Aus der Klinik und Poliklinik für Herzchirurgie, herzchirurgische Intensivmedizin und Thoraxchirurgie der Universität zu Köln
Direktor: Universitätsprofessor Dr. med. Th. Wahlers

Plasma proteome of brain-dead organ donors predicts heart-transplant outcome

Inaugural-Dissertation zur Erlangung der Doktorwürde
der Medizinischen Fakultät
der Universität zu Köln

vorgelegt von
Jan Lukac
aus Düsseldorf

promoviert am 29. Januar 2024

Gedruckt mit Genehmigung der Medizinischen Fakultät der Universität zu Köln
2024

Dekan: Universitätsprofessor Dr. med. G. R. Fink

1. Gutachter: Professor Dr. med. P. Baradaran Rahmanian
2. Gutachter: Universitätsprofessor Dr. med. S. Baldus
3. Gutachter: Professor Dr. R. Zimmermann

Erklärung:

Ich erkläre hiermit, dass ich die vorliegende Dissertationsschrift ohne unzulässige Hilfe Dritter und ohne Benutzung anderer als der angegebenen Hilfsmittel angefertigt habe; die aus fremden Quellen direkt oder indirekt übernommenen Gedanken sind als solche kenntlich gemacht.

Bei der Auswahl und Auswertung des Materials sowie bei der Herstellung des Manuskriptes habe ich Unterstützungsleistungen von folgenden Personen erhalten:

Herr Dr. K. Dhaygude
Herr Dr. M. Saraswat
Herr S. Joenväärä
Herr Dr. med. S. Syrjälä
Herr Dr. med. E. Holmström
Herr Dr. R. Krebs
Frau E. Rouvinen
Herr Dr. med. A. Nykänen
Herr Professor R. Renkonen
Herr Professor K. Lemström

Weitere Personen waren an der Erstellung der vorliegenden Arbeit nicht beteiligt. Insbesondere habe ich nicht die Hilfe einer Promotionsberaterin/eines Promotionsberaters in Anspruch genommen. Dritte haben von mir weder unmittelbar noch mittelbar geldwerte Leistungen für Arbeiten erhalten, die im Zusammenhang mit dem Inhalt der vorgelegten Dissertationsschrift stehen.

Die Dissertationsschrift wurde von mir bisher weder im Inland noch im Ausland in gleicher oder ähnlicher Form einer anderen Prüfungsbehörde vorgelegt.

Die dieser Arbeit zugrunde liegende Konzeptualisierung und Forschungsfinanzierung wurde mit meiner Mitarbeit von Herr Dr. med. A. Nykänen, Herr Professor K. Lemström und Herr Professor R. Renkonen durchgeführt.

Das dieser Arbeit zugrunde liegende Forschungsdesign wurde mit meiner Mitarbeit von Herr Dr. med. A. Nykänen, Herr Professor K. Lemström, Herr Dr. K. Dhaygude und Herr Professor R. Renkonen erstellt.

Der dieser Arbeit zugrunde liegende Datensatz wurde mit meiner Mitarbeit an der Universitätsklinik Helsinki in Finnland in der Abteilung für Herz- und Thoraxchirurgie und im Transplantationslaboratorium von Herr Dr. med. A. Nykänen, Herr Dr. med. S.

Syrjälä, Herr Dr. K. Dhaygude, Herr S. Joenväärä, Herr Dr. M. Saraswat, Herr Dr. med. E. Holmström, Herr Dr. R. Krebs und Frau E. Rouvinen erhoben. Dabei wurden die Plasmaproben von Herr Dr. R. Krebs und Frau E. Rouvinen gesammelt, aufbereitet und gelagert, das Proteom der Plasmaproben von Herr S. Joenväärä und Herr Dr. M. Saraswat bestimmt und von Herr Dr. K. Dhaygude und mir statistisch analysiert. Die klinischen Daten wurden von Herr Dr. med. A. Nykänen, Herr Dr. med. S. Syrjälä, Herr Dr. med. E. Holmström und mir zusammengetragen und statistisch analysiert.

Die dieser Arbeit zugrunde liegenden analytischen Methoden wurden mit meiner Mitarbeit von Herr Dr. med. S. Syrjälä, Herr Dr. M. Saraswat, Herr Dr. K. Dhaygude und Herr Professor R. Renkonen eingebracht.

Die dieser Arbeit zugrunde liegende Datenanalyse wurde mit einer Mitarbeit von Herr Dr. K. Dhaygude, Herr Dr. med. S. Syrjälä, Herr S. Joenväärä und Herr Dr. M. Saraswat durchgeführt. Dabei wurde die Flüssigchromatographie mit Massenspektrometrie-Kopplung von Herr S. Joenväärä und und Herr Dr. M. Saraswat, die Statistik-Programmiersprache RStudio von Herr Dr. K. Dhaygude und die Statistiksoftware SPSS von Herr Dr. med. S. Syrjälä und mir verwendet. Zusätzlich wurde die IPA Canonical Pathway Analysis-Software von mir verwendet.

Die dieser Arbeit zugrunde liegenden Ergbnisse wurde mit meiner Mitarbeit von Herr Dr. med. A. Nykänen, Herr Dr. K. Dhaygude, Herr Dr. M. Saraswat, Herr Dr. med. S. Syrjälä, Herr S. Joenväärä und Herr Professor K. Lemström interpretiert.

Die dieser Arbeit zugrunde liegende Publikation wurde mit meiner Mitarbeit von Herr Dr. med. A. Nykänen, Herr Dr. K. Dhaygude, Herr Dr. med. S. Syrjälä, Herr Dr. M. Saraswat, Herr S. Joenväärä, Herr Dr. R. Krebs und Herr Professor K. Lemström verfasst.

Erklärung zur guten wissenschaftlichen Praxis:

Ich erkläre hiermit, dass ich die Ordnung zur Sicherung guter wissenschaftlicher Praxis und zum Umgang mit wissenschaftlichem Fehlverhalten (Amtliche Mitteilung der Universität zu Köln AM 132/2020) der Universität zu Köln gelesen habe und verpflichte mich hiermit, die dort genannten Vorgaben bei allen wissenschaftlichen Tätigkeiten zu beachten und umzusetzen.

Järvenpää, den 23.05.2023

Unterschrift: .....

Danksagung

Mein Dank gilt meinem Doktorvater Prof. Dr. Parwis Rahmanian für die Betreuung dieser Dissertationsarbeit und die zugewandte und freundliche Unterstützung. Zudem möchte ich mich bei dem Transplantationslabor der Universität Helsinki für die fruchtvolle Zusammenarbeit und bei der Medizinischen Fakultät zu Köln für die Möglichkeit des Medizinstudiums sowie die Unterstützung während des Studiums und des Dissertationsvorhabens bedanken. Darüber hinaus gilt ein großer Dank meiner Lebensgefährtin Ella für ihre unentwegte Unterstützung.

Table of contents

LIST OF NON-STANDARD ABBREVIATIONS 6

1. SUMMARY IN GERMAN 7

2. INTRODUCTION 10

3. MATERIAL AND METHODS 14

4. RESULTS 18

4. DISCUSSION 25

5. REFERENCES 35

6. APPENDIX 46

6.1 FIGURES 46

6.2 TABLES 49

7. PRE-PUBLICATION OF RESULTS AND SUPPLEMENTARY MATERIALS 49

List of non-standard abbreviations

- CRP: c-reactive protein
- FDR: false discovery rate
- HTx: heart transplantation
- IPA: ingenuity pathway analysis
- NO: nitric oxide
- OPLS-DA: orthogonal projections to latent structure-discriminant analysis
- PCA: principal component analysis
- ROC: receiver operating characteristic
- ROS: reactive oxygen species
- S-Plot: variance vs correlation plot
- SOM: self-organizing map
- hsTnI: high-sensitivity troponin I
- hsTnT: high-sensitivity troponin T

1. SUMMARY IN GERMAN

Die Herztransplantation ist die Therapie der Wahl für Patienten mit terminaler Herzinsuffizienz aus verschiedenen Gründen. Aufgrund der Alterung der Gesellschaft steigt die Zahl an Patienten, die ein Spenderherz benötigen, während gleichzeitig die Zahl an geeigneten Spenderherzen sinkt. Um den daraus entstehenden und stetig wachsenden Organmangel entgegenzuwirken, wird zunehmend auf marginale Spenderorgane zurückgegriffen. Jedoch führt die Verwendung dieser Organe mit eingeschränkter Qualität zu einem häufigeren Auftreten von primären Transplantatversagen und einer verkürzten Überlebenszeit.[1] Dabei werden auftretende Komplikationen der Spenderorgane häufig zu spät diagnostiziert und deren Ätiologie bleibt nur unzureichend bekannt und geklärt.

Um eine optimierte Verwendung von Spenderherzen zu erreichen, ist es von großer Wichtigkeit Spenderherzen mit einem erhöhten Risiko für Transplantatversagen frühzeitig zu identifizieren und die Behandlung entsprechend anzupassen. Jedoch ist hierfür ein verbessertes Verständnis der zugrundeliegenden molekularen Pathophysiologie vonnöten. Ein vielversprechender Ansatz für die Erforschung der molekularen Pathologie stellt die Proteomik dar. Unter Proteomik versteht man die Erforschung des Proteoms mit biochemischen Methoden. Das Proteom umfasst die Gesamtheit der Proteine in einer Zelle, einem Organ oder eines Organismus. So kann durch die Verwendung der Liquid-Chromatographie Massenspektrometrie/Massenspektrometrie (LC-MS/MS) auf der Proteinebene ein detaillierter Einblick in die Pathophysiologie und die molekularen Fingerabdrücke von Spenderorganen mit einer schlechteren klinischen Prognose gewonnen werden.

In dieser retrospektiven monozentrischen Studie, die an der Universitätsklinik Helsinki durchgeführt wurde, wurden Plasmaproben von 54 hirntoten Organspendern sowie 24 gesunden Kontrollprobanden im Zeitraum von 2010 bis 2016 gesammelt und in Hinblick auf einen möglichen Einfluss auf das Ergebnis nach Herztransplantation hin untersucht. In der anschließenden Ultra-Performance-Flüssigchromatographie-gekoppelten Tandemmassenspektrometer (UPLC-MS/MS) Analyse der Plasmaproben wurden insgesamt 463 Proteine identifiziert. Als Nächstes wurden mithilfe von uni- und multivariaten Analysen die Unterschiede in der Proteinexpression zwischen den Organspendern und den gesunden Kontrollprobanden untersucht. Von 463 Proteinen waren 237 Proteine unterschiedlich zwischen den beiden Gruppen exprimiert, wobei 90 Proteine eine verminderte und 149 eine erhöhte Expression in den Organspendern zeigten. Für die Erforschung der zugrundeliegenden biologischen Mechanismen wurde die Pathway-Enrichment-Analyse angewendet. Es wurden 6 Pathways gefunden von denen Glukoneogenese, Glykolyse und Koagulation in den Organspendern hochreguliert, und Komplementsystem, LXR/RXR-Aktivierung und Produktion von Stickstoffmonoxid und reaktiven Sauerstoffspezies in Makrophagen herunterreguliert waren. Um potenzielle Biomarker für ein negatives Outcome zu finden, wurde die Assoziation zwischen dem Plasmaproteom der Organspender und den klinischen Endpunkten der Organempfänger wie primäres Transplantatversagen, akute Abstoßungsreaktion mit hämodynamischer Instabilität, sowie transplantatbedingte Sterblichkeit analysiert. In punktbiserialer Korrelationsanalyse war das Protein *Lysine-specific demethylase 3A* moderat mit dem Auftreten von jeglichen und schweren primären Transplantatversagen assoziiert. In der uni- und and multivariaten Cox-Regressionsanalyse wurden *Myosin Va* und *Proteasome activator complex subunit 2* als Prädiktoren für die Entstehung einer akuten Abstoßungsreaktion mit hämodynamischer Instabilität innerhalb von 30 Tagen identifiziert. In der

univariaten Analyse war eine erhöhte Expression von *Lysine-specific demethylase 3A* and *Moesin* mit einer erhöhten transplantatbedingten 1-Jahres-Sterblichkeit vergesellschaftet.

Unsere Ergebnisse zeigen, dass der Hirntod eine signifikante Auswirkung auf das Plasmaproteom der Organspender hat. Das Proteinprofil der Organspender ist charakterisiert u.a. durch Dysregulation von Blutgerinnung, Komplementsystem, Immunsystem, sowie Verletzung des Endothels und Myokardiums. Wir haben Plasmaproteine gefunden, die mit dem klinischen Ergebnis nach Herztransplantation assoziiert sind. Diese Proteine stellen womöglich potenzielle Biomarker dar, die dabei helfen könnten Spenderorgane mit einem erhöhten Risiko für Komplikationen bereits vor der Transplantation zu identifizieren und das weitere Management von Organspender, Spenderorgan und Organempfänger zu optimieren.

2. INTRODUCTION

Heart transplantation (HTx) is the only curative treatment for patients with end-stage heart failure that cannot be managed with maximum medical therapy. Annually, around 8000 HTx are performed worldwide, out of which around 20 HTx are performed in Finland, and around 329 in Germany.[2,3,4] Heart transplants come either from donation after brain death or donation after circulatory death. Despite recent advances in donation after circulatory death, donation after brain death remains the mainstay of heart transplantation. However, brain death causes progressive and detrimental tissue damage in the central nervous system leading to massive circulatory, hormonal, and metabolic changes and systemic inflammation. This may expose donor organs to injury and increase the risk of acute rejection, primary graft dysfunction (PGD), and mortality in heart transplant recipients.[5,6,7,8] However, the molecular mechanisms and pathways affecting donor organ quality in brain-dead organ donors are still not fully understood and studies have relied on examining clinical parameters, donor demographics, and a small number of proteins such as *Donor B-type natriuretic peptide*.[9,10]

Currently, most heart transplants are retrieved from brain-dead multiple organ donors and clinical outcomes have markedly improved over the decades.[11] Nevertheless, PGD is an early postoperative complication that occurs in up to 28 to 36% of cases and is still the leading cause of early mortality, accounting for about 43% of deaths that occur within 30 days after HTx.[12,13,14] PGD-related mortality within 30-days is up to 19% compared to 4.5% all-cause mortality in patients without PGD.[15] Long-term PDG-related mortality has been reported to be up to 42% compared to 8% all-cause mortality in patients without PGD.[16] The International Society for Heart and Lung Transplantation (ISHLT) established the diagnostic and grading criteria for PGD in a

consensus statement in 2014.[17] PGD is defined as the presentation of left, right, or biventricular dysfunction occurring within the first 24 hours after HTx. Additionally, other secondary causes of graft dysfunction such as hyperacute rejection, pulmonary hypertension, or known surgical complications must be ruled out. Left ventricle PGD can be further categorized into mild, moderate, or severe PGD. The severity of PGD is determined based on ejection fraction, hemodynamics, and the need for ionotropic or mechanical support. Risk factors for the development of PGD include donor, recipient, and procedural factors. Donor factors include inter alia age and the cause of brain death. Recipient factors encompass overweight, diabetes, and pre-operative inotropic and mechanical circulatory support. Procedural factors include donor heart ischemic time, donor-recipient weight mismatching, and cardiopulmonary bypass time.[18,19,20,21,22,23] However, not all risk factors of PGD are known, and underlying molecular processes have not been fully explained. Such multifactorial etiology complicates the diagnostic evaluation and makes it difficult to distinguish between heart transplant patients with a high risk of PGD on the one hand and patients with a low risk on the other hand.

The ongoing shortage of heart organ donors is a major limiting factor for heart transplantation. Organ shortage is aggravated by population aging which leads to an increasing number of patients with end-stage heart failure on the organ waiting list while the number of older donors with comorbidities and lower organ quality is growing.[24] To extend the donor organ pool, more clinicians accept marginal donors for transplantation. Marginal donors are suboptimal donors who do not meet the criteria of an optimal donor. It is generally accepted that an optimal donor can be characterized amongst others by a maximum age of 55 years, absence of left ventricular hypertrophy, ischemic time of less than 4 hours, suitable donor to recipient predicted heart mass

ratio, having no coronary artery disease, no history of alcohol abuse, and gender-matched transplantation.[25,26,27,28,29,30.] However, the increased use of marginal donors is complicated by the fact that marginal donors have a higher risk of transplant failure including the occurrence of PGD as well as death.[31,32] Therefore, it is important to further investigate the effect of known and unknown risk factors on the clinical outcome of marginal heart donors.

As brain death has specific implications for the heart transplant quality and the use of marginal donors with higher risk of complications is increasing, making efforts to prevent and minimize acute rejection, PGD, and mortality are of immense importance. However, a thorough understanding of the pathophysiology in brain-dead organ donors at the molecular level is needed. Based on the investigation and improved understanding of molecular mechanisms and pathways, novel biomarker candidates could be discovered. So far, clinical biomarkers to detect and monitor the quality of transplants in human brain-dead donors are unavailable. Liquid biopsies based on plasma samples may offer the possibility to identify heart transplants with lower quality and an increased risk of transplant failure. Early detection of high-risk transplants could lay the basis for improved management of the heart transplant during procurement, preservation, reperfusion, transplantation, and post-transplant treatment.

The underlying molecular level of pathophysiology can be investigated with different omics-based methods such as genomics, miRNA omics, and proteomics. Using proteomics with ultra-high-performance liquid chromatography, connected to tandem mass spectrometry (UPLC-MS/MS), offers a promising approach to accurately measure the protein expressions in plasma. Furthermore, proteomics can be embedded in a systemic biology approach to ease the systemic characterization of

plasma proteins.[33] Uni- and multivariate statistical analyses can be used to find significant differences in protein expression between two groups. Next, biological pathway analyses and literature research pinpoint modulated key proteins, pathways, and biological mechanisms, and therefore help to elucidate the complex pathophysiology of brain-dead organ donors.[34]

In this study, a label-free proteomics approach was used to reveal the plasma proteomic profile of brain-dead organ donors. We sought to find key proteins, biological pathways, and pathogenic mechanisms that are affected by the brain death of organ donors. Moreover, we aimed to enhance the understanding of the complex unphysiological state of brain-dead donors and to search for novel biomarker candidates for the risk evaluation of cardiac donor organs.

3. MATERIAL AND METHODS

This study is a post hoc analysis of multi-organ donors participating in a prospective, randomized clinical trial on the effects of donor simvastatin treatment on ischemia-reperfusion injury after heart transplantation (Nykänen et al.) Nykänen et al. included heart transplantations performed at Helsinki University Hospital between 2010 and 2016 unless they did not meet the inclusion criteria. 84 heart donors were randomly assigned to receive 80 mg of simvastatin (42 donors) via nasogastric tube within 2 hours after the declaration of brain death or to receive no simvastatin (42 donors). They found that donor treatment with simvastatin reduces biomarkers of myocardial injury and heart failure as well as the number of acute rejections with hemodynamic compromise early after heart transplantation.[35] Out of the original 84 trial donors and recipients, 54 donor samples were chosen for proteomics analysis as they had complete sets of all time points samples available of the donor and recipient pair (1h to 24h). Out of 54 donor samples, 27 donors belonged to the simvastatin treatment group. In addition to the 54 donor samples, control samples were collected from 24 healthy controls. Next, we analyzed the 54 donor and 24 plasma protein samples by nano ultra-high-performance liquid chromatography and quantified them with UPLC-MS/MS before we compared the plasma proteome with clinical outcome after HTx.

The study was reviewed and approved by the Institutional Ethical Committee of the Helsinki University Hospital (Permission 358/13/03/02/2009 amendment), Helsinki, Finland. The Institutional Review Board concluded that consent would not be required for the use of samples collected after the declaration of brain death. Control samples from healthy volunteers were obtained from employees of the research institute. The

study was carried out adhering to the International Conference on Harmonization E6 guidelines for Good Clinical Practice and the principles of the Declaration of Helsinki.

Heart transplant donors with the following criteria were excluded from the study: >60 years of age, located outside of Finland, low left ventricular ejection fraction (ejection fraction <45%), severe left ventricular hypertrophy (posterior wall or septal thickness >14 mm), abnormal coronary angiography requirement of high-dose inotropic agent treatment at organ procurement (dopamine or dobutamine >20 ugs/kg/min or norepinephrine >0.2 ugs/kg/min), or previous statin drug treatment. At least one echocardiogram was acquired from all donors and coronary angiogram was performed in donors with the age of >40 years, a strong family history of coronary artery disease, or a smoking history. Clinical donor management and follow-up were carried out based on the clinical protocol of the Heart and Lung Transplantation Program at the Helsinki University Hospital.[36] Immediately after the declaration of brain death, donors received 1g of methylprednisolone and 1g of meropenem intravenously.

Plasma samples were taken by employees of the transplantation laboratory and collected in lithium heparin tubes before heparinization and organ procurement. After cooling down, we used the “Top 12 Abundant Protein Depletion kit” (Pierce, Thermo Fisher) to deplete greater than 95% of the most abundant proteins from 10 µl of plasma. The list of 12 depleted proteins included *alpha-1-1acid-glycoprotein, alpha-1-antitrypsin, alpha-2-macroglobulin, albumin, apolipoprotein A-I, apolipoprotein A-II, fibrinogen, haptoglobin, IgA, IgG, IgM,* and *transferrin,* and the remaining proteins were digested by trypsin. In addition, donor hemoglobin (Hb), platelets, hsTnT, hsTnI, CRP, total cholesterol, high-density lipoprotein, low-density lipoprotein, and triglycerides were analyzed from plasma samples by an accredited clinical laboratory (HUSLAB,

Helsinki University Hospital). UPLC-MS/MS was performed as described.[37] Label-free quantification failed on 1 donor sample due to the batch effect, therefore this sample was excluded from the study. One control sample failed normalization and was removed from the study. Therefore, finally 53 donor and 23 control samples were considered for subsequent statistical analysis.

In statistical analyses, unsupervised PCA and SOM and supervised OPLS-DA modeling methods were applied to illustrate the clustering of all 463 quantified proteins. Grouping patterns, trends, and outliers were examined on scatter plots and heatmap. We used the ropls and pheatmap packages in R software. Next, we performed univariate and multivariate analyses to find differentially expressed proteins between donors and healthy controls. First, we performed univariate analysis on all 463 quantified proteins including the Wilcoxon-Mann-Whitney test, fold change analysis, and the S-Plot for OPLS-DA. Wilcoxon-Mann-Whitney test p value was corrected using the Benjamini-Hochberg method and an FDR-corrected p value of <0.05 was considered significant. Multivariate analysis was carried out with OPLS-DA to generate an S-Plot. For S-Plot, the cut-offs, ±0.1 for p(1) and ±0.7 for p(corr)[1] were used. S-Plot proteins were filtered by FDR-corrected p value to see which were also significant by Benjamin-Hochberg procedure for added statistical stringency. Moreover, we performed receiver operating characteristic (ROC) analysis with MetaboAnalyst 4.0 (metaboanalyst.ca/) to quantify how accurately S-Plot proteins can discriminate between the 2 groups. An AUC value of more than 0.8 is considered good.

Following the identification of significant proteins, enrichment pathway analysis was used to explore the biological pathways of identified proteins of brain-dead donors. Enrichment pathway analysis was performed by Canonical Pathway Analysis in the

web-based bioinformatics application QIAGEN Ingenuity Pathway Analysis (IPA). In this study, a -log(p value) of >3 corresponding to a p value of <0.001 was applied for more statistical robustness. In addition, a z-score greater than 1 or smaller than -1 was considered significant.

Then, we performed outcome analysis on recipient freedom from any primary graft dysfunction (PGD) and from severe PGD, recipient freedom from acute rejection with hemodynamic compromise within 30 days after transplantation, and on graft-related 1-year mortality to evaluate the impact of donor plasma protein levels on these clinical endpoints. In outcome analysis on recipient freedom from any primary graft dysfunction (PGD) and from severe PGD, point-biserial correlation analysis was applied on brain-dead donor donors. A correlation coefficient of 0 to 0.4 is considered a weak relationship, a correlation coefficient of 0.4 to 0.7 a moderate relationship, and a correlation coefficient of more than 0.7 is considered a strong relationship.

In outcome analysis on recipient freedom from acute rejection with hemodynamic compromise within 30 days and on graft-related 1-year mortality, univariate Cox regression analysis was performed with brain-dead donor plasma proteins. Next, maximally selected rank statistics algorithms were used to divide donors into high- and low-level subgroups based on different plasma protein levels. Then, the log-rank test was applied to compare recipient rejection and mortality freedom curves between the donor subgroups. Afterward, we generated Kaplan-Meier plots for significant proteins in each subgroup and considered donor proteins with $p < 0.05$ as having a statistically significant effect on recipient rejection and mortality episodes. Finally, multivariate Cox regression was carried out to see the combined predictive effect for significant proteins.

All outcome analyses were performed using survival and survminer packages in R software.

For more details about plasma sample processing, pathway analysis, definitions of clinical outcomes, and statistical analyses, see Methods in Supplementary Materials.

4. RESULTS

Brain-dead donors showed a unique but heterogeneous proteomic profile

The final proteomic analysis consisted of 53 multi-organ donors for HTx, and 23 healthy controls (**Figure 1**). The median age of the organ donors was 44 years, and 10 were female (**Table 1**). We detected 1259 plasma proteins with a minimum of 1 unique peptide by UPLC-MS/MS. For sufficient stringency and confidence in proteomics data, we filtered the proteins with 2 or more unique peptides and obtained 463 quantified proteins. To describe the changes in protein abundance between donors and healthy controls, the fold change was calculated by dividing the mean protein expression of a single protein among donors by the mean expression in controls. The fold change ranged from 0.11 to 2584. For more details on the study population and demographic data, see Results in Supplementary Materials.

Of note is that donor treatment with simvastatin did not classify the treated and untreated donor groups, and therefore was not considered a confounding factor (**Figure S1**).

PCA was performed on all 463 quantified proteins (**Figure 2A).** The scatter plot (t1 versus t2) revealed that samples of donors and healthy controls were only partially separated. Four donors were outside of the 95% confidence ellipse of measurement. The unsupervised learning method of SOM displayed 2 main clusters of protein expression in donors (Donor A and Donor B), 1 of them having 2 subclusters (Donor B1 and Donor B2) (**Figure 2B,** red color for donor samples), and 2 clusters in healthy controls (**Figure 2B,** blue color for healthy control samples), confirming the findings of PCA. A subset of healthy controls and donors merged into the same cluster which was due to the similarity of a few proteins in those samples and the use of the complete set of all 463 quantified proteins in SOM clustering.

To further characterize the separation between donors and healthy controls, supervised multivariate OPLS-DA model and univariate S-Plot were performed. OPLS-DA showed a clear separation between the 2 groups, confirming the findings suggested by PCA and SOM (**Figure 2C**). S-Plot analysis revealed that 32 proteins were statistically significant in both univariate and multivariate analyses between donors and healthy controls, and thereby represent proteins mostly contributing to the differences between donors and healthy controls (**Figure 2D**). Three proteins were upregulated, while 29 proteins were downregulated. Of these proteins, *apolipoprotein A-IV, complement C1q C chain, leucine-rich alpha-2-glycoprotein 1*, and *14-3-3 protein beta/alpha* showed a good area under the ROC curve (AUC) value of >0.8 (**Table S1**).

Next, we performed univariate analysis to calculate log2(fold change) and p value using the Wilcoxon-Mann-Whitney test to find out which of 463 proteins were statistically significantly different between donors and healthy controls. Univariate

analysis based on FDR-corrected p value of <0.05 revealed 237 differently expressed proteins between the donors and healthy controls of which 90 proteins were upregulated, while 147 proteins were downregulated (**Table S2**).

Brain-dead donor protein profile revealed significantly altered pathways

IPA pathway analysis of 237 differentially expressed proteins revealed 65 significant pathways with a p value of <0.05. Furthermore, using more stringent statistical criteria for protein data set in IPA pathway analysis, we found that 118 proteins with log2(fold change) ≥1 belonged to 58 significant pathways, while 66 proteins with log2(fold change) ≥1.5 showed 50 significant pathways (**Table S3**).

In IPA pathway analysis based on z-score orientation (absolute z-score greater than 1) and the most stringent FDR-corrected p value of <0.001, we saw that on the one hand coagulation, gluconeogenesis, and glycolysis were significantly enriched, and these pathways showed a trend towards upregulation. On the other hand, complement system, LXR/RXR activation, and production of NO and ROS in macrophages showed a trend toward downregulation (z-score ≤-1) (**Table 2, Figure S2A-F**). When considering log2(fold change) ≥1, we found that only gluconeogenesis, glycolysis, and xenobiotic metabolism pathways were significant and that they were upregulated. No significant pathway was found with log2(fold change) ≥1.5 (**Table 2**)**.**

Out of 32 S-Plot proteins, 10 S-Plot proteins belonged to the pathways with an absolute z-score greater than 1 and a p value of <0.001, while the remaining 22 S-Plot proteins were present in other significant pathways. We found that these 10 S-Plot proteins were mostly enriched in coagulation, complement, LXR/RXR activation, and production of NO and ROS in macrophages pathways (**Table 2**)**.**

Proteome profile discriminated 3 subclusters within brain-dead donors

To exclude a methodological artifact of healthy controls to brain-dead donors, we carried out separate statistical analyses including only brain-dead donors and found 3 subclusters within donors with only minor changes in their demographics (**Figure S3**, **Table 1)**. When comparing the recipient outcomes between Donor A and Donor B groups, we could not see any statistically significant difference in PGD, acute rejection, or graft-related survival (**Table 3**). Detailed information, stratified by the Donor subgroups, on the donor demographics and recipient outcomes is given in Tables 1 and 3, and on enriched pathways in Tables S4 and S5, and Supplementary Materials.

Donor plasma *lysine-specific demethylase 3A* was moderately associated with PGD

Next, we investigated whether donor plasma proteins could predict any PGD grade or severe PGD after transplantation. Out of 53 recipients, 17 (32%) recipients developed PGD, and only 6 (11%) had severe PGD. The characteristics of respective donors of recipients with any PGD grade or severe PGD were not statistically different **(Table S6)**. However, the recipients with any or severe PGD had longer intubation time, longer stay at ICU and index hospitalization, and higher levels of proBNP, hsTnI, hsTnT, and lactate **(Table S7)**.

The point-biserial correlation analysis revealed that only 5 proteins correlated with any PGD, while 6 proteins correlated with severe PGD. Only *lysine-specific demethylase 3A* showed a moderate correlation with any PGD and severe PGD **(Table S8)**.

High donor plasma *myosin Va* and *proteasome activator subunit 2* predicted acute rejection episodes with hemodynamic compromise

Next, we investigated whether donor plasma proteins could predict episodes of acute rejections with hemodynamic compromise. Three patients were excluded from the analysis as they expired due to graft-related reasons within 30 days **(Table S9)**. Sixteen patients received treatment for acute rejection with hemodynamic compromise. The characteristics of respective donors were not different **(Table S10)**. However, the recipients with rejection episodes had significantly higher plasma levels of troponins and lactate during the first 24 hours, higher ProBNP and lower left-ventricle ejection fraction at 1 month, and longer ICU and hospital stay after transplantation **(Table S11)**. For more details about specific treatment for acute rejection with hemodynamic compromise, see Results in Supplemental Material.

Univariate Cox regression analysis of differentially expressed 237 proteins revealed that 7 donor plasma proteins were significantly associated with acute rejections with hemodynamic compromise within 30 days. These proteins included *CD163*, *CRP*, *keratin 76, myosin Va, proteasome subunit alpha type 6, proteasome activator subunit 2*, and *transaldolase 1*. We further explored the possibility of an association between acute rejections with hemodynamic compromise and concentration thresholds for these proteins in univariate analysis. After stratification of patients based on each protein expression level, we found that higher donor plasma levels of all these proteins were associated with a significantly increased number of acute rejections with hemodynamic compromise. In Kaplan-Meier analysis, all 7 donor plasma proteins passed the log-rank test with a p value less than 0.05 **(Figure 3A-G, Table 4)**. Higher expression of these 7 proteins was linked to higher hazard/risk **(Table 4)**.

Additionally, a donor plasma proteomic predictive risk score was calculated based on the concentration levels of these proteins and corresponding regression coefficients. This predictive risk score was calculated by giving 1 point for each of the 7 proteins that were within their respective high-risk levels, therefore yielding a score of 0 to 7 for each donor. In risk score calculation, 18 patients had a score of 0, 16 patients had a score of 1, 6 patients had a score of 2, 5 patients had a score of 3, and 5 patients had a score greater than 3. Based on the donor proteomics risk score, we found that a higher score significantly predicted acute rejection with hemodynamic compromise (Figure 3H). In addition, we observed that donors with a high-risk score (score ≥3) had an 80% probability of acute rejection with hemodynamic compromise within 30 days **(Figure S4)**.

In multivariate Cox regression analysis, *myosin Va* and *proteasome activator subunit 2* remained significant suggesting that these 2 proteins are key candidates for prediction of acute rejection with hemodynamic compromise within 30 days after transplantation **(Figure S5)**.

High levels of *moesin* and *lysine-specific demethylase 3A* were associated with worse graft-related 1-year survival

Next, we investigated whether donor proteome could predict graft-related mortality. Out of 53 recipients, 7 recipients died due to graft-related reasons, 6 of them during the first year, and 1 patient died 730 days after transplantation. PGD was the cause of death in 4 patients, acute rejection in 2 patients, and chronic rejection in 1 patient (**Table S9**). Therefore, we tested whether donor proteome could predict 1-year graft-related mortality.

In univariate analysis, we found that 5 proteins were significantly associated with 1-year graft-related mortality (**Figure 4A-E**). After stratification of donors using maximally selected rank statistics algorithms, we found that high donor plasma levels of *moesin* and *lysine-specific demethylase 3A* were associated with increased graft-related 1-year mortality, while low plasma levels of *D-dopachrome decarboxylase, leucine-rich alpha-2-glycoprotein,* and *keratin 79* were associated with decreased graft-related 1-year mortality. In multivariate analysis of 1-year graft-related survival analyses, none of the proteins were significant (**Table 4**).

A summary of the possible biological role of key proteins predicting heart transplant outcome discussed further below, can be found in **Table S12**.

4. DISCUSSION

Heart transplantation using heart allografts from brain-dead organ donors has been established as the gold standard in the treatment of patients with end-stage heart failure. Due to aggravating donor shortage, marginal hearts are increasingly used to improve the availability of donor organs. However, the use of marginal donors with lower organ quality worsens clinical outcomes. Despite remarkable improvements in the management of heart transplants, strategies to optimize the use of scarce donor organs are essential. Novel insights into the molecular pathophysiology of brain-dead organ donors integrated into existing knowledge of involved biological processes may provide liquid biomarker candidates for the detection, prognosis, and treatment of heart transplants with lower quality and increased risk of complication.

Using a label-free proteomics approach, we present the plasma proteomic profile of brain-dead organ donors. We were able to show that brain death induces alterations in protein expression, biological pathways, and pathogenic mechanisms. We found 237 proteins that distinguished brain-dead donors from healthy controls. Based on these 237 identified proteins, 6 significant pathways were enriched, and 32 most significant proteins were filtered by S-Plot, out of which 10 were present in enriched pathways. Enriched pathways were coagulation, complement system, gluconeogenesis, glycolysis, LXR/RXR activation, and production of nitric oxide (NO) and reactive oxygen species (ROS) in macrophages. Moreover, plasma proteins were linked to arteriogenesis and vascular growth, cardiomyocyte and endothelial cell function, and inflammation. Altered biological pathways, mechanisms, and single proteins may play a pivotal role in the pathophysiology of organ injury, acute rejection, primary graft dysfunction (PGD), and mortality. Moreover, single proteins were able to predict heart transplant outcome and thus may be valuable for transplant evaluation

and personalized treatment. If the proteomic profile of an individual donor shows an increased risk of complications after HTx, the care of the donor, transplant, and recipient can be potentially personalized. For example, if a donor proteomic profile indicates a high risk of the development of PGD, enhanced hormonal replacement therapy in donors, faster transport of the transplant, and closer monitoring of cardiac enzymes in recipients may help to decrease the risk of the occurrence of PGD.[38,39,40]

The crosstalk between complement and coagulation is central to the innate immune response to injury.[41,42] A key study by Atkinson et al. has demonstrated that brain death triggers complement activation and ischemia-reperfusion injury in heart transplants. Moreover, Atkinson et al. recognized that recipients of brain-dead donor grafts have a higher risk of acute rejection and graft failure than recipients of living donor grafts. This may be due to more complement activation and cardiac injury, suggesting that a complement inhibition treatment in recipients may alleviate cardiac injury and result in better clinical outcomes.[43] In our study, brain death was linked to an overall upregulation of coagulation and a downregulation of the complement system whilst S-Plot proteins being present in pathways were downregulated in donors. In donor subgroup analyses, the Donor B subgroup with more hypertension and traumatic brain injury as well as the Donor B1 subgroup with higher CRP and troponin within 24h and reduced heart function 7 days after HTx showed an upregulation of complement pathway. Nevertheless, our findings indicate that the shortage of anticoagulant proteins *antithrombin-III*, *plasminogen* and *protein C* may aggravate microvascular thrombosis, and reduce optimal myocardial reperfusion in the heart recipient. In a study performed by Labarrere et al., endomyocardial biopsies were taken from 141 heart transplant recipients 3 months after HTx, and the presence of vascular *antithrombin* was assessed by immunohistochemistry. Interestingly, heart transplants with a lack of

vascular *antithrombin* had an increased risk of cardiac allograft vasculopathy and heart transplant failure, while transplants with recovered vascular *antithrombin* showed better clinical outcome after HTx.[44]

Excessive coagulation, inappropriate innate immune response, and ischemia-reperfusion injury may have led to the depletion of the LXR/RXR pathway in brain-dead donors. Prior studies have noted the importance of LXR/RXR as lipid-sensing transcription factors that link lipid metabolism with protective immune response and attenuation of ischemia-reperfusion injury.[45,46] One study by Xu et al. has assessed the impact of *apolipoprotein A4* on thrombosis in human plasma samples and reported that *apolipoprotein A4* inhibited thrombocyte aggregation and thrombus formation.[47] In our study, we observed decreased *apolipoprotein A4* levels which may worsen thrombosis after brain death. A considerable amount of literature has been published on the kinin-kallikrein system which contributes to coagulation, vascular inflammation, and vasodilatation. *Kininogen-1* plays a key role as it mediates the assembly of the kinin-kallikrein system.[48,49] Griangreco et al have analyzed 88 pre-transplant samples and found that a decreased plasma level of *kallikrein* was a robust predictor of PGD, particularly in combination with pre-transplant ionotropic treatment.[50] The impact of *paraoxonase-1* on endothelium was studied by García-Heredia et al. They reported that *paraoxonase-1* has anti-apoptotic and anti-oxidative effects on endothelial cells.[51] We found that levels of *paraoxonase-1* were lower in brain-dead donors compared to controls. Taken together, the low levels of *paraoxonase-1* may make heart transplants more susceptible to endothelial cell damage by oxidation and apoptosis.

On one hand, myocardial injury may be aggravated by increasing decoupling of glycolysis and glucose oxidation as reported by Opie et al. and Lee et al..[52,53] In our

brain-dead donors, glycolysis may be upregulated for anaerobic ATP production, while normal cardiac ATP production from fatty acid oxidation may be downregulated.[54] Several studies have shown that upregulation of gluconeogenesis may worsen hyperglycemia and systemic inflammation in brain-dead donors.[55,56,57] In a study conducted by Aljiffry et al., 15 human brain-dead organ donors were divided into one group which was treated with high-dose insulin, and one control group without insulin treatment. The insulin-treatment group showed preserved normoglycemia and suppressed systemic inflammation, providing support for the hypothesis that insulin treatment of brain-dead donors may mitigate transplant injury and improve clinical outcome.[58]

On the other hand, oxidative myocardial stress may be worsened by the observed downregulation of the production of NO and ROS in macrophages pathway which may lead to less NO bioavailability. Because generation of NO activates *aldose reductase*, less NO availability may weaken the *aldose reductase* activity which metabolizes lipid peroxidation products and protects the heart against oxidative injury. To investigate the cardioprotective properties of *aldose reductase*, Kaiserova et al. have treated the hearts of rats with NO synthase inhibitors before initiating ischemia. After reperfusion, the absence of *aldose reductase* activation was seen which resulted in the intensification of ischemia-reperfusion injury.[59]

After protein set enrichment analysis, we used uni- and multivariate analyses to investigate if donor plasma proteins may predict heart transplant outcomes such as any or severe PGD, acute rejection with hemodynamic compromise, and graft-related 1-year mortality. Interestingly, we found a couple of proteins that were in addition to any or severe PGD associated with multiple clinical endpoints. *Keratin 76* was

associated with severe PGD and acute rejection with hemodynamic compromise, *Lysine-specific demethylase 3A* with any and severe PGD, and 1- survival, *moesin* with severe PGD and 1-year survival, and *proteasome 20s subunit alpha 6* with severe PGD and acute rejection with hemodynamic compromise.

In univariate analysis of acute rejection with hemodynamic compromise, higher donor plasma levels of *CD163*, *CRP, keratin 76, myosin Va, proteasome subunit alpha type-6, proteasome activator subunit 2*, and *transaldolase 1* were correlated with acute rejection during the first month after HTx. In multivariate analysis of acute rejection with hemodynamic compromise, we found *myosin Va* and *proteasome activator subunit 2* as the best predictors for the development of acute rejection episodes.

The study by Schumacher-Bass et al. (2014) offers probably the most comprehensive analysis of the intracellular motor protein *myosin Va* which takes part in cardiac ion channel trafficking. They found that *myosin Va* mediates the cell surface trafficking of the human voltage-gated potassium channel Kv1.5 in cardiac myocytes. Activation of Kv1.5 generates the cardiac ultra-rapid delayed rectifier potassium current (IKur) which is a major repolarizing current in human atrial myocytes. Due to their central role in atrial action potential, *myosin Va* and Kv1.5 have been suggested as promising therapeutical targets to maintain atrial rhythm and treat atrial fibrillation.[60,61] Over the past years, research has highlighted that atrial fibrillation after HTx is an important determinant of clinical outcome. Early posttransplant atrial fibrillation was shown to be associated with acute rejection and increased mortality, especially in recipients receiving heart transplants from donors with older age.[62,63,64,65] In 2021, Darche et al. included 639 heart recipients in a study at Heidelberg Heart Center to analyze the association between atrial fibrillation before HTx and 1-month after HTx. They found

that atrial fibrillation before HTx is a central risk factor for posttransplant atrial fibrillation, permanent pacemaker implantation, and mortality after HTx.[66] We hypothesize that heart transplants from donors with elevated *myosin Va* levels may be more prone to pre- and posttransplant atrial fibrillation and ultimately to acute rejection. However, in our study we have not collected the data about the occurrence of atrial fibrillation. If our hypothesis can be proven by future studies, we suggest that heart transplants with high *myosin Va* levels may be possibly treated with either established antiarrhythmic drugs such as amiodarone or so far non-established drugs such as peptide inhibitors to minimize the risk of development of atrial fibrillation.[67,68]

Proteasome activator subunit 2 is a proteasome activator (PA28) subunit that activates the circulating 20s proteasome. Faries et al. took vascular biopsies from 70 patients to study the effects of proteasome activation on the human vascular system. They have been able to show that abnormal proteasome activation enhances intimal hyperplasia which represents the early stage of atherosclerosis.[69] When comparing intimal hyperplasia and atherosclerosis in non-transplant patients with acute graft rejection and cardiac vascular vasculopathy in transplant patients, it appears that their pathophysiology is based on initial endothelial response to injury. In HTx, alloimmune-responses cause a severely injured and dysfunctional endothelium which is a key contributor to acute and long-term graft failure. The injury of microvascular endothelial cells causes permeability dysfunction, hemorrhage, and thrombosis which precede ischemic graft damage, acute rejection, or fibrosis. The injury of macrovascular endothelial cells alters endothelial permeability which stimulates vascular smooth muscle cell-mediated intimal hyperplasia and vasodilatory dysfunction.[70] Intimal hyperplasia can be seen as a precursor of cardiac allograft vasculopathy, a particular

type of coronary atherosclerosis that represents the most common cause of late graft failure.[71]

Next, we investigated if the individual risk of brain-dead donors for acute rejection with hemodynamic compromise can be detected by a donor plasma proteomic immunological risk score. Our results showed that the individual risk increases depending on how many of the 7 proteins were increasingly expressed. On this basis, we conclude that the risk score may be used for pre-transplant risk assessment and management of the therapy regimen.

In univariate Cox regression analysis of graft-related 1-year mortality, higher donor plasma levels of *lysine-specific demethylase 3A* and *moesin* were related to a higher risk of mortality. An animal study by Zhang et al. investigated the central regulators of pathological myocardial fibrosis. It was shown that *lysine-specific demethylase 3A* controls myocardial fibrosis, and thus it has been discussed as a novel pharmacological target to treat fibrosis and cardiac hypertrophy.[72] *Moesin* is primarily expressed in vascular endothelial cells and promotes endothelial hyperpermeability and vascular inflammation. In the question of the clinical utility of *moesin* as a biomarker, Chen et al. found that increased *moesin* levels were associated with microvascular injury in septic patients and suggested *moesin* as a novel biomarker for the evaluation of sepsis severity.[73] Yamani et al. examined the progression of coronary vasculopathy in 140 heart transplant patients within 1-year after HTx by intravascular ultrasound. They found that pretransplant myocardial ischemia injury triggers early fibrosis and that early fibrosis is associated with the early development of coronary allograft vasculopathy after HTx.[74] Together, our findings lead to a similar conclusion where high expression of *lysine-specific demethylase 3A* and *moesin* in brain-dead

organ donors may be closely linked to the occurrence of microvascular injury, myocardial fibrosis, and cardiac allograft vasculopathy by which they may indicate a worse transplant quality.

Our data show that single donor plasma proteins, enriched biological pathways as well as pathogenic mechanisms play a pivotal role in the pathophysiology of brain death-induced heart transplant injury which affects the risk of later transplant complications. We filtered a panel of donor plasma proteins which may be promising liquid biomarker candidates to assess the risk of individual heart transplants. In future clinical practice, minimally invasive peripheral plasma samples could be taken from organ donors immediately after declaration of brain death. The proteomics-derived biomarker profile could be analyzed in vitro by LC-MS/MS for real-time assessment of heart transplant's individual risk of acute rejection with hemodynamic compromise, PGD, and mortality. Once the individual heart transplant risk is assessed, medical treatment could be adjusted during donor management, organ retrieval, organ preservation, heart transplantation, and post-transplant follow-up. For example, if a brain-dead organ donor shows a suspicious protein biomarker profile predicting a high risk of development of PGD, enhanced hormonal replacement therapy with thyroid hormones and high-dose steroids could be administered to the donor to protect against PGD.[75,76,77] Furthermore, insulin could be given to maintain normoglycemia and reduce the inflammatory response in brain-dead organ donors.[78,79] After retrieval of the donor organ, the fastest possible transport, in case of long travel distances with an ambulance jet or helicopter, should be chosen to minimize the ischemic time.[80] During heart transplantation, the cardiopulmonary bypass time should be as short as possible to mitigate PGD-associated ischemic injury.[81] In addition to the use of protein biomarker signatures in brain-dead donor assessment, cardiac troponin

measurements in recipients could be used to monitor the remaining risk of the development of PGD. In our study, heart recipients with any and severe PGD showed significantly higher hsTnI and hsTnT levels at 6, 12, and 24 hours after transplantation. Our observation is supported by a recently published study on the potential role of elevated troponin levels in the risk of the development of PGD.[82]

As shown in this discovery study, LC-MS/MS can be used to find plasma protein panels that may be successfully implemented in future clinical practice. LC-MS is becoming increasingly popular in clinical practice, having previously been used primarily in clinical research. Today LC-MS/MS is already an established tool in clinical practice for in vitro diagnostics. Dried blood spots are analyzed for therapeutic drug monitoring during the treatment with immunosuppressive drugs after solid organ transplantation or newborns are screened for metabolic disorders.[83,84] However, the LC-MS/MS analysis workflow of a whole blood sample still requires numerous manual steps, and thus more technical advances are needed to run the LC-MS/MS in an increasingly fully automated and faster manner.[85]

Despite its relatively small sample size and single-center approach, we consider this study meaningful. The size of the brain-dead organ group is naturally small due to the overall rather small number of HTx performed in Finland. However, all HTx in Finland are performed at the Helsinki University Hospital and therefore our sample size covers Finland representatively.

In conclusion, we present the plasma proteome signature of brain-dead organ donors using an open-label proteomic approach. We show that brain death alters plasma protein expression and characterize these changes in a systems biology approach.

Our results elucidate the complex unphysiological state of brain-dead organ donors and highlight key proteins that may play a vital role in altered biological mechanisms and pathways of brain-dead organ donors. Several of those proteins and biological processes are associated with the clinical outcome after HTx. Our results cast a new light on the potential of donor plasma proteome in biomarker discovery research. Further research on the effects of the proteins, the potential of novel treatment targets, and the utility of proposed biomarker candidates in acute rejection with hemodynamic compromise, PGD, and 1-year mortality is needed.

While this study successfully elucidates the proteomic signature of brain-dead heart organ donors in Finland, the plasma proteome of our heart donors may partly differ from the heart donor proteome in other world regions for two reasons. Firstly, our heart donor group consists of “high-quality” donors as donors with high age, low ejection fraction, severe left ventricular hypertrophy, and high-dose inotropic treatment were excluded from the study. Therefore, our preselected donor group may not include those donors who are increasingly considered and used as suboptimal donors in other transplantation cohorts.[86] Secondly, our donor group is characterized by the genetic homogeneity of the Finnish population. Therefore, we suggest international multi-center studies with more heterogeneous donor cohorts to compare the results of a Finnish cohort with HTx cohorts in other countries. Furthermore, further studies with larger sample sizes are necessary to validate and test suggested biomarker candidates before aiming for a successful clinical implementation in the future.

Nevertheless, our results suggest that plasma proteome analysis may improve the outcome of HTx.

5. REFERENCES

[1] Galeone A, Lebreton G, Coutance G, et al. A single-center long-term experience with marginal donor utilization for heart transplantation. *Clin Transplant* 2020; **34**(11): e14057. doi:10.1111/ctr.14057

[2] Global Observatory on Donation and Transplantation. Total number of total heart transplantations globally in year 2021. Available from: http://www.transplant-observatory.org/data-charts-and-tables/chart/ (last accessed on 19.06.2022)

[3] Scandiatransplant. Transplantation and donation figures 2021. Available from: http://www.scandiatransplant.org/data/sctp_figures_2021_4Q.pdf (last accessed on 19.06.2022)

[4] Bundeszentrale für gesundheitliche Aufklärung (BZgA). Die Herztransplantation. Available from: https://www.organspende-info.de/organspende/transplantierbare-organe/herztransplantation/ (last accessed on 22.09.2022)

[5] Mayer CL, Huber BR, Peskind E. Traumatic brain injury, neuroinflammation, and post-traumatic headaches. *Headache* 2013; **53**(9): 1523-30. doi:10.1111/head.12173

[6] Anthony DC, Couch Y, Losey P, Evans MC. The systemic response to brain injury and disease. *Brain Behav Immun* 2012; **26**(4): 534-40. doi: 10.1016/j.bbi.2011.10.011

[7] Freeman WD, Wadei HM. A brain-kidney connection: the delicate interplay of brain and kidney physiology. *Neurocrit Care* 2015; **22**(2): 173-5. doi:10.1007/s12028-015-0119-8

[8] Watts RP, Thom O, Fraser JF. Inflammatory signalling associated with brain dead organ donation: from brain injury to brain stem death and posttransplant ischaemia reperfusion injury. *J Transplant* 2013; **2013**: 521369. doi:10.1155/2013/521369

[9] Vorlat A, Conraads VM, Jorens PG, et al. Donor B-type natriuretic peptide predicts early cardiac performance after heart transplantation. *J Heart Lung Transplant* 2012; **31**(6): 579-84. doi: 10.1016/j.healun.2012.02.009

[10] Madan S, Saeed O, Shin J, et al. Donor Troponin and Survival After Cardiac Transplantation: An Analysis of the United Network of Organ Sharing Registry. *Circ Heart Fail* 2016; **9**(6). doi: 10.1161/CIRCHEARTFAILURE.115.002909

[11] Deuse T, Haddad F, Pham M, et al. Twenty-year survivors of heart transplantation at Stanford University. *Am J Transplant* 2008; **8**(9): 1769-1774. doi:10.1111/j.1600-6143.2008.02310.x

[12] Squiers JJ, DiMaio JM, Van Zyl J, et al. Long-term outcomes of patients with primary graft dysfunction after cardiac transplantation. *Eur J Cardiothorac Surg* 2021; **60**(5): 1178-1183. doi:10.1093/ejcts/ezab177

[13] Avtaar Singh SS, Banner NR, Rushton S, Simon AR, Berry C, Al-Attar N. ISHLT Primary Graft Dysfunction Incidence, Risk Factors, and Outcome: A UK National Study. *Transplantation* 2019; **103**(2): 336-343. doi:10.1097/TP.0000000000002220

[14] Lund LH, Edwards LB, Kucheryavaya AY, et al. The Registry of the International Society for Heart and Lung Transplantation: Thirty-second Official Adult Heart Transplantation Report--2015; Focus Theme: Early Graft Failure. *J Heart Lung Transplant* 2015; **34**(10): 1244-1254. doi: 10.1016/j.healun.2015.08.003

[15] Avtaar Singh SS, Banner NR, Rushton S, Simon AR, Berry C, Al-Attar N. ISHLT Primary Graft Dysfunction Incidence, Risk Factors, and Outcome: A UK National Study. *Transplantation* 2019; **103**(2): 336-343. doi:10.1097/TP.0000000000002220

[16] Dronavalli VB, Rogers CA, Banner NR. Primary Cardiac Allograft Dysfunction-Validation of a Clinical Definition. *Transplantation* 2015; **99**(9): 1919-25. doi:10.1097/TP.0000000000000620

[17] Kobashigawa J, Zuckermann A, Macdonald P, et al. Report from a consensus conference on primary graft dysfunction after cardiac transplantation. *J Heart Lung Transplant* 2014; **33**(4): 327-40. doi: 10.1016/j.healun.2014.02.027

[18] Segovia J, Cosio MD, Barcelo JM, et al. RADIAL: a novel primary graft failure risk score in heart transplantation. *J Heart Lung Transplant* 2011; **30**(6): 644-51. doi: 0.1016/j.healun.2011.01.721

[19] Yamani MH, Lauer MS, Starling RC, et al. Impact of donor spontaneous intracranial hemorrhage on outcome after heart transplantation. *Am J Transplant* 2004; **4**(2): 257-61. doi:10.1046/j.1600-6143.2003.00314.x

[20] Guisado Rasco A, Sobrino Marquez JM, Nevado Portero J, et al. Impact of overweight on survival and primary graft failure after heart transplantation. *Transplant Proc* 2010; **42**(8): 3178-80. doi: 10.1016/j.transproceed.2010.05.139

[21] Russo MJ, Iribarne A, Hong KN, et al. Factors associated with primary graft failure after heart transplantation. *Transplantation* 2010; **90**(4): 444-50. Doi: 10.1097/TP.0b013e3181e6f1eb

[22] Young JB, Hauptman PJ, Naftel DC, et al. Determinants of early graft failure following cardiac transplantation, a 10-year, multi-institutional, multivariable analysis. *J Heart Lung Transplant* 2001; **20**(2): 212. doi: 10.1016/s1053-2498(00)00460-5

[23] Singh SSA, Dalzell JR, Berry C, Al-Attar N. Primary graft dysfunction after heart transplantation: a thorn amongst the roses. *Heart Fail Rev* 2019; **24**(5): 805-20. doi: 10.1007/s10741-019-09794-1

[24] Khush KK, Potena L, Cherikh WS, et al. The International Thoracic Organ Transplant Registry of the International Society for Heart and Lung Transplantation: 37th adult heart transplantation report-2020; focus on deceased donor characteristics. *J Heart Lung Transplant* 2020; **39**(10): 1003-15. doi: 10.1016/j.healun.2020.07.010

[25] Galeone A, Lebreton G, Coutance G, et al. A single-center long-term experience with marginal donor utilization for heart transplantation. *Clin Transplant* 2020; **34**(11): e14057. doi: 10.1111/ctr.1405

[26] Lund LH, Khush KK, Cherikh WS, et al. The Registry of the International Society for Heart and Lung Transplantation: Thirty-fourth Adult Heart Transplantation Report-2017; Focus Theme: Allograft ischemic time. *J Heart Lung Transplant* 2017; **36**(10): 1037-46. doi: 10.1016/j.healun.2017.07.019

[27] Bergenfeldt H, Stehlik J, Hoglund P, Andersson B, Nilsson J. Donor-recipient size matching and mortality in heart transplantation: Influence of body mass index and gender. *J Heart Lung Transplant* 2017; **36**(9): 940-7. doi: 10.1016/j.healun.2017.02.002

[28] Gao HZ, Hunt SA, Alderman EL, Liang D, Yeung AC, Schroeder JS. Relation of donor age and preexisting coronary artery disease on angiography and intracoronary ultrasound to later development of accelerated allograft coronary artery disease. *J Am Coll Cardiol* 1997; **29**(3): 623-9. doi: 10.1016/s0735-1097(96)00521-9 96)00521-9

[29] Newman J, Liebo M, Lowes BD, et al. The effect of donor alcohol abuse on outcomes following heart transplantation. *Clin Transplant* 2019; **33**(2): e13461. doi: 10.1111/ctr.13461

[30] Peled Y, Lavee J, Arad M, et al. The impact of gender mismatching on early and late outcomes following heart transplantation. *ESC Heart Fail* 2017; **4**(1): 31-9. doi: 10.1002/ehf2.12107

[31] Iyer A, Kumarasinghe G, Hicks M, et al. Primary graft failure after heart transplantation. *J Transplant* 2011; **2011**: 175768. doi: 10.1155/2011/175768

[32] Galeone A, Lebreton G, Coutance G, et al. A single-center long-term experience with marginal donor utilization for heart transplantation. *Clin Transplant* 2020; **34**(11): e14057. doi: 10.1111/ctr.1405

[33] Bontha SV, Maluf DG, Mueller TF, Mas VR. Systems Biology in Kidney Transplantation: The Application of Multi-Omics to a Complex Model. *Am J Transplant* 2017; **17**(1): 11-21. doi: 10.1111/ajt.13881

[34] Lukac J, Dhaygude K, Saraswat M, et al. Plasma proteome of brain-dead organ donors predicts heart transplant outcome. *J Heart Lung Transplant* 2022; **41**(3): 311-24. doi: 10.1016/j.healun.2021.11.011

[35] Nykanen AI, Holmstrom EJ, Tuuminen R, et al. Donor Simvastatin Treatment in Heart Transplantation. *Circulation* 2019; **140**(8): 627-40. doi: 10.1161/CIRCULATIONAHA.119.039932

[36] Zaroff JG, Rosengard BR, Armstrong WF, et al. Consensus conference report: maximizing use of organs recovered from the cadaver donor: cardiac recommendations, March 28-29, 2001, Crystal City, Va. *Circulation* 2002; **106**(7): 836-41. doi: 10.1161/01.cir.0000025587.40373.75

[37] Holm M, Joenväärä S, Saraswat M, et al. Plasma protein expression differs between colorectal cancer patients depending on primary tumor location. *Cancer Med* 2020; **9**(14):5221-5234. doi:10.1002/cam4.3178

[38] Zaroff JG, Rosengard BR, Armstrong WF, et al. Consensus conference report: maximizing use of organs recovered from the cadaver donor: cardiac recommendations, March 28-29, 2001, Crystal City, Va. *Circulation* 2002; **106**(7): 836-41. doi: 10.1161/01.cir.0000025587.40373.75

[39] Rylski B, Berchtold-Herz M, Olschewski M, et al. Reducing the ischemic time of donor hearts will decrease morbidity and costs of cardiac transplantations. *Interact Cardiovasc Thorac Surg* 2010; **10**(6): 945-7. doi: 10.1510/icvts.2009.223719

[40] Liu Z, Perry LA, Penny-Dimri JC, et al. Prognostic Significance of Elevated Troponin in Adult Heart Transplant Recipients: A Systematic Review and Meta-Analysis. *Exp Clin Transplant* 2022. doi: 10.6002/ect.2021.0386

[41] Foley JH, Conway EM. Cross Talk Pathways Between Coagulation and Inflammation. *Circ Res* 2016; **118**(9): 1392-1408. doi: 10.1161/CIRCRESAHA.116.306853

[42] Amara U, Flierl MA, Rittirsch D, et al. Molecular intercommunication between the complement and coagulation systems. *J Immunol* 2010; **185**(9):5628-5636. doi: 10.4049/jimmunol.0903678

[43] Atkinson C, Floerchinger B, Qiao F, et al. Donor brain death exacerbates complement-dependent ischemia/reperfusion injury in transplanted hearts. *Circulation* 2013; **127**(12): 1290-9. doi: 10.1161/CIRCULATIONAHA.112.000784

[44] Labarrere CA, Torry RJ, Nelson DR, et al. Vascular antithrombin and clinical outcome in heart transplant patients. *Am J Cardiol* 2001; **87**(4): 425-31. doi: 0.1016/s0002-9149(00)01395-3

[45] A-Gonzalez N, Bensinger SJ, Hong C, et al. Apoptotic cells promote their own clearance and immune tolerance through activation of the nuclear receptor LXR. *Immunity* 2009; **31**(2): 245-258. doi: 10.1016/j.immuni.2009.06.018

[46] Lei P, Baysa A, Nebb HI, et al. Activation of Liver X receptors in the heart leads to accumulation of intracellular lipids and attenuation of ischemia-reperfusion injury. *Basic Res Cardiol* 2013; **108**(1): 323. doi: 10.1007/s00395-012-0323-z

[47] Xu XR, Wang Y, Adili R, et al. Apolipoprotein A-IV binds alphaIIbbeta3 integrin and inhibits thrombosis. *Nat Commun* 2018; **9**(1): 3608. doi: 10.1038/s41467-018-05806-0

[48] Weidmann H, Heikaus L, Long AT, Naudin C, Schlüter H, Renné T. The plasma contact system, a protease cascade at the nexus of inflammation, coagulation and immunity. *Biochim Biophys Acta Mol Cell Res* 2017; **1864**(11 Pt B): 2118-2127. doi: 10.1016/j.bbamcr.2017.07.009

[49] Lopatko Fagerstrom I, Stahl AL, Mossberg M, et al. Blockade of the kallikrein-kinin system reduces endothelial complement activation in vascular inflammation. *EBioMedicine* 2019; **47**: 319-28. doi: 10.1016/j.ebiom.2019.08.020

[50] Giangreco NP, Lebreton G, Restaino S, et al. Plasma kallikrein predicts primary graft dysfunction after heart transplant. *J Heart Lung Transplant* 2021; **40**(10): 1199-211. 10.1016/j.healun.2021.07.001

[51] Garcia-Heredia A, Marsillach J, Rull A, et al. Paraoxonase-1 inhibits oxidized low-density lipoprotein-induced metabolic alterations and apoptosis in endothelial cells: a nondirected metabolomic study. *Mediators Inflamm* 2013; **2013**: 156053. doi: 10.1155/2013/156053

[52] Opie LH. Myocardial ischemia--metabolic pathways and implications of increased glycolysis. *Cardiovasc Drugs Ther* 1990; **4** Suppl 4: 777-90. doi: 10.1007/BF00051275

[53] Lee L, Horowitz J, Frenneaux M. Metabolic manipulation in ischaemic heart disease, a novel approach to treatment. *Eur Heart J* 2004; **25**(8): 634-41. doi: 10.1016/j.ehj.2004.02.018

[54] Wende AR, Brahma MK, McGinnis GR, Young ME. Metabolic Origins of Heart Failure. *JACC Basic Transl Sci* 2017; **2**(3): 297-310. doi: 10.1016/j.jacbts.2016.11.009

[55] Masson F, Thicoipe M, Gin H, et al. The endocrine pancreas in brain-dead donors. A prospective study in 25 patients. *Transplantation* 1993; **56**(2): 363-7. doi: 10.1097/00007890-199308000-00022

[56] Aljiffry M, Hassanain M, Schricker T, et al. Effect of Insulin Therapy using Hyper-insulinemic Normoglycemic Clamp on Inflammatory Response in Brain Dead Organ Donors. *Exp Clin Endocrinol Diabetes* 2016; **124**(5): 318-323. doi: 10.1055/s-0042-101240

[57] Ranasinghe AM, McCabe CJ, Quinn DW, et al. How does glucose insulin potassium improve hemodynamic performance? Evidence for altered expression of beta-

adrenoreceptor and calcium handling genes. *Circulation* 2006; **114**(1 Suppl): I239-I244. doi: 10.1161/CIRCULATIONAHA.105.000760

[58] Aljiffry M, Hassanain M, Schricker T, et al. Effect of Insulin Therapy using Hyperinsulinemic Normoglycemic Clamp on Inflammatory Response in Brain Dead Organ Donors. *Exp Clin Endocrinol Diabetes* 2016; **124**(5): 318-323. doi: 10.1055/s-0042-101240

[59] Kaiserova K, Tang XL, Srivastava S, Bhatnagar A. Role of nitric oxide in regulating aldose reductase activation in the ischemic heart. *J Biol Chem* 2008; **283**(14): 9101-12. doi: 10.1074/jbc.M709671200

[60] Schumacher-Bass SM, Vesely ED, Zhang L, et al. Role for myosin-V motor proteins in the selective delivery of Kv channel isoforms to the membrane surface of cardiac myocytes. *Circ Res* 2014; **114**(6): 982-92. doi: 10.1161/CIRCRESAHA.114.302711

[61] Borrego J, Feher A, Jost N, Panyi G, Varga Z, Papp F. Peptide Inhibitors of Kv1.5: An Option for the Treatment of Atrial Fibrillation. *Pharmaceuticals (Basel)* 2021; **14**(12). doi: 10.3390/ph14121303

[62] Cui G, Tung T, Kobashigawa J, Laks H, Sen L. Increased incidence of atrial flutter associated with the rejection of heart transplantation. *Am J Cardiol* 2001; **88**(3): 280-4. doi: 10.1016/s0002-9149(01)01641-1

[63] Cohn WE, Gregoric ID, Radovancevic B, Wolf RK, Frazier OH. Atrial fibrillation after cardiac transplantation: experience in 498 consecutive cases. *Ann Thorac Surg* 2008; **85**(1): 56-8. doi: 10.1016/j.athoracsur.2007.07.037

[64] Chokesuwattanaskul R, Bathini T, Thongprayoon C, et al. Atrial fibrillation following heart transplantation: A systematic review and meta-analysis of observational studies. *J Evid Based Med* 2018; **11**(4): 261-71. doi: 10.1111/jebm.12323

[65] Ferretto S, Giuliani I, Sanavia T, et al. Atrial fibrillation after orthotopic heart transplantation: Pathophysiology and clinical impact. *Int J Cardiol Heart Vasc* 2021; **32**: 100710. doi: 10.1016/j.ijcha.2020.100710

[66] Darche, Fabrice F et al. Atrial fibrillation before heart transplantation is a risk factor for post-transplant atrial fibrillation and mortality. *ESC heart failure* 2021; **8** (5): 4265-4277. doi: 10.1002/ehf2.13552

[67] Thajudeen A, Stecker EC, Shehata M, et al. Arrhythmias after heart transplantation: mechanisms and management. *J Am Heart Assoc* 2012; **1**(2): e001461. doi: 10.1161/JAHA.112.001461

[68] Borrego J, Feher A, Jost N, Panyi G, Varga Z, Papp F. Peptide Inhibitors of Kv1.5: An Option for the Treatment of Atrial Fibrillation. *Pharmaceuticals (Basel)* 2021; **14**(12). doi: 10.3390/ph14121303

[69] Faries PL, Rohan DI, Wyers MC, et al. Relationship of the 20S proteasome and the proteasome activator PA28 to atherosclerosis and intimal hyperplasia in the human vascular system. *Ann Vasc Surg* 2001;**15**(6): 628-633. doi: 10.1007/s10016-001-0055-2

[70] von Rossum A, Laher I, Choy JC. Immune-mediated vascular injury and dysfunction in transplant arteriosclerosis. *Front Immunol* 2014; **5**: 684. doi: 10.3389/fimmu.2014.00684

[71] Rahmani M, Cruz RP, Granville DJ, McManus BM. Allograft vasculopathy versus atherosclerosis. *Circ Res* 2006; **99**(8): 801-15. doi: 10.1161/01.RES.0000246086.93555.f3

[72] Zhang QJ, Tran TAT, Wang M, et al. Histone lysine dimethyl-demethylase KDM3A controls pathological cardiac hypertrophy and fibrosis. *Nat Commun* 2018; **9**(1): 5230. doi: 10.1038/s41467-018-07173-2

[73] Chen Y, Wang J, Zhang L, Zhu J, Zeng Y, Huang JA. Moesin Is a Novel Biomarker of Endothelial Injury in Sepsis. *J Immunol Res* 2021; **2021**: 6695679. doi: 10.1155/2021/6695679

[74] Yamani MH, Haji SA, Starling RC, et al. Myocardial ischemic-fibrotic injury after human heart transplantation is associated with increased progression of vasculopathy, decreased cellular rejection and poor long-term outcome. *J Am Coll Cardiol* 2002; **39**(6):970-977. doi: 10.1016/s0735-1097(02)01714-x

[75] Zaroff JG, Rosengard BR, Armstrong WF, et al. Consensus conference report: maximizing use of organs recovered from the cadaver donor: cardiac recommendations, March 28-29, 2001, Crystal City, Va. *Circulation* 2002; **106**(7): 836-41. doi: 10.1161/01.cir.0000025587.40373.75

[76] Novitzky D, Cooper DK, Rosendale JD, Kauffman HM. Hormonal therapy of the brain-dead organ donor: experimental and clinical studies. *Transplantation* 2006; **82**(11): 1396-401. doi: 10.1097/01.tp.0000237195.12342.f1

[77] Nagy A, Szecsi B, Eke C, et al. Endocrine Management and Hormone Replacement Therapy in Cardiac Donor Management: A Retrospective Observational Study. Transplant Proc 2021; **53**(10): 2807-15. doi: 10.1016/j.transproceed.2021.08.048

[78] Wood KE, Becker BN, McCartney JG, D'Alessandro AM, Coursin DB. Care of the potential organ donor. *N Engl J Med* 2004; **351**(26): 2730-9. doi: 10.1056/NEJMra013103

[79] Aljiffry M, Hassanain M, Schricker T, et al. Effect of Insulin Therapy using Hyper-insulinemic Normoglycemic Clamp on Inflammatory Response in Brain Dead Organ Donors. *Exp Clin Endocrinol Diabetes* 2016; **124**(5): 318-323. doi: 10.1055/s-0042-101240

[80] Rylski B, Berchtold-Herz M, Olschewski M, et al. Reducing the ischemic time of donor hearts will decrease morbidity and costs of cardiac transplantations. *Interact Cardiovasc Thorac Surg* 2010; **10**(6): 945-7. doi: 10.1510/icvts.2009.223719

[81] Singh SSA, Dalzell JR, Berry C, Al-Attar N. Primary graft dysfunction after heart transplantation: a thorn amongst the roses. *Heart Fail Rev* 2019; **24**(5): 805-20. doi: 10.1007/s10741-019-09794-1

[82] Liu Z, Perry LA, Penny-Dimri JC, et al. Prognostic Significance of Elevated Troponin in Adult Heart Transplant Recipients: A Systematic Review and Meta-Analysis. *Exp Clin Transplant* 2022. doi: 10.6002/ect.2021.0386

[83] Banerjee S. Empowering Clinical Diagnostics with Mass Spectrometry. *ACS Omega* 2020; **5**(5): 2041-8. doi: 10.1021/acsomega.9b03764

[84] Ombrone D, Giocaliere E, Forni G, Malvagia S, la Marca G. Expanded newborn screening by mass spectrometry: New tests, future perspectives. *Mass Spectrom Rev* 2016; **35**(1): 71-84. doi: 10.1002/mas.21463

[85] Zhang YV, Rockwood A. Impact of automation on mass spectrometry. *Clin Chim Acta* 2015; **450**: 298-303. doi: 10.1016/j.cca.2015.08.027

[86] Khush KK. Donor selection in the modern era. *Ann Cardiothorac Surg* 2018; **7**(1): 126-34. doi: 10.21037/acs.2017.09.09

6. APPENDIX

6.1 FIGURES

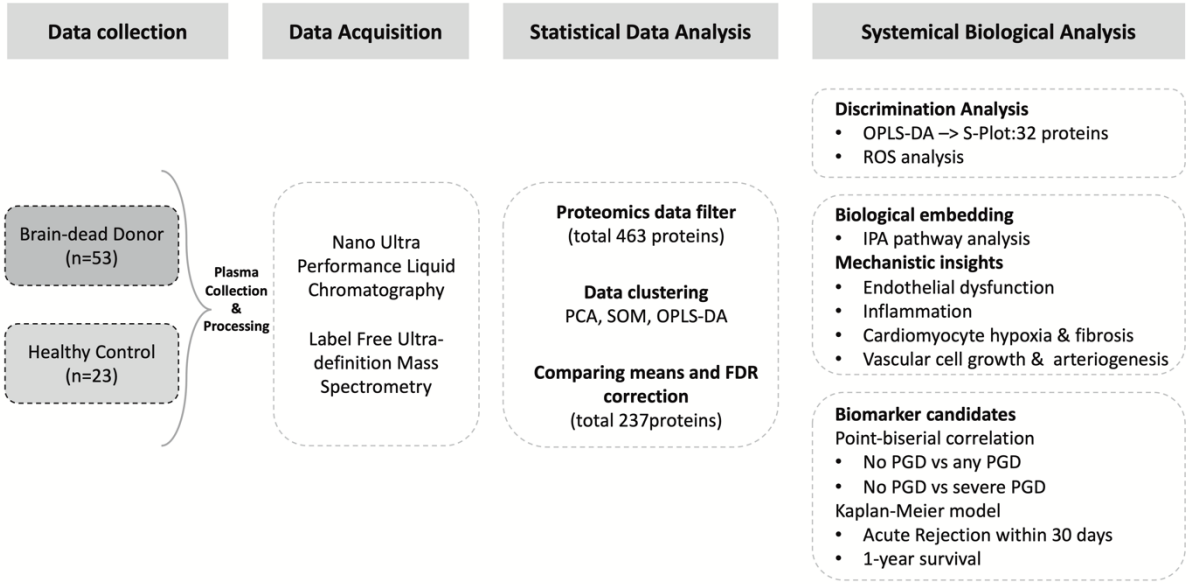

Figure 1. Flow chart of the study

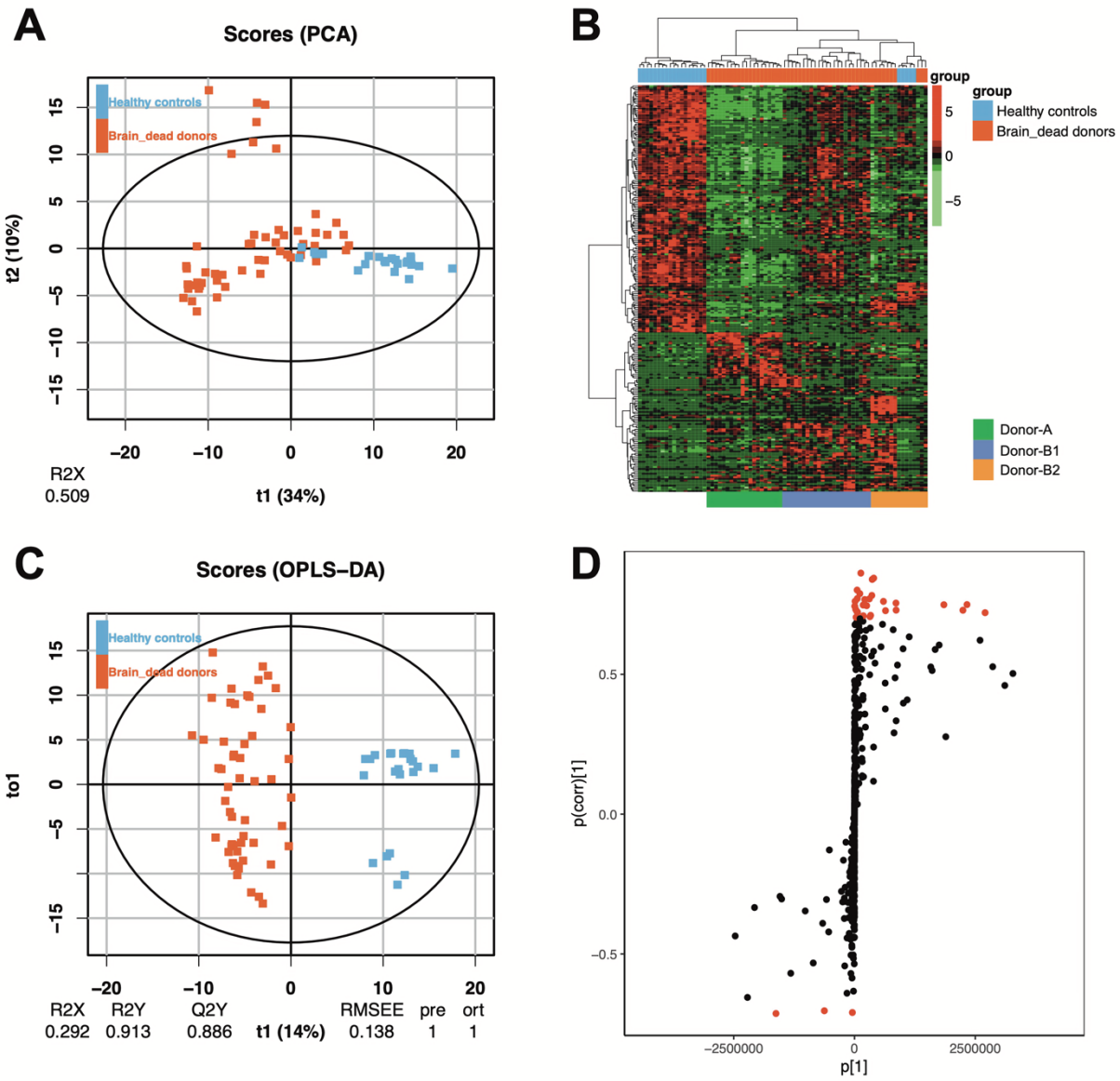

Figure 2. Comparison of differentially expressed plasma proteins between brain-dead donors and healthy controls.

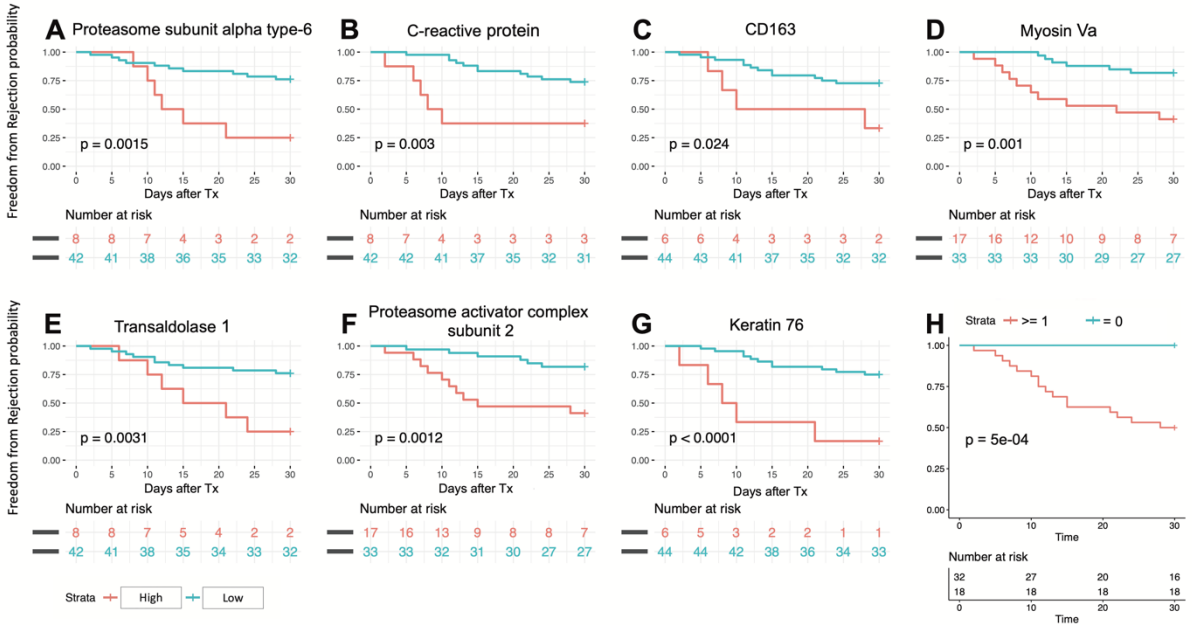

Figure 3. Impact of donor plasma protein levels on the development of acute rejection with hemodynamic compromise within the first 30 days after heart transplantation.

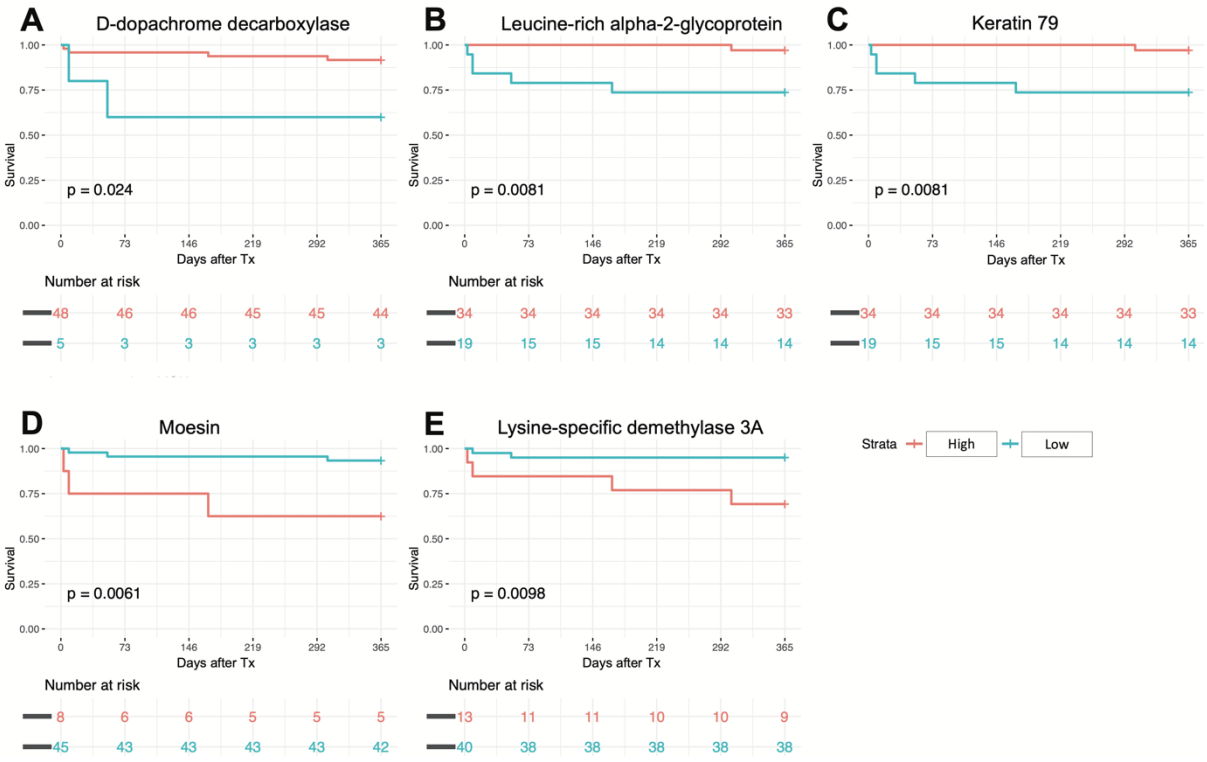

Figure 4. Impact of donor plasma protein levels on graft-related 1-year survival after heart transplantation.

6.2 TABLES

Table 1. Clinical characteristics of brain-dead heart transplant donors and allocation of other solid organs based on different donor plasma proteome profiles.

Donor characteristics	**All donors (N=53)**	**Donor A (N=20)**	**Donor B (N=33)**	**Donor B1 (N=26)**	**Donor B2 (N=7)**
Age, y	44 (33-51)	44 (35-52)	43 (33-50)	44 (34.5-50)	43 (27-49.5)
Female sex, No. (%)	10 (18.9)	2 (10)	8 (24.2)	5 (19.2)	3 (42.9)
Body mass index, kg/m^2	25.2±4.8	24.3±6.2	25.7±3.7	25.7±3.9	25.8±3.2
Simvastatin treatment, No. (%)	27 (51)	13 (65)	14 (42.4)	13 (50)	1 (14.3)
Previous medical history† , No. (%)					
Hypertension	6 (11)	**0 (0)***	6 (18.2)	6 (23.1)	0 (0)
Smokin, No. (%)					
Current	23 (43)	8 (40)	15 (45.5)	10 (38.5)	5 (71.4)
Former	4 (8)	3 (15)	1 (3)	1 (3.8)	0 (0.0)

Donor characteristics	All donors (N=53)	Donor A (N=20)	Donor B (N=33)	Donor B1 (N=26)	Donor B2 (N=7)
Never	15 (28)	4 (20)	11 (33.3)	10 (38.5)	1 (14.3)
Unknown	11 (21)	5 (25)	6 (18.2)	5 (19.2)	1 (14.3)
CMV-positive, No. (%)	44 (83)	16 (80)	28 (84.8)	21 (80.8)	7 (100)
Cause of brain death, No. (%)					
Intracranial hemorrhage	26 (49.1)	10 (50)	16 (48.5)	11 (42.3)	5 (71.4)
Traumatic brain injury	19 (35.8)	5 (25)	14 (42.4)	12 (46.2)	2 (28.6)
Cerebral infarction	6 (11.3)	**5 (25)***	1 (3)	1 (3.8)	0 (0.0)
Other	2 (3.8)	0 (0.0)	2 (6.1)	2 (7.7)	0 (0.0)
P-troponin I, ng/l	47 (9-207)	38 (8-88)	76 (14-293)	78 (14-286)	27 (6-250)
P-troponin T, ng/l	21 (9-55)	16 (9-33)	25 (11-67)	27 (10-90)	20 (14-60)
Hemoglobin, g/L	121±23	117±26	124±20	126±22	116±14
CRP, mg/L	43 (12-122)	95 (27.8-177)	31 (9-89)	34 (9.8-89.8)	21 (10-43.5)
Thrombocytes, E9/L	186±80	171±62	196±89	208±89	**111±13*****
Total P-cholesterol, mmol/l	2.72±0.94	2.76±0.89	2.68±0.98	2.93±0.93	1.87±0.7
P-HDL, mmol/l	1±0.37	0.97±0.38	0.91±0.37	0.95±0.37	0.76±0.37
P-LDL, mmol/l	1.23±0.72	1.20±0.73	1.24±0.73	1.40±0.73	**0.71±0.41***
P-triglycerides, mmol/l	0.86±0.5 1	1.02±0.58	0.79±0.44	0.82±0.47	0.59±0.27

Donor characteristics	All donors (N=53)	Donor A (N=20)	Donor B (N=33)	Donor B1 (N=26)	Donor B2 (N=7)
Echocardiogram					
Left ventricle ejection fraction, %	62 (59-65)	61 (60-65)	62 (58-66)	63 (58-66)	61 (60-65)
Presence of regional wall motion abnormality, No. (%)	6 (11)	2 (10)	4 (12.1)	2 (7.7)	2 (28.6)
Diastolic posterior wall thickness, mm	11 (9-12)	10.5 (10-11)	11 (10-13)	11 (10-13)	9.7 (9-10)
Diastolic septum thickness, mm	11 (10-12)	10.75 (10-11)	11 (10-12)	11 (10-12)	10.75 (11-11)
Coronary angiography‡					
Performed, No.(%)	30 (57)	13 (65)	17 (51.5)	14 (53.8)	3 (42.9)
Abnormal finding angiography, No. (%)	6 (11)	3 (15)	3 (9.1)	3 (11.5)	0 (0.0)
Inotropic support, No. (%)	37 (70)	12 (60)	25 (75.8)	18 (69.2)	7 (100)
Resuscitation, No. (%)	9 (17)	2 (10)	7 (21.2)	7 (26.9)	0 (0.0)
Time of ROSC for resuscitated donors, min	17±13	30±0	14±12	14±12	0.0

Donor characteristics	All donors (N=53)	Donor A (N=20)	Donor B (N=33)	Donor B1 (N=26)	Donor B2 (N=7)
The time between the declaration of brain death and organ procurement, h	14.86±4	14.58±3.7	14.76±4	14.86±4	14.39±3
Organs transplanted from donors, No. (%)					
Heart	53 (100)	20 (100)	33 (100)	26 (100)	7 (100)
Lung	17 (32)	6 (30)	11 (33.3)	8 (30.8)	3 (42.9)
Liver	36 (68)	12 (60)	24 (72.7)	20 (76.9)	4 (57.1)
Kidneys	86 (90.6)	29 (85)	57 (93.9)	46 (96.1)	11 (85.7)
Pancreas	31 (58)	10 (50)	21 (63.6)	16 (61.5)	5 (71.4)

Plus-minus values are mean ±SD; values with the range in parentheses are median (interquartile range). P values are marked as asterisks (*P<0.05. **P<0.01. ***P<0.001). CMV, indicates cytomegalovirus; HDL, high-density lipoprotein; LDL, low-density lipoprotein; ROSC, return of spontaneous circulation; and Tx, transplantation. †In the previous medical history of the donors there was no coronary artery disease, chronic obstructive pulmonary disease, peripheral vascular disease, previous malignancy, prior stroke, and no history of sternotomy. ‡Donor coronary angiography was performed for donors with >40 years of age, strong family history of coronary disease, or smoking.

Table 2. Effect of log2 fold change on Ingenuity Pathway Analysis of identified proteins in heart transplant donors.

Pathway (z-score =>1)	Donor vs Controls No fold change (237 proteins)	-log(p value)	Donor vs Controls Fold change ≥1 (118 proteins)	-log(p value)	Donor vs Controls Fold change ≥1.5 (66 proteins)	-log(p value)	Donor A vs. B No fold change (164 proteins)	Donor B1 vs B2 No fold change (107 proteins)	S-Plot proteins
Coagulation System	1,732	15,7	-	-	-	-	-	-	plasma kallkrein, kininogen 1, plasminogen, protein C,antithrombin-III
Complement System	-1,265	15,2	-	-	-	-	-1,265	1	complement C1q C chain,

Pathway (z-score =>1)	Donor vs Controls No fold change (237 proteins)	-log(p value)	Donor vs Controls Fold change ≥1 (118 proteins)	-log(p value)	Donor vs Controls Fold change ≥1.5 (66 proteins)	-log(p value)	Donor A vs. B No fold change (164 proteins)	Donor B1 vs B2 No fold change (107 proteins)	S-Plot proteins
									mannan binding lectin serine peptidase 1
Gluconeogenesis I	1,633	5,33	1,342	5,62	-	-	-2,236	-	
Glycolysis I	1,633	5,62	1,342	5,87	-	-	-2,236	-	
LXR/RXR Activation	-4,536	29,6	-0,816	4,52	-	-	-3,13	3	alpha 2-HS glycoprotein ,

Pathway (z-score =>1)	Donor vs Controls No fold change (237 proteins)	-log(p value)	Donor vs Controls Fold change ≥1 (118 proteins)	-log(p value)	Donor vs Controls Fold change ≥1.5 (66 proteins)	-log(p value)	Donor A vs. B No fold change (164 proteins)	Donor B1 vs B2 No fold change (107 proteins)	S-Plot proteins
									apolipoprotein A4, kininogen 1, paraoxonase 1
Production of Nitric Oxide and Reactive Oxygen Species in	-2,111	6,46	-	-	-	-	-2,121	-	apolipoprotein A4, paraoxonase 1

Pathway (z-score =>1)	Donor vs Controls No fold change (237 proteins)	-log(p value)	Donor vs Controls Fold change ≥1 (118 proteins)	-log(p value)	Donor vs Controls Fold change ≥1.5 (66 proteins)	-log(p value)	Donor A vs. B No fold change (164 proteins)	Donor B1 vs B2 No fold change (107 proteins)	S-Plot proteins
Macrophages									
Role of Pattern Recognition Receptors in Recognition of Bacteria	-	-	-	-	-	-	-1,342	-	complement C1q C chain

Pathway (z-score =>1)	Donor vs Controls No fold change (237 proteins)	-log(p value)	Donor vs Controls Fold change ≥1 (118 proteins)	-log(p value)	Donor vs Controls Fold change ≥1.5 (66 proteins)	-log(p value)	Donor A vs. B No fold change (164 proteins)	Donor B1 vs B2 No fold change (107 proteins)	S-Plot proteins
and Viruses									
Xenobiotic Metabolism CAR Signaling Pathway	-	-	1,633	3,63	-	-	-	-	glutathione S-transferase mu 2

In IPA pathway analysis, we considered pathways with a -log(p value) of >3.0 (p value <0.001) and a z-score of ±1 as significant. Upregulated pathways are highlighted in red and downregulated in green. S-Plot proteins enriched into specific pathways are presented.

Table 3. Clinical characteristics and outcomes of the heart transplant recipients based on different donor plasma proteome profiles.

	All donors (N=53)	**Donor A (N=20)**	**Donor B (N=33)**	**Donor B1 (N=26)**	**Donor B2 (N=7)**
Recipient characteristics					
Age, y	58 (46.5-61)	55 (46-59)	59 (49-62)	61 (49-63)	58 (48-60)
Female sex, No. (%)	13 (24.5)	3 (15)	10 (30.3)	7 (26.9)	3 (42.9)
Body mass index, kg/m^2	26±4.4	26±4.6	25.6±4.5	25.9±4.7	24.4±3.3
Previous medical history† No. (%)					
Hypertension	8 (15.1)	1 (5)	7 (21.2)	6 (23.1)	1 (14.3)
Coronary artery disease	11 (20.8)	5 (25)	6 (18.2)	4 (15.4)	2 (28.6)
Chronic obstructive pulmonary disease	2 (3.8)	0 (0.0)	2 (6.1)	2 (7.7)	0 (0.0)
Diabetes	7 (13.2)	1 (20)	6 (18.2)	5 (19.2)	1 (14.3)
Previous malignancy	5 (9.4)	1 (5)	4 (12.1)	3 (11.5)	1 (14.3)

	All donors (N=53)	Donor A (N=20)	Donor B (N=33)	Donor B1 (N=26)	Donor B2 (N=7)
Prior stroke	7 (13.2)	2 (10)	5 (15.2)	4 (15.4)	1 (14.3)
Amiodarone <6 months prior transplantation, No. (%)	14 (26.4)	4 (20)	10 (30.3)	9 (34.6)	1 (14.3)
History of sternotomy	15 (28.3)	5 (25)	10 (30.3)	7 (26.9)	3 (42.9)
Primary disease, No. (%)					
Endstage coronary disease	12 (22.6)	4 (20)	8 (24.2)	6 (23.1)	2 (28.6)
Dilatative cardiomyopathy	26 (49)	11 (55)	15 (45.5)	12 (46.2)	3 (42.9)
Congenital	4 (7.6)	2 (10)	2 (6.1)	1 (3.8)	1 (14.3)
Myocarditis	3 (5.7)	0 (0.0)	3 (9.1)	3 (11.5)	0 (0.0)
Other	8 (15.1)	3 (15)	5 (15.2)	4 (15.4)	1 (4.3)

	All donors (N=53)	Donor A (N=20)	Donor B (N=33)	Donor B1 (N=26)	Donor B2 (N=7)
Donor-recipient sex mismatch, No. (%)	6 (11.3)	4 (20)	2 (6.1)	2 (7.7)	0 (0.0)
Mechanical circulatory support prior to HTx, No. (%)	13 (24.5)	2 (10)	11 (33.3)	9 (34.6)	2 (28.6)
ECMO, No. (%)	6 (11.3)	2 (10)	4 (12.1)	4 (15.4)	0 (0.0)
LVAD, No. (%)	7 (13.2)	**0 (0.0)***	7 (21.2)	5 (19.2)	2 (28.6)
Days on waiting list	190 (41.8-352.5)	203 (49-360)	180 (28.5-330)	157 (29.3-335)	200 (68-221)
Graft ischemia, min					
Cold	97±50.1	94±50.2	98±50.8	96±47.1	106±65.8
Warm	80±20.2	86±21.4	77±19.2	77±21.4	78±8.9
Total	173±54.1	170±59.3	175±51.5	172±49.1	184±63
Organ functions before heart transplantation					
PVR, Wood units	3±1.3	2.7±1.1	3.2±1.5	3.1±1.4	3.8±1.9
TPG, mmHg	10 (7-12)	11 (10-12)	8 (7-13)	8 (7-11)	10 (6.3-13.5)

	All donors (N=53)	Donor A (N=20)	Donor B (N=33)	Donor B1 (N=26)	Donor B2 (N=7)
SPAP, mmHg	43±12.8	43±10.9	43±14.3	40±12.6	55.5±17.1
P-bilirubin, µmol/L	13 (10-19)	14 (10-22.5)	11 (9-15)	11 (9-15.8)	10 (9.5-14)
Glomerular filtration rate, mL/min per 1.73 square meters	55.7 (45-73)	51.7 (44-65.3)	57 (48-73)	56.4 (45.7-72.5)	58.3 (55.5-69.5)
NT-proBNP, ng/L	3171 (1075-5686)	3304 (2263-5208)	3100 (852-5942)	3132 (934-6146)	1982 (756-4619)
Immunosuppressive therapy, No. (%)					
Induction Therapy					
Anti-thyomocyte	21 (39.6)	10 (50)	11 (33.3)	11 (42.3)	0 (0.0)
Maintenance therapy					
Cyclosporine A	10 (18.9)	4 (20)	6 (18.2)	4 (15.4)	2 (28.6)
Tacrolismus	39 (73.6)	14 (70)	25 (75.8)	21 (80.8)	4 (57.1)
Azathioprine	2 (3.8)	1 (5)	1 (3.3)	1 (3.8)	0 (0.0)
Mycophenlic acid	46 (86.8)	16 (80)	30 (90.1)	24 (92.3)	6 (85.7)
Prednisolone	53 (100)	20 (100)	33 (100)	26 (100)	7 (100)
Recipient Outcome					

	All donors (N=53)	Donor A (N=20)	Donor B (N=33)	Donor B1 (N=26)	Donor B2 (N=7)
Intubation time, h	42 (20-125)	60 (24-111)	42 (18-180)	23 (18-183)	19 (16-63)
Time on ICU, h	216 (144-480)	204 (168-372)	216 (120-492)	264 (120-552)	168 (90-378)
Hospital length of stay, d	44±29	48±37	42±24	45±24	29±18
Inotropic support, No. (%)	47 (88.7)	19 (95)	28 (84.8)	23 (88.46)	5 (71.4)
30-day survival. No. (%)	50 (94.3)	19 (95)	31 (93.9)	25 (96.2)	6 (85.7)
1-year survival, No. (%)	46 (86.8)	18 (90)	28 (84.8)	22 (84.6)	6 (85.7)
LV-EF at 7 days	59±9.4	58±7	59±10.9	57±10.6	**69±6.3***
Primary graft dysfunction, No. (%)					
Any PGD	17 (32.1)	6 (20)	11 (33.3)	9 (34.6)	2 (28.6)
Severe PGD	6 (11.3)	2 (10)	4 (12.1)	4 (15.4)	0 (0.0)
30-day acute rejection with	16 (30.2)	5 (25)	11 (33.3)	10 (38.5)	1 (14.3)

	All donors (N=53)	Donor A (N=20)	Donor B (N=33)	Donor B1 (N=26)	Donor B2 (N=7)
hemodynamic compromise, No. (%)*					
30-day acute rejection with myocyte damage, No. (%)*	3 (5.7)	1 (5)	2 (6.1)	2 (7.7)	0 (0.0)
1-year acute rejection with hemodynamic compromise, No. (%)	20 (37.7)	7 (35)	13 (39.4)	11 (42.3)	2 (28.6)
1-year acute rejection with myocyte damage, No. (%)	8 (15.1)	3 (15)	5 (15.2)	4 (16.7)	1 (14.3)
P-troponin I, ng/l					

	All donors (N=53)	Donor A (N=20)	Donor B (N=33)	Donor B1 (N=26)	Donor B2 (N=7)
6h	86310 (40324 - 149706)	88155 (45683-162006.25)	79373 (39820 – 149187)	86957(44060-215360)	**43188 (21286-75966)****
12h	95187.5(42482-195580)	101563 (48698-181267)	91186 (41185-186515)	115680.5(4492 – 267527)	**50133 (23255-67453)****
24h	57679 (32912 - 106589)	69300 (36760-124360)	49437 (31803 – 103140)	60123 (33374-110863)	**34828 (21565-57794)***
P-troponin T, ng/l					
6h	8940 (4637-17150)	8896 (5712-14588)	8940 (4217-17150)	11665 (4830-18535)	**4153 (2818-9120) ****
12h	8460 (4399-14453)	7947 (4531 -14555)	9593 (4421 -14220)	12080 (5505-16310)	**4421 (2345-6115) ****
24h	5918 (3262-9269)	5713 (3847-9458)	6055 (2706-8425)	7563.5 (3288-9202)	**2313 (2079-4829)***
hsCRP, Mg/L					
1h	2.8 (1.9-7)	3.22 (2-7)	2.8 (1.5-6.5)	2.2 (1.6-6.7)	4.7 (1.9-5.7)
6h	5.6 (3.8-12.6)	6.8 (5-11.8)	5.5 (3.2-12.6)	5 (3.2-12.4)	6.5 (4-13.2)

	All donors (N=53)	Donor A (N=20)	Donor B (N=33)	Donor B1 (N=26)	Donor B2 (N=7)
12h	26.2 (16.2-44.8)	25.3 (15-48.6)	26.9 (19.6-43.2)	28.5 (21.6-44.6)	20 (15.5-32.8)
24h	87.1 (61.4-123.1)	99.3 (66.3-119.1)	85.5 (63.6-122.2)	96.5 (77.8-126.6)	**63.6 (45.4-74.5)***

Plus-minus values are mean ±SD; values with range in parentheses are median (interquartile range). P values are *P<0.05. **P<0.01. ***P<0.001. During the first 24 hours, there was no difference in CKMB, lactate, and leukocytes between the donor groups. In addition, there was no difference in the function of heart transplants measured by ProBNP, and LV-EF between the donor groups after 7 days. †In the previous medical history of the heart transplant recipients, there was no peripheral vascular disease. *Acute rejection with hemodynamic compromise was diagnosed based on clinical decisions such as a clinically significant decrease in left-ventricular function, an increase in left-ventricular wall thickness, and/or arrhythmias. The diagnosis of acute rejection with hemodynamic compromise always required that the patient was treated with a high dose of intravenous pulse steroids and/or antithymocyte globulin. *Acute rejection with myocyte damage is equal to or more than G1Rb rejection. In this study cohort, we did not see any cases of antibody-mediated rejection within 30-days or 1-year after HTx.

Table 4. Donor plasma proteins as prognostic biomarkers for acute rejection with hemodynamic compromise within 30 days and graft-related 1-year survival after heart transplantation.

Clinical endpoint	Protein	Level	Maxstat Cut-off	Number	Event	Percentage	HR (CPH univariable)	HR (CPH multivariable)
Acute rejection with hemodynamic compromise within 30d	CD163	Low	41407,8	44	12	72,70 %	reference	reference
	CD163	High	41407,8	6	4	33,30 %	3.41 (1.09-10.64, p=0.034)	0.15 (0.02-1.44, p=0.101)
	C-reactive protein	Low	490182,7	42	11	73,00 %	reference	reference
	C-reactive protein	High	490182,7	8	5	14,30 %	4.38 (1.50-12.76, p=0.007)	3.19 (0.62-16.30, p=0.164)
	Keratin 76	Low	16211,1	44	11	75,00 %	reference	reference
	Keratin 76	High	16211,1	6	5	16,70 %	7.31 (2.47-21.60, p<0.001)	2.18 (0.30-15.62, p=0.439)
	Myosin Va	Low	2143,2	33	6	81,80 %	reference	reference
	Myosin Va	High	2143,2	17	10	41,20 %	4.70 (1.70-12.97, p=0.003)	5.18 (1.17-22.91, p=0.030)
	Proteasome subunit alpha type-6	Low	798,6	42	10	76,20 %	reference	reference

Clinical endpoint	Protein	Level	Maxstat Cut-off	Number	Event	Percentage	HR (CPH univariable)	HR (CPH multivariable)
	Proteasome subunit alpha type-6	High	798,6	8	6	25,00 %	4.64 (1.65-13.06, p=0.004)	3.80 (0.62-23.15, p=0.147)
	Proteasome activators ubunit 2	Low	81,6	33	6	81,80 %	reference	reference
	Proteasome activators ubunit 2	High	81,6	17	10	41,20 %	4.65 (1.68-12.87, p=0.003)	4.19 (1.16-15.14, p=0.029)
	Transaldolase1	Low	11926,2	42	10	76,20 %	reference	reference
	Transaldolase 1	High	11926,2	8	6	25,00 %	4.16 (1.50-11.58, p=0.006)	3.68 (0.70-19.44, p=0.124)
	Protein	**Level**	**Maxstat Cut-off**	**Number**	**Event**	**Percentage**	**HR (CPH univariable)**	**HR (CPH multivariable)**
	D-dopachrome decarboxylase	high	105,9	48	4	91,70 %	reference	reference
	D-dopachrome decarboxylase	low	105,9	5	2	60,00 %	5.77 (1.05-31.74, p=0.044)	2.09 (0.34-12.98, p=0.428)
1-year survival	Moesin	low	6807,7	45	3	93,30 %	reference	reference

Clinical endpoint	Protein	Level	Maxstat Cut-off	Number	Event	Percentage	HR (CPH univariable)	HR (CPH multivariable)
	Moesin	high	6807,7	8	3	62,50 %	6.94 (1.40-34.51, p=0.018)	1.14 (0.11-11.40, p=0.909)
	Leucine Rich Alpha-2-Glycoprotein 1	high	508587,7	34	1	97,10 %	reference	reference
	Leucine Rich Alpha-2-Glycoprotein 1	low	508587,7	19	5	73,70 %	10.40 (1.21-89.13, p=0.033)	6.78 (0.56-81.50, p=0.131)
	Lysine-specific demethylase 3A	low	2434,8	40	2	95,00 %	reference	reference
	Lysine-specific demethylase 3A	high	2434,8	13	4	69,20 %	6.87 (1.26-37.55, p=0.026)	5.50 (0.61-49.65, p=0.129)
	Keratin 79	high	4271,7	34	1	97,10 %	reference	-
	Keratin 79	low	4271,7	19	5	73,70 %	10.40 (1.21-89.13, p=0.033)	-

Number, the group size of donors with higher protein expression and of donors with lower protein expression. Event, number of acute rejections, or number of graft-related deaths. Percentage, freedom from rejection. HR, hazard ratio; CPH, cox proportion hazard. Significant proteins in univariate COX regression analyses of acute rejection: CD163, HR 3.41, p value 0.034; C-reactive protein, HR 4.38, p value 0.007; KRT76, HR 7.31, p value <0.001; Myosin Va5, HR 4.7, p value 0.003; Proteasome subunit

alpha type-6, HR 4.64, p value 0.004; Proteasome activator subunit 2, HR 4.65, p value 0.003; and Transaldolase 1, HR 4.16, p value 0.006. Significant proteins in multivariate COX regression analyses of acute rejection: MYOA5, HR 5.18, p value 0.030; and PSME2 HR 4.19, p value 0.029. Significant proteins in univariate COX regression analysis of survival: D-dopachrome decarboxylase, HR 5.77, p value 0.044; Moesin, HR 6.94, p value 0.018; Leucine rich alpha-2-glycoprotein 1, HR 10.4, p value 0.033; Lysine-specific demethylase 3A, HR 6.87, p value 0.026; Keratin 79, HR 10.4, p value 0.033. There were no significant proteins in multivariate COX regression analyses of survival.

7. PRE-PUBLICATION OF RESULTS AND SUPPLEMENTARY MATERIALS

Urheberrecht

Die dieser kumulativen Dissertationsarbeit zugrundeliegende Originalarbeit (DOI:https://doi.org/10.1016/j.healun.2021.11.011) ist unter den Bedingungen der Creative Commons Attribution License (CC BY) (https://creativecommons.org/licenses/by/4.0/) verfügbar. Der Text der Kapitel Methoden sowie Ergebnisse ist aus der Originalveröffentlichung abgeleitet und wurde zur Verbesserung der Lesbarkeit überarbeitet.

ELSEVIER

The Journal of Heart and Lung Transplantation

http://www.jhltonline.org

Plasma proteome of brain-dead organ donors predicts heart transplant outcome

Jan Lukac, MD,[a,b] Kishor Dhaygude, PhD,[a] Mayank Saraswat, PhD,[a,c] Sakari Joenväärä, MSc,[a,d] Simo O Syrjälä, MD, PhD,[a,e] Emil J Holmström, MD,[a] Rainer Krebs, PhD,[a] Risto Renkonen, MD, PhD,[a,d] Antti I Nykänen, MD, PhD,[a,e] and Karl B Lemström, MD, PhD[a]

From the [a]Translational Immunology Research Program and Transplantation Laboratory, University of Helsinki, Helsinki, Finland; [b]Department of Cardiothoracic Surgery, University Hospital Cologne and University of Cologne, Germany; [c]Department of Laboratory Medicine and Pathology, Mayo Clinic, Rochester, Minnesota; [d]HUSLAB, Helsinki University Hospital, Helsinki, Finland; and the [e]Department of Cardiothoracic Surgery, Helsinki University Hospital and University of Helsinki, Helsinki, Finland.

KEYWORDS:
Basic;
Translational;
Clinical Research;
Proteomics

BACKGROUND: The pathophysiological changes related to brain death may affect the quality of the transplanted organs and expose the recipients to risks. We probed systemic changes reflected in donor plasma proteome and investigated their relationship to heart transplant outcomes.

METHODS: Plasma samples from brain-dead multi-organ donors were analyzed by label-free protein quantification using high-definition mass spectrometry. Unsupervised and supervised statistical models were used to determine proteome differences between brain-dead donors and healthy controls. Proteome variation and the corresponding biological pathways were analyzed and correlated with transplant outcomes.

RESULTS: Statistical models revealed that donors had a unique but heterogeneous plasma proteome with 237 of 463 proteins being changed compared to controls. Pathway analysis showed that coagulation, gluconeogenesis, and glycolysis pathways were upregulated in donors, while complement, LXR/RXR activation, and production of nitric oxide and reactive oxygen species in macrophages pathways were downregulated. In point-biserial correlation analysis, lysine-specific demethylase 3A was moderately correlated with any grade and severe PGD. In univariate and multivariate Cox regression analyses myosin Va and proteasome activator complex subunit 2 were significantly associated with the development of acute rejections with hemodynamic compromise within 30 days. Finally, we found that elevated levels of lysine-specific demethylase 3A and moesin were identified as predictors for graft-related 1-year mortality in univariate analysis.

CONCLUSIONS: We show that brain death significantly changed plasma proteome signature Donor plasma protein changes related to endothelial cell and cardiomyocyte function, inflammation, and vascular growth and arteriogenesis could predict transplant outcome suggesting a role in donor evaluation.
J Heart Lung Transplant 2022;41:311−324

Abbreviation: CRP, c-reactive protein; FDR, false discovery rate; HTx, heart transplantation; IPA, ingenuity pathway analysis; NO, nitric oxide; OPLS-DA, orthogonal projections to latent structure-discriminant analysis; PCA, principal component analysis; ROC, receiver operating characteristic; ROS, reactive oxygen species; S-Plot, variance vs correlation plot; SOM, self-organizing map; hsTnI, high-sensitivity troponin I; hsTnT, high-sensitivity troponin T

Reprint requests: Jan Lukac, Translational Immunology Research Program and Transplantation Laboratory, University of Helsinki, Helsinki, Finland, P.O.Box 21 (Haartmaninkatu 3, 4th Floor, Building-B). FIN-00014.

E-mail address: jan.lukac@helsinki.fi

1053-2498/$ - see front matter © 2021 The Author(s). Published by Elsevier Inc. on behalf of International Society for Heart and Lung Transplantation. This is an open access article under the CC BY license (http://creativecommons.org/licenses/by/4.0/)
https://doi.org/10.1016/j.healun.2021.11.011

© 2021 The Author(s). Published by Elsevier Inc. on behalf of International Society for Heart and Lung Transplantation. This is an open access article under the CC BY license (http://creativecommons.org/licenses/by/4.0/)

Brain death is the result of irreversible injury of the central nervous system. The injury may lead to systemic inflammatory, hormonal, and metabolic changes, as well as affect peripheral organs and compromise cardiorespiratory function. This may increase the risk of primary graft dysfunction, acute rejection, and survival of the recipient.[1–4]

Most of our understanding of donor organ quality is based on studies investigating donor demographics, clinical parameters, and a limited number of cytokines or proteins.[5,6] In the last few years, high-throughput technologies have advanced the discovery of pathophysiological molecular signatures. The ultra-high-performance liquid chromatography, connected to tandem mass spectrometry (UPLC-MS/MS), has facilitated a detailed measurement of the plasma proteome. In systemic biology approach, uni- and multivariate statistical analyses identify proteins that distinguish a group from another. This allows the integration of proteomics data with existing knowledge of involved biological processes and detailed examination of potential.[7]

Our results show that brain death induced prominent protein expression and pathway alterations in the donor plasma proteome. Furthermore, changes in donor plasma protein related to endothelial cell and cardiomyocyte function, inflammation, and vascular growth and arteriogenesis could predict transplant outcome suggesting their role in donor evaluation. To conclude, our results enhance the understanding of the plasma proteome in brain-dead donors, and changes in their signature may be used to predict the heart transplant outcome.

Methods

Study design and study population

This study is a post hoc analysis of multi-organ donors participating in a prospective, randomized clinical trial on the effects of donor simvastatin treatment on ischemia-reperfusion injury after heart transplantation (Nykänen et al.).[8] We analyzed donor plasma protein samples by nano ultra-performance liquid chromatography and quantified them with UPLC-MS/MS and investigated their relationship to heart transplant outcome. Plasma samples were collected in lithium heparin tubes before heparinization and organ procurement. After cooling down, we used the "Top 12 Abundant Protein Depletion kit" (Pierce, Thermo Fisher) to deplete greater than 95% of the most abundant proteins from 10 μl of plasma. The list of 12 depleted proteins was alpha-1-1acid-glycoprotein, alpha-1-antitrypsin, alpha-2-macroglobulin, albumin, apolipoprotein A-I, apolipoprotein A-II, fibrinogen, haptoglobin, IgA, IgG, IgM, and transferrin and the remaining proteins were digested by trypsin. UPLC-MS/MS was performed as described.[9] Out of the original 84 trial donors and recipients, 54 donors were chosen for proteomics analysis as they had complete sets of all time points samples available of the donor and recipient pair. Label-free quantification failed on 1 donor sample due to batch effect, therefore this sample was excluded from the study. Control samples were collected from 24 healthy controls. One control sample failed normalization and was removed from the study. For details about donor inclusion and exclusion criteria, donor management, plasma sample processing, definitions of clinical outcomes, and bioinformatics and statistical analyses, see Methods in Supplemental Material.

Results

Brain-dead donors showed a unique but heterogenous proteomic profile

The final proteomic analysis consisted of 53 multi-organ donors for HTx, and 23 healthy controls (Figure 1). The median age of the organ donors was 44 years, and 10 were female (Table 1). We detected 1259 plasma proteins with a minimum of 1 unique peptide by UPLC-MS/MS. For sufficient stringency and confidence in proteomics data, we filtered to the proteins with 2 or more unique peptides and obtained 463 quantified proteins. To describe the changes in protein abundance between donors and healthy controls, the fold change was calculated by dividing the mean protein expression of a single protein in donors by mean expression in controls. The fold change ranged from 0.11 to 2584.

Of note is that donor treatment with simvastatin did not classify the treated and untreated donor groups, and therefore was not considered a confounding factor (Figure S1).

PCA was performed on all 463 quantified proteins (Figure 2A). The scatter plot (t1 versus t2) revealed that samples of donors and healthy controls were only partially separated. Four donors were outside of the 95% confidence ellipse of measurement. The unsupervised learning method of SOM displayed 2 main clusters of protein expression in donors (Donor A and Donor B), 1 of them having 2 subclusters (Donor B1 and Donor B2) (Figure 2B, red color for donor samples), and 2 clusters in healthy controls (Figure 2B, blue color for healthy control samples), confirming the findings of PCA. A subset of healthy controls and donors merged into the same cluster which was due to the similarity of few proteins in those samples and the use of the complete set of all 463 quantified proteins in SOM clustering.

To further characterize the separation between donors and healthy controls, supervised multivariate OPLS-DA model and univariate S-Plot were performed. OPLS-DA showed a clear separation between the 2 groups, confirming the findings suggested by PCA and SOM (Figure 2C). S-Plot analysis revealed that 32 proteins were statistically significant in both univariate and multivariate analyses between donors and healthy controls, and thereby represent proteins mostly contributing to the differences between donors and healthy controls (Figure 2D). Three proteins were upregulated, while 29 proteins were downregulated. Of these proteins, apolipoprotein A-IV, complement C1q C chain, leucine-rich alpha-2-glycoprotein 1, and 14-3-3

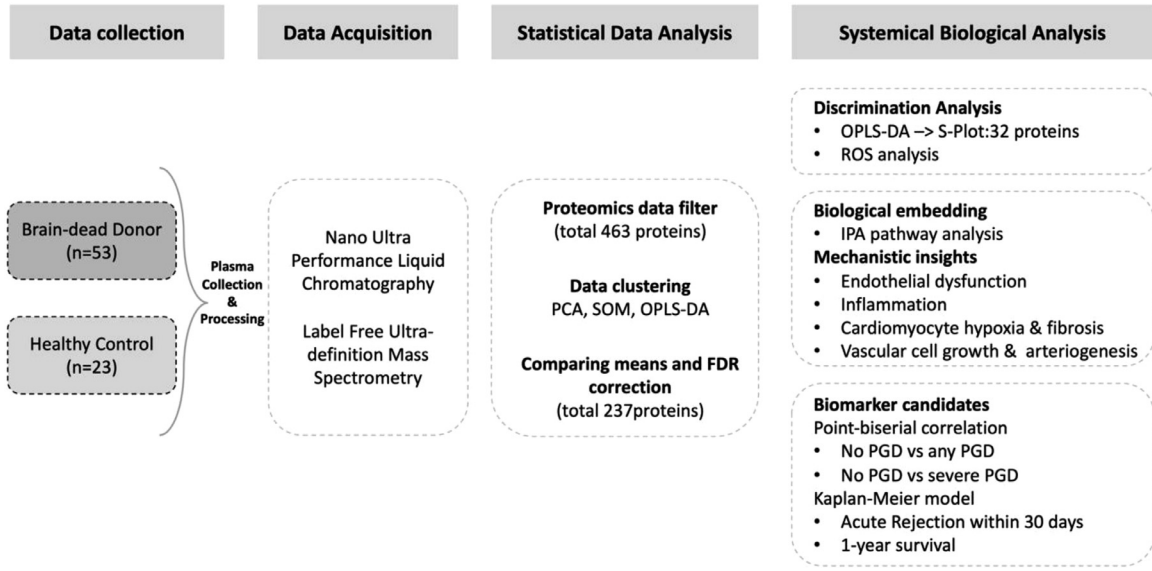

Figure 1 Flow chart of the study.

Data collection. One control sample failed normalization and was removed. One donor sample failed due to batch effect and was removed. Data acquisition. Label-free ultra-definition mass spectrometry presents the structural identity of the individual peptides based on the mass to charge ratio. Nano ultra performance liquid chromatography as the second part of this tandem method (UPLC-MS) separates peptides within the plasma sample. Statistical Data Analysis. 463 proteins were quantified which contained 2 or more unique peptides. Principal component analysis (PCA) was used as a clustering technique to determine if the protein expression separates organ donors and healthy controls as two classes and to find the expressed proteins that explain the majority of the variance noticed in a much bigger number of measured protein expressions. Self-organizing map (SOM) was used to visualize and analyze high-dimensional proteomics datasets by presenting them as lower-dimensional ones. Orthogonal projections to latent structure-discriminant analysis (OPLS-DA) is a regression model method to discriminate 2 or more classes using multivariate proteomics data. Benjamini-Hochberg FDR correction revealed 237 identified proteins with FDR-corrected p value <0.05, accounting for differences between the classes which are visualized in PCA, SOM, and OPLS-DA. Systemical Biological Analysis. S-Plot was created based on OPLS-DA loadings plot to extract 32 statistically most significant proteins between brain-dead donors and healthy controls. IPA pathway enrichment analysis was performed on 237 identified proteins. Point-biserial correlation analysis was applied to investigate the correlation between donor plasma proteome and any PGD or severe PGD. Kaplan-Meier model was applied on the clinical outcome endpoints 30 days rejection with hemodynamic compromise and 1-year survival to find biomarker candidates among 237 identified proteins in brain-dead donors.

protein beta/alpha showed a good area under the ROC curve (AUC) value of >0.8 (Table S1).

Next, we performed univariate analysis to calculate log2 (fold change) and p value using the Wilcoxon-Mann-Whitney test to find out which of 463 proteins were statistically significantly different between donors and healthy controls. Univariate analysis based on FDR-corrected p value of <0.05 revealed 237 differently expressed proteins between the donors and healthy controls of which 90 proteins were upregulated, while 147 proteins were downregulated (Table S2).

Brain-dead donor protein profile revealed significantly altered pathways

IPA pathway analysis of 237 differentially expressed proteins revealed 65 significant pathways with a p value of <0.05. Furthermore, using more stringent statistical criteria for protein data set in IPA pathway analysis, we found that 118 proteins with log2(fold change) ≥1 belonged to 58 significant pathways, while 66 proteins with log2(fold change) ≥1.5 showed 50 significant pathways (Table S3).

In IPA pathway analysis based on z-score orientation (absolute z-score greater than 1) and the most stringent FDR-corrected p value of <0.001, we observed that on the one hand coagulation, gluconeogenesis, and glycolysis were significantly enriched, and these pathways showed a trend towards upregulation. On the other hand, complement system, LXR/RXR activation, and production of NO and ROS in macrophages showed a trend towards downregulation (z-score ≤-1) (Table 2, Figure S2A-F). When considering log2 (fold change) ≥1, we found that only gluconeogenesis, glycolysis, and xenobiotic metabolism pathways were significant and that they were upregulated. No significant pathway was found with log2(fold change) ≥1.5 (Table 2).

Out of 32 S-Plot proteins, 10 S-Plot proteins belonged to the pathways with absolute z-score greater than 1 and p value of <0.001, while the remaining 22 S-Plot proteins were present in other significant pathways. We found that these 10 S-Plot proteins were mostly enriched in coagulation, complement, LXR/RXR activation, and production of NO and ROS in macrophages pathways (Table 2).

Proteome profile discriminated 3 subclusters within brain-dead donors

To exclude a methodological artifact of healthy controls to brain-dead donors, we carried out separate statistical

Table 1 Clinical Characteristics of Brain-Dead Heart Transplant Donors and Allocation of Other Solid Organs Based on Different Donor Plasma Proteome Profiles

Donor characteristics	All donors (N=53)	Donor A (N=20)	Donor B (N=33)	Donor B1 (N=26)	Donor B2 (N=7)
Age, y	44 (33-51)	44 (35-52)	43 (33-50)	44 (34.5-50)	43 (27-49.5)
Female sex, No. (%)	10 (18.9)	2 (10)	8 (24.2)	5 (19.2)	3 (42.9)
Body mass Index, kg/m^2	25.2±4.8	24.3±6.2	25.7±3.7	25.7±3.9	25.8±3.2
Simvastatin treatment, No. (%)	27 (51)	13 (65)	14 (42.4)	13 (50)	1 (14.3)
Previous medical history[a], No. (%)					
Hypertension	6 (11)	0 (0)*	6 (18.2)	6 (23.1)	0 (0)
Smokin, No. (%)					
Current	23 (43)	8 (40)	15 (45.5)	10 (38.5)	5 (71.4)
Former	4 (8)	3 (15)	1 (3)	1 (3.8)	0 (0.0)
Never	15 (28)	4 (20)	11 (33.3)	10 (38.5)	1 (14.3)
Unknown	11 (21)	5 (25)	6 (18.2)	5 (19.2)	1 (14.3)
CMV-positive, No. (%)	44 (83)	16 (80)	28 (84.8)	21 (80.8)	7 (100)
Cause of brain death, No. (%)					
Intracranial hemorrhage	26 (49.1)	10 (50)	16 (48.5)	11 (42.3)	5 (71.4)
Traumatic brain injury	19 (35.8)	5 (25)	14 (42.4)	12 (46.2)	2 (28.6)
Cerebral infarction	6 (11.3)	5 (25)*	1 (3)	1 (3.8)	0 (0.0)
Other	2 (3.8)	0 (0.0)	2 (6.1)	2 (7.7)	0 (0.0)
P-troponin I, ng/l	47 (9-207)	38 (8-88)	76 (14-293)	78 (14-286)	27 (6-250)
P-troponin T, ng/l	21 (9-55)	16 (9-33)	25 (11-67)	27 (10-90)	20 (14-60)
Hemoglobin, g/L	121±23	117±26	124±20	126±22	116±14
CRP, mg/L	43 (12-122)	95 (27.8-177)	31 (9-89)	34 (9.8-89.8)	21 (10-43.5)
Thrombocytes, E9/L	186±80	171±62	196±89	208±89	111±13***
Total P-cholesterol, mmol/l	2.72±0.94	2.76±0.89	2.68±0.98	2.93±0.93	1.87±0.7
P-HDL, mmol/l	1±0.37	0.97±0.38	0.91±0.37	0.95±0.37	0.76±0.37
P-LDL, mmol/l	1.23±0.72	1.20±0.73	1.24±0.73	1.40±0.73	0.71±0.41*
P-triglycerides, mmol/l	0.86±0.5 1	1.02±0.58	0.79±0.44	0.82±0.47	0.59±0.27
Echocardiogram					
Left ventricle ejection fraction, %	62 (59-65)	61 (60-65)	62 (58-66)	63 (58-66)	61 (60-65)
Presence of regional wall motion abnormality, No. (%)	6 (11)	2 (10)	4 (12.1)	2 (7.7)	2 (28.6)
Diastolic posterior wall thickness, mm	11 (9-12)	10.5 (10-11)	11 (10-13)	11 (10-13)	9.7 (9-10)
Diastolic septum thickness, mm	11 (10-12)	10.75 (10-11)	11 (10-12)	11 (10-12)	10.75 (11-11)
Coronary angiography[b]					
Performed, No.(%)	30 (57)	13 (65)	17 (51.5)	14 (53.8)	3 (42.9)
Abnormal finding angiography, No. (%)	6 (11)	3 (15)	3 (9.1)	3 (11.5)	0 (0.0)
Inotropic support, No. (%)	37 (70)	12 (60)	25 (75.8)	18 (69.2)	7 (100)
Resuscitation, No. (%)	9 (17)	2 (10)	7 (21.2)	7 (26.9)	0 (0.0)
Time of ROSC for resuscitated donors, min	17±13	30±0	14±12	14±12	0.0
The time between the declaration of brain death and organ procurement, h	14.86±4	14.58±3.7	14.76±4	14.86±4	14.39±3
Organs transplanted from donors, No. (%)					
Heart	53 (100)	20 (100)	33 (100)	26 (100)	7 (100)
Lung	17 (32)	6 (30)	11 (33.3)	8 (30.8)	3 (42.9)
Liver	36 (68)	12 (60)	24 (72.7)	20 (76.9)	4 (57.1)
Kidneys	86 (90.6)	29 (85)	57 (93.9)	46 (96.1)	11 (85.7)
Pancreas	31 (58)	10 (50)	21 (63.6)	16 (61.5)	5 (71.4)

Plus-minus values are mean ±SD; values with the range in parentheses are median (interquartile range). P values are marked as asterisks (*p<0.05. **p<0.01. ***p<0.001). CMV, indicates cytomegalovirus; HDL, high-density lipoprotein; LDL, low-density lipoprotein; ROSC, return of spontaneous circulation; and Tx, transplantation.

[a]In the previous medical history of the donors there was no coronary artery disease, chronic obstructive pulmonary disease, peripheral vascular disease, previous malignancy, prior stroke, and no history of sternotomy.

[b]Donor coronary angiography was performed for donors with >40 years of age, strong family history of coronary disease, or smoking.

analyses including only brain-dead donors and found 3 subclusters within donors with only minor changes in their demographics (Figure S3, Table 1). When comparing the recipient outcomes between Donor A and Donor B groups, we could not see any statistically significant difference in PGD, acute rejection, or graft-related survival (Table 3). Detailed information, stratified by the Donor subgroups, on the donor demographics and recipient outcomes is given in Tables 1 and 3, and on enriched pathways in Tables S4 and S5, and Supplement.

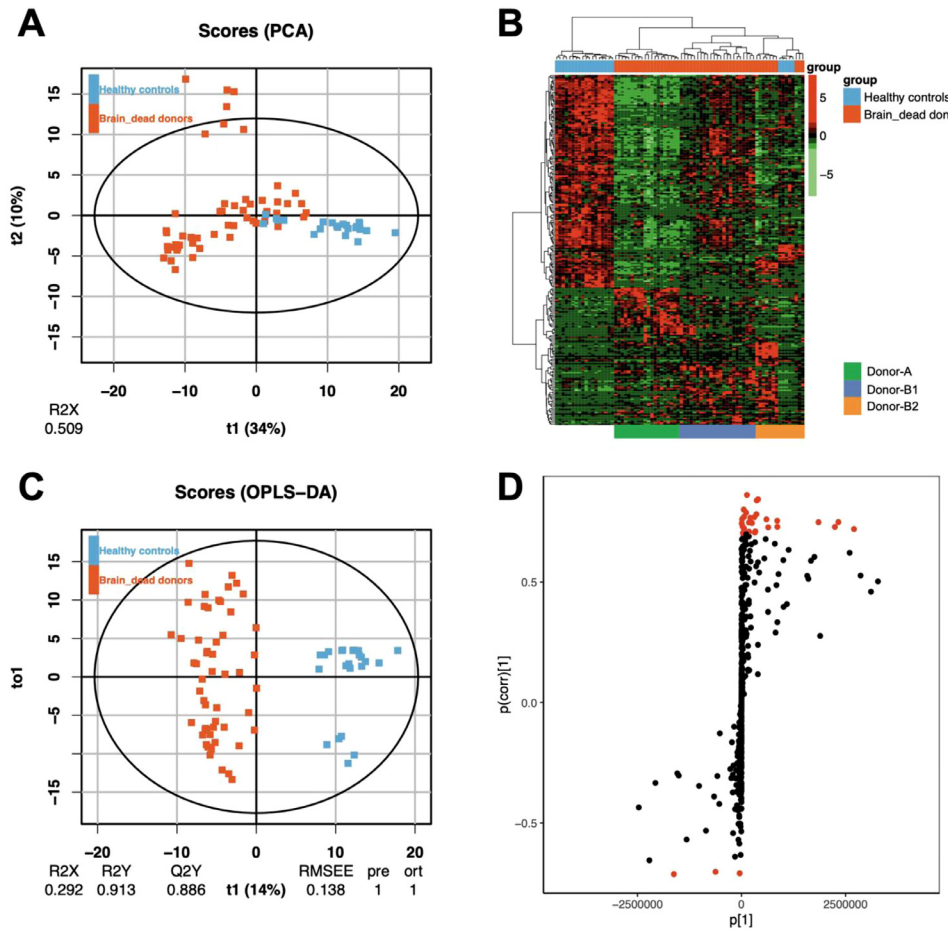

Figure 2 Comparison of differentially expressed plasma proteins between brain-dead donors and healthy controls.

Unsupervised PCA analysis was performed on 463 quantified proteins. In PCA analysis, the t1 axis showed the variation of plasma proteins between the brain-dead donors (orange dots) and healthy controls (blue dots), whereas the t2 axis showed the variation of protein profile within the same group. The 95% confidence ellipse showed that 4 out of 53 heart donors had increased protein expression heterogeneity. Within 95% confidence ellipse, brain-dead donor samples, as well as healthy control samples, were grouped into two major clusters. (B) SOM clustering of all 463 quantified plasma proteins in the heatmap showed separate clusters in brain-dead donors (orange) and healthy controls (blue), confirming the observation of the PCA plot. Red color represents upregulated, and green color downregulated protein expression in samples. Donor samples grouped into Donor A (dark green), Donor B1 (pink), and Donor B2 (orange). Subsets of healthy controls (blue, right side) and Donor B2 (orange, right side) grouped into the same cluster. (C) Supervised OPLS-DA analysis on 463 quantified plasma proteins showed a clear separation between the 2 groups, confirming the findings suggested by PCA and SOM. (D) S-Plot generated from the OPLS-DA analysis revealed 32 significant differentially expressed proteins between brain dead donors and healthy controls. The right upper corner of the Figure shows that 29 proteins were downregulated, whereas the left lower corner shows that 3 proteins were upregulated in brain dead donors. Proteins with the cut-offs, ± 0.1 for p[1] and $> +0.7$ or < -0.7 for p(corr) [1] were considered as significant proteins. (Color version of figure is available online)

Donor plasma lysine-specific demethylase 3A was moderately associated with PGD

Next, we investigated whether donor plasma proteins could predict and any PGD grade or severe PGD after transplantation. 17 of 53 recipients (32%) recipients developed PGD and only 6 (11%) had severe PGD. The characteristics of respective donors of recipients with any PGD grade or severe PGD were not statistically different (Table S6). However, the recipients with any or severe PGD had longer intubation time, longer stay at ICU and index hospitalization, and higher levels of proBNP, hsTnI, hsTnT, and lactate (Table S7).

The point-biserial correlation analysis revealed that only 5 proteins correlated with any PGD, while 6 proteins correlated with severe PGD. Only lysine-specific demethylase 3A showed a moderate correlation with any PGD and severe PGD (Table S8).

High donor plasma myosin Va and proteasome activator subunit 2 predicted acute rejection episodes with hemodynamic compromise

Next, we investigated whether donor plasma proteins could predict episodes of acute rejections with hemodynamic compromise. The prerequisite to establish the diagnosis of acute rejection with hemodynamic compromise was that the patient was treated by high dose of intravenous pulse steroids and/or anti-thymocyte globulin. Three patients

were excluded from the analysis as they expired due to graft-related reasons within 30 days (Table S9). Sixteen patients received treatment for acute rejection with hemodynamic compromise. The characteristics of respective donors were not different (Table S10). However, the recipients with rejection episodes had significantly higher plasma levels of troponins and lactate during the first 24 hours, higher ProBNP and lower left-ventricle ejection fraction at 1 month, and longer ICU and hospital stay after transplantation (Table S11).

Univariate Cox regression analysis of differentially expressed 237 proteins revealed that 7 donor plasma proteins were significantly associated with acute rejections with hemodynamic compromise within 30 days. These proteins included CD163, CRP, keratin 76, myosin Va, proteasome subunit alpha type 6, proteasome activator subunit 2, and transaldolase 1. We further explored the possibility of an association between hemodynamically compromised acute rejection rejections and concentration thresholds for these proteins in univariate analysis. After stratification of patients based on each protein expression level, we found that higher donor plasma levels of all these proteins were associated with a significantly increased number of acute rejections with hemodynamic compromise. In Kaplan-Meier analysis, all the 7 donor plasma proteins passed the log-rank test with a p value less than 0.05 (Figure 3A-G, Table 4). Higher expression of these 7 proteins was linked to higher hazard/risk (Table 4).

Table 2 Effect of log2 Fold Change on Ingenuity Pathway Analysis of Identified Proteins in Heart Transplant Donors

Pathway (z-score =>1)	Donor vs Controls No fold change (237 proteins)	-log(p value)	Donor vs Controls Fold change ≥1 (118 proteins)	-log(p value)	Donor vs Controls Fold change ≥1.5 (66 proteins)	-log(p value)	Donor A vs. B No fold change (164 proteins)	Donor B1 vs B2 No fold change (107 proteins)	S-Plot proteins
Coagulation System	1,732	15,7	-	-	-	-	-	-	plasma kallkrein, kininogen 1, plasminogen, protein C,antithrombin-III
Complement System	-1,265	15,2	-	-	-	-	-1,265	1	complement C1q C chain, mannan binding lectin serine peptidase 1
Gluconeogenesis I	1,633	5,33	1,342	5,62	-	-	-2,236	-	
Glycolysis I	1,633	5,62	1,342	5,87	-	-	-2,236	-	
LXR/RXR Activation	-4,536	29,6	-0,816	4,52	-	-	-3,13	3	alpha 2-HS glycoprotein, apolipoprotein A4, kininogen 1, paraoxonase1

(*continued on next page*)

Pathway (z-score =>1)	Donor vs Controls No fold change (237 proteins)	-log(p value)	Donor vs Controls Fold change ≥1 (118 proteins)	-log(p value)	Donor vs Controls Fold change ≥1.5 (66 proteins)	-log(p value)	Donor A vs. B No fold change (164 proteins)	Donor B1 vs B2 No fold change (107 proteins)	S-Plot proteins
Production of Nitric Oxide and Reactive Oxygen Species in Macrophages	-2,111	6,46	-	-	-	-	-2,121	-	apolipoprotein A4, paraoxonase 1
Role of Pattern Recognition Receptors in Recognition of Bacteria and Viruses	-	-	-	-	-	-	-1,342	-	complement C1q C chain
Xenobiotic Metabolism CAR Signaling Pathway	-	-	1,633	3,63	-	-	-	-	glutathione S-transferase mu 2

In IPA pathway analysis, we considered pathways with a -log(*p* value) of >3.0 (*p* value <0.001) and a z-score of ±1 as significant. Upregulated pathways are highlighted in red and downregulated in green. S-Plot proteins enriched into specific pathways are presented.

Additionally, a donor plasma proteomic predictive risk score was calculated based on the concentration levels of these proteins and corresponding regression coefficients. This predictive risk score was calculated by giving 1 point for each of the 7 proteins that were within their respective high-risk levels, therefore yielding a score of 0 to 7 for each donor. In risk score calculation, 18 patients had a score of 0, 16 patients a score of 1, 6 patients a score of 2, 5 patients a score of 3, and 5 patients had a score greater than 3. Based on the donor proteomics risk score, we found that a higher score significantly predicted acute rejection with hemodynamic compromise (Figure 3H). In addition, we observed that donors with high-risk score (score ≥3) had an 80% probability of acute rejection with hemodynamic compromise within 30 days (Figure S4).

In multivariate Cox regression analysis, myosin Va and proteasome activator subunit 2 remained significant suggesting that these 2 proteins are key candidates for prediction of acute rejection with hemodynamic compromise within 30 days after transplantation (Figure S5).

High levels of moesin and lysine-specific demethylase 3A were associated with worse graft-related 1-year survival

Next, we investigated whether donor proteome could predict graft-related mortality. 7 of 53 recipients died due to graft-related reasons, and 6 of them during the first year, and 1 patient died 730 days after transplantation. PGD was the cause of death in 4 patients, acute rejection in 2 patients, and chronic rejection in 1 patient (Table S9). Therefore, we tested whether donor proteome could predict 1-year graft-related mortality.

In univariate analysis, we found that 5 proteins were significantly associated with 1-year graft-related mortality (Figure 4A-E). After stratification of donors using the Maxstat method, we found that high donor plasma levels of moesin and lysine-specific demethylase 3A were associated with increased graft-related 1-year mortality, while low plasma levels of D-dopachrome decarboxylase, leucine-rich alpha-2-glycoprotein, and keratin 79 were associated

Table 3 Clinical Characteristics and Outcomes of the Heart Transplant Recipients Based on Different Donor Plasma Proteome Profiles

	All donors (N=53)	Donor A (N=20)	Donor B (N=33)	Donor B1 (N=26)	Donor B2 (N=7)
Recipient characteristics					
Age, y	58 (46.5-61)	55 (46-59)	59 (49-62)	61 (49-63)	58 (48-60)
Female sex, No. (%)	13 (24.5)	3 (15)	10 (30.3)	7 (26.9)	3 (42.9)
Body mass index, kg/m^2	26±4.4	26±4.6	25.6±4.5	25.9±4.7	24.4±3.3
Previous medical history† No. (%)					
Hypertension	8 (15.1)	1 (5)	7 (21.2)	6 (23.1)	1 (14.3)
Coronary artery disease	11 (20.8)	5 (25)	6 (18.2)	4 (15.4)	2 (28.6)
Chronic obstructive pulmonary disease	2 (3.8)	0 (0.0)	2 (6.1)	2 (7.7)	0 (0.0)
Diabetes	7 (13.2)	1 (20)	6 (18.2)	5 (19.2)	1 (14.3)
Previous malignancy	5 (9.4)	1 (5)	4 (12.1)	3 (11.5)	1 (14.3)
Prior stroke	7 (13.2)	2 (10)	5 (15.2)	4 (15.4)	1 (14.3)
Amiodarone <6 months prior transplantation, No. (%)	14 (26.4)	4 (20)	10 (30.3)	9 (34.6)	1 (14.3)
History of sternotomy	15 (28.3)	5 (25)	10 (30.3)	7 (26.9)	3 (42.9)
Primary disease, No. (%)					
Endstage coronary disease	12 (22.6)	4 (20)	8 (24.2)	6 (23.1)	2 (28.6)
Dilatative cardiomyopathy	26 (49)	11 (55)	15 (45.5)	12 (46.2)	3 (42.9)
Congenital	4 (7.6)	2 (10)	2 (6.1)	1 (3.8)	1 (14.3)
Myocarditis	3 (5.7)	0 (0.0)	3 (9.1)	3 (11.5)	0 (0.0)
Other	8 (15.1)	3 (15)	5 (15.2)	4 (15.4)	1 (4.3)
Donor-recipient sex mismatch, No. (%)	6 (11.3)	4 (20)	2 (6.1)	2 (7.7)	0 (0.0)
Mechanical circulatory support prior to HTx, No. (%)	13 (24.5)	2 (10)	11 (33.3)	9 (34.6)	2 (28.6)
ECMO, No. (%)	6 (11.3)	2 (10)	4 (12.1)	4 (15.4)	0 (0.0)
LVAD, No. (%)	7 (13.2)	0 (0.0)*	7 (21.2)	5 (19.2)	2 (28.6)
Days on waiting list	190 (41.8-352.5)	203 (49-360)	180 (28.5-330)	157 (29.3-335)	200 (68-221)
Graft ischemia, min					
Cold	97±50.1	94±50.2	98±50.8	96±47.1	106±65.8
Warm	80±20.2	86±21.4	77±19.2	77±21.4	78±8.9
Total	173±54.1	170±59.3	175±51.5	172±49.1	184±63
Organ functions before heart transplantation					
PVR, Wood units	3±1.3	2.7±1.1	3.2±1.5	3.1±1.4	3.8±1.9
TPG, mmHg	10 (7-12)	11 (10-12)	8 (7-13)	8 (7-11)	10 (6.3-13.5)
SPAP, mmHg	43±12.8	43±10.9	43±14.3	40±12.6	55.5±17.1
P-bilirubin, μmol/L	13 (10-19)	14 (10-22.5)	11 (9-15)	11 (9-15.8)	10 (9.5-14)
Glomerular filtration rate, mL/min per 1.73 square meters	55.7 (45-73)	51.7 (44-65.3)	57 (48-73)	56.4 (45.7-72.5)	58.3 (55.5-69.5)
NT-proBNP, ng/L	3171 (1075-5686)	3304 (2263-5208)	3100 (852-5942)	3132 (934-6146)	1982 (756-4619)
Immunosuppressive therapy, No. (%)					
Induction Therapy					
Anti-thyomocyte	21 (39.6)	10 (50)	11 (33.3)	11 (42.3)	0 (0.0)
Maintenance therapy					
Cyclosporine A	10 (18.9)	4 (20)	6 (18.2)	4 (15.4)	2 (28.6)
Tacrolismus	39 (73.6)	14 (70)	25 (75.8)	21 (80.8)	4 (57.1)
Azathioprine	2 (3.8)	1 (5)	1 (3.3)	1 (3.8)	0 (0.0)
Mycophenlic acid	46 (86.8)	16 (80)	30 (90.1)	24 (92.3)	6 (85.7)
Prednisolone	53 (100)	20 (100)	33 (100)	26 (100)	7 (100)
Recipient Outcome					
Intubation time, h	42 (20-125)	60 (24-111)	42 (18-180)	23 (18-183)	19 (16-63)
Time on ICU, h	216 (144-480)	204 (168-372)	216 (120-492)	264 (120-552)	168 (90-378)
Hospital length of stay, d	44±29	48±37	42±24	45±24	29±18
Inotropic support, No. (%)	47 (88.7)	19 (95)	28 (84.8)	23 (88.46)	5 (71.4)
30-day survival. No. (%)	50 (94.3)	19 (95)	31 (93.9)	25 (96.2)	6 (85.7)
1-year survival, No. (%)	46 (86.8)	18 (90)	28 (84.8)	22 (84.6)	6 (85.7)
LV-EF at 7 days	59±9.4	58±7	59±10.9	57±10.6	69±6.3*
Primary graft dysfunction, No. (%)					
Any PGD	17 (32.1)	6 (20)	11 (33.3)	9 (34.6)	2 (28.6)
Severe PGD	6 (11.3)	2 (10)	4 (12.1)	4 (15.4)	0 (0.0)
30-day acute rejection with hemodynamic compromise, No. (%)*	16 (30.2)	5 (25)	11 (33.3)	10 (38.5)	1 (14.3)
30-day acute rejection with myocyte damage, No. (%)*	3 (5.7)	1 (5)	2 (6.1)	2 (7.7)	0 (0.0)
1-year acute rejection with hemodynamic compromise, No. (%)	20 (37.7)	7 (35)	13 (39.4)	11 (42.3)	2 (28.6)
1-year acute rejection with myocyte damage, No. (%)	8 (15.1)	3 (15)	5 (15.2)	4 (16.7)	1 (14.3)
P-troponin I, ng/l					
6h	86310 (40324- 149706)	88155 (45683- 162006.25)	79373 (39820 −149187)	86957(44060-215360)	43188 (21286-75966)**
12h	95187.5(42482-195580)	101563 (48698-181267)	91186 (41185- 186515)	115680.5(4492 −267527)	50133 (23255-67453)**
24h	57679 (32912- 106589)	69300 (36760-124360)	49437 (31803 −103140)	60123 (33374-110863)	34828 (21565-57794)*

(*continued on next page*)

Table 3 (*Continued*)

	All donors (N=53)	Donor A (N=20)	Donor B (N=33)	Donor B1 (N=26)	Donor B2 (N=7)
P-troponin T, ng/l					
6h	8940 (4637-17150)	8896 (5712-14588)	8940 (4217-17150)	11665 (4830-18535)	4153 (2818-9120) **
12h	8460 (4399- 14453)	7947 (4531-14555)	9593 (4421-14220)	12080 (5505- 16310)	4421 (2345- 6115) **
24h	5918 (3262-9269)	5713 (3847-9458)	6055 (2706- 8425)	7563.5 (3288-9202)	2313 (2079- 4829)*
hsCRP, Mg/L					
1h	2.8 (1.9-7)	3.22 (2-7)	2.8 (1.5-6.5)	2.2 (1.6-6.7)	4.7 (1.9-5.7)
6h	5.6 (3.8-12.6)	6.8 (5-11.8)	5.5 (3.2-12.6)	5 (3.2-12.4)	6.5 (4-13.2)
12h	26.2 (16.2-44.8)	25.3 (15-48.6)	26.9 (19.6-43.2)	28.5 (21.6-44.6)	20 (15.5-32.8)
24h	87.1 (61.4-123.1)	99.3 (66.3-119.1)	85.5 (63.6-122.2)	96.5 (77.8-126.6)	63.6 (45.4-74.5)*

Plus-minus values are mean ±SD; values with range in parentheses are median (interquartile range). *p* values are *$p<0.05$. **$p<0.01$. ***$p<0.001$. During the first 24 hours, there was no difference in CKMB, lactate, and leukocytes between the donor groups. In addition, there was no difference in the function of heart transplants measured by ProBNP, and LV-EF between the donor groups after 7 days. †In the previous medical history of the heart transplant recipients, there was no peripheral vascular disease. *Acute rejection with hemodynamic compromise was diagnosed based on clinical decisions such as clinically significant decrease in left-ventricular function, increase in left-ventricular wall thickness and/or arrhythmias. The diagnose of acute rejection with hemodynamic compromise always required that the patient was treated by high dose of intravenous pulse steroids and/or antithymocyte globulin. *Acute rejection with myocyte damage is equal or more than G1Rb rejection. In this study cohort, we did not see any cases of antibody-mediated rejection within 30-days or 1-year after HTx.

with decreased graft-related 1-year mortality. In multivariate analysis of 1-year graft-related survival analyses, none of the proteins were significant (Table 4).

A summary of the possible biological role of key proteins predicting heart transplant outcome discussed further below, can be found in Table S12.

Discussion

In this study, we observed that brain-dead donors had a unique but heterogeneous proteomic signature. The changes were related to coagulation system, gluconeogenesis, and glycolysis pathways, complement, LXR/RXR activation, and production of NO and ROS in macrophages pathways. Furthermore, changes in donor plasma protein related to endothelial cell and cardiomyocyte function, inflammation, and vascular growth and arteriogenesis could predict transplant outcome suggesting their role in donor evaluation.

Despite our protein set enrichment analysis approach, making sound biological conclusions from high-dimensional MS data is still challenging.[10] Therefore, data filtering is crucially important for stringent statistical analysis. However, the relevant pathophysiology of the disease process must also be considered. In this study, FDR-corrected p value without further filtering by log2 fold change reproduced the results of the pathophysiology of donors when compared to earlier results and our recent observations in plasma extracellular vesicle transcriptomics (SeoJeong et al., unpublished).[11] Based on this, we found that donor plasma showed a distinct protein profile from healthy controls, with 237 differentially expressed proteins and 6 significantly altered pathways. Out of these, 32 proteins were identified by S-Plot as the most distinguishing proteins of donors, and 10 of these proteins were enriched into 6 significantly changed pathways.

Complement and coagulation are evolutionary-related proteolytic cascades that are critical in the innate immune response to injury.[12,13] In preclinical studies, brain death enhances complement activation and ischemia-reperfusion injury in heart transplants.[14] In our study, brain death was associated with the downregulation of complement and the upregulation of coagulation. The most significantly differentially expressed S-Plot proteins of complement and coagulation were downregulated in donors. In the comparison of donor subgroups, the complement pathway was upregulated in the Donor B group which showed more traumatic brain injury and hypertension, and in the B1 subgroup which had higher troponin and CRP within 24h and reduced cardiac function 7 days after HTx. However, lack of natural anticoagulants such as plasminogen, protein C, and antithrombin-III may lead to microvascular blood clot formation and thereby no-reflow during reperfusion of the transplant in the recipient. In addition, loss of vascular antithrombin has been linked to cardiac allograft vasculopathy and heart failure after HTx.[15]

Brain-dead donors showed significant downregulation of the LXR/RXR pathway. LXR/RXR are cholesterol-sensing nuclear receptors and key regulators of lipid metabolism. They may also control the innate immune response and reduce myocardial ischemia-reperfusion injury.[16,17] The downregulated proteins of the LXR/RXR pathway were alpha-2-HS-glycoprotein, apolipoprotein A4, plasma kallikrein, kininogen 1, and paraoxonase 1. Apolipoprotein A4 attenuates platelet aggregation, thrombosis, and platelet hyperactivity, and therefore the decreased levels of apolipoprotein A4 may reflect the aggravation of prothrombotic state in brain-dead donors.[18] In the kinin−kallikrein system, kininogen-1 is the precursor protein of high- and low-molecular kininogen, and bradykinin. The kinin-kallikrein system promotes blood coagulation, vasodilatation, and vascular inflammation.[19,20] Recently, decreased levels of pre-transplant kallikrein have been shown to predict PGD after HTx.[21] Paraoxonase-1 inhibits oxidation and apoptosis in endothelial cells and low serum levels may predispose donors to increased endothelial cell damage.[22] The downregulation of LXR/RXR suggests that this pathway was possibly depleted due to inappropriate activation of inflammatory and coagulation responses in brain-dead donors.

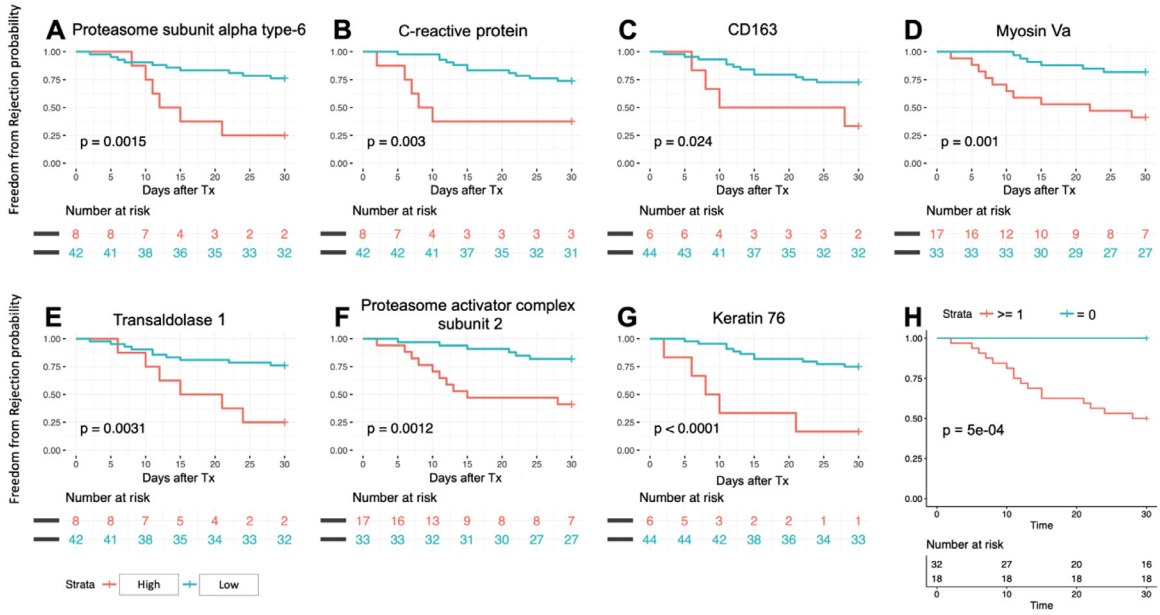

Figure 3 Impact of donor plasma protein levels on the development of acute rejection with hemodynamic compromise within the first 30 days after heart transplantation.

(A-G) Kaplan-Meier analysis on 50 heart transplant recipients showing the curves of high (red) and low (blue) protein levels of 7 donor proteins that were significantly associated with acute rejection with hemodynamic compromise episodes within 30 days after HTx. *p* value was calculated by log-rank test and revealed that rejection-free curves were significantly different between the high and low protein level groups. (A) Proteasome subunit alpha type-6 (PSMA6): *p* value = 0.0015, (B) CRP: *p* value = 0.003, (C) CD163: *p* value = 0.024, (D) myosin Va (MYO5A): *p* value = 0.001, (E) transaldolase 1 (TALDO1): *p* value = 0.0031, (F) proteasome activator subunit 2 (PSME2): *p* value = 0.0012, (G) keratin 76 (KRT76): *p* value < 0.0001. (H) Donor plasma proteomic immunological risk score was calculated based on the expression values of the 7 proteins. For high-risk level 1 point and for low-risk level zero points were given. A donor score of ≥1 was able to predict the risk of rejection. (Color version of figure is available online)

Under normal conditions, cardiac ATP is mainly derived from fatty acid oxidation. However, under stress conditions carbohydrates are predominantly used as an energy substrate.[23] This shift in glucose metabolism is reflected by the upregulation of the glycolysis pathway in brain-dead donors. The increased glycolysis is pivotal for anaerobic ATP production, but at the same time increased uncoupling of glycolysis and glucose oxidation may contribute to myocardial injury.[24,25] In aerobic glucose metabolism, accumulating lipid peroxidation products are metabolized by aldose reductase via the polyol pathway protecting the heart against oxidative injury. The protective activity of aldose reductase is dependent on the generation of NO.[26] In our donors, we observed a downregulation of the production of NO and ROS in macrophages pathway which may result in reduced NO bioavailability, and therefore increased aldose reductase activity and less myocardial oxidative stress. Moreover, brain-dead donors showed a substantial increase in the gluconeogenesis pathway resulting in hyperglycemia and worsening of systemic inflammation.[27–29]

Finally, we investigated whether donor plasma proteins may predict heart transplant outcomes. Interestingly, most of the proteins being correlated with any PGD or severe PGD were significantly associated with other recipient outcomes as well. Lysine-specific demethylase 3A was associated with any and severe PGD, and 1- survival, proteasome 20s subunit alpha 6 with severe PGD and acute rejection with hemodynamic compromise, moesin with severe PGD and 1-year survival, and keratin 76 with severe PGD and acute rejection with hemodynamic compromise.

In univariate Cox regression analysis, we found that higher donor plasma levels of CD163, CRP, keratin 76, myosin Va, proteasome subunit alpha type-6, proteasome activator subunit 2, and transaldolase 1 were associated with the development of acute rejection episodes with hemodynamic compromise during the first month after transplantation. Interestingly, multivariate analysis showed that the 2 proteins myosin Va and proteasome activator subunit 2 were the best predicting proteins for acute rejection with hemodynamic compromise episodes. Myosin Va is an intracellular motor protein that plays a role in channel trafficking in cardiomyocyte membrane and has been suggested as a novel therapeutic target in cardiovascular disease.[30] The circulating 20s proteasome is modulated by proteasome activator (PA28) subunits such as proteasome activator subunit 2. Abnormalities of this modulation contribute to increased intimal hyperplasia and atherosclerosis.[31]

Of note is that 7 proteins found in univariate analysis on acute rejection with hemodynamic compromise were not clearly related to the top pathways observed in brain-dead donors. However, they were related to inflammation, endothelial dysfunction, and cardiovascular protein trafficking. Therefore, we hypothesize that these proteins may reflect donors' cardiovascular morbidity or endothelial and cardiomyocyte injury induced during brain death. Based on the donor plasma proteomic immunological risk score, we

Table 4 Donor Plasma Proteins as Prognostic Biomarkers for acute Rejection with Hemodynamic Compromise Within 30 Days and Graft-Related 1-Year Survival After Heart Transplantation

Clinical endpoint	Protein	Level	Maxstat Cut-off	Number	Event	Percentage	HR (CPH univariable)	HR (CPH multivariable)
Acute rejection with hemodynamic compromise within 30d	CD163	Low	41407,8	44	12	72,70 %	reference	reference
	CD163	High	41407,8	6	4	33,30 %	3.41 (1.09-10.64, p=0.034)	0.15 (0.02-1.44, p=0.101)
	C-reactive protein	Low	490182,7	42	11	73,00 %	reference	reference
	C-reactive protein	High	490182,7	8	5	14,30 %	4.38 (1.50-12.76, p=0.007)	3.19 (0.62-16.30, p=0.164)
	Keratin 76	Low	16211,1	44	11	75,00 %	reference	reference
	Keratin 76	High	16211,1	6	5	16,70 %	7.31 (2.47-21.60, p<0.001)	2.18 (0.30-15.62, p=0.439)
	Myosin Va	Low	2143,2	33	6	81,80 %	reference	reference
	Myosin Va	High	2143,2	17	10	41,20 %	4.70 (1.70-12.97, p=0.003)	5.18 (1.17-22.91, p=0.030)
	Proteasome subunit alpha type-6	Low	798,6	42	10	76,20 %	reference	reference
	Proteasome subunit alpha type-6	High	798,6	8	6	25,00 %	4.64 (1.65-13.06, p=0.004)	3.80 (0.62-23.15, p=0.147)
	Proteasome activatorsubunit 2	Low	81,6	33	6	81,80 %	reference	reference
	Proteasome activatorsubunit 2	High	81,6	17	10	41,20 %	4.65 (1.68-12.87, p=0.003)	4.19 (1.16-15.14, p=0.029)
	Transaldolase1	Low	11926,2	42	10	76,20 %	reference	reference
	Transaldolase 1	High	11926,2	8	6	25,00 %	4.16 (1.50-11.58, p=0.006)	3.68 (0.70-19.44, p=0.124)
1-year survival	D-dopachrome decarboxylase	high	105,9	48	4	91,70 %	reference	reference
	D-dopachrome decarboxylase	low	105,9	5	2	60,00 %	5.77 (1.05-31.74, p=0.044)	2.09 (0.34-12.98, p=0.428)
	Moesin	low	6807,7	45	3	93,30 %	reference	reference
	Moesin	high	6807,7	8	3	62,50 %	6.94 (1.40-34.51, p=0.018)	1.14 (0.11-11.40, p=0.909)
	Leucine Rich Alpha-2-Glycoprotein 1	high	508587,7	34	1	97,10 %	reference	reference
	Leucine Rich Alpha-2-Glycoprotein 1	low	508587,7	19	5	73,70 %	10.40 (1.21-89.13, p=0.033)	6.78 (0.56-81.50, p=0.131)
	Lysine-specific demethylase 3A	low	2434,8	40	2	95,00 %	reference	reference
	Lysine-specific demethylase 3A	high	2434,8	13	4	69,20 %	6.87 (1.26-37.55, p=0.026)	5.50 (0.61-49.65, p=0.129)
	Keratin 79	high	4271,7	34	1	97,10 %	reference	-
	Keratin 79	low	4271,7	19	5	73,70 %	10.40 (1.21-89.13, p=0.033)	-

Number, the group size of donors with higher protein expression and of donors with lower protein expression. Event, number of acute rejections, or number of graft-related deaths. Percentage, freedom from rejection. HR, hazard ratio; CPH, cox proportion hazard. Significant proteins in univariate COX regression analyses of acute rejection: CD163, HR 3.41, p value 0.034; C-reactive protein, HR 4.38, p value 0.007; KRT76, HR 7.31, p value <0.001; Myosin Va5, HR 4.7, p value 0.003; Proteasome subunit alpha type-6, HR 4.64, p value 0.004; Proteasome activator subunit 2, HR 4.65, p value 0.003; and Transaldolase 1, HR 4.16, p value 0.006. Significant proteins in multivariate COX regression analyses of acute rejection: MYOA5, HR 5.18, p value 0.030; and PSME2 HR 4.19, p value 0.029. Significant proteins in univariate COX regression analysis of survival: D-dopachrome decarboxylase, HR 5.77, p value 0.044; Moesin, HR 6.94, p value 0.018; Leucine rich alpha-2-glycoprotein 1, HR 10.4, p value 0.033; Lysine-specific demethylase 3A, HR 6.87, p value 0.026; Keratin 79, HR 10.4, p value 0.033. There were no significant proteins in multivariate COX regression analyses of survival.

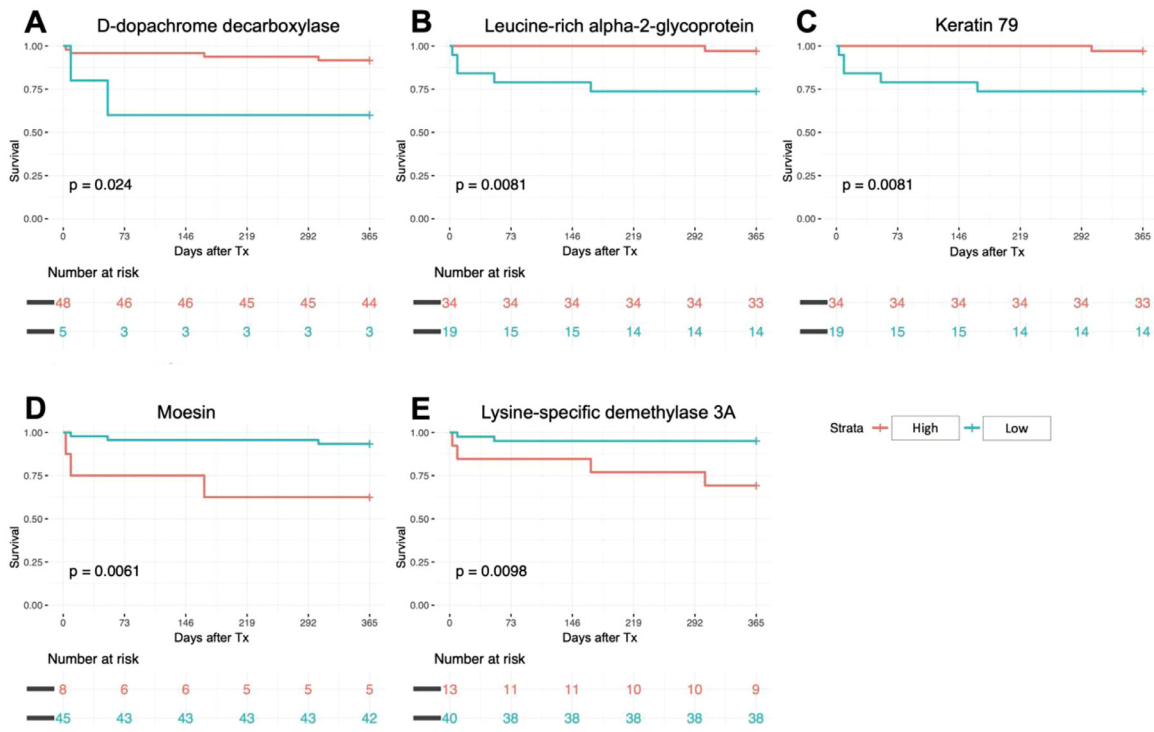

Figure 4 Impact of donor plasma protein levels on graft-related 1-year survival after heart transplantation.

Kaplan-Meier survival analysis on 50 heart transplant recipients showed that on the one hand, (A) donors with low levels of d-dopachrome decarboxylase, (B) leucine rich alpha-2-glycoprotein 1, and (C) keratin 79 had worse overall 1-year survival than donors with high levels of d-dopachrome decarboxylase (60% in low vs. 91.70% in high), leucine-rich alpha-2-glycoprotein (73.70% in low vs. 97.10% in high) and keratin 79 (73.70% in low vs. 97.10% in high). On the other hand, (D) donors with high levels of moesin and (E) lysine-specific demethylase 3A had worse overall 1-year survival than donors with low levels of moesin (93.30% in low vs. 62.50% in high) and lysine-specific demethylase 3A (95% in low vs. 69.20% in high).

showed that if any of the 7 donor proteins were upregulated, there was an increased risk of acute rejections with hemodynamic compromise within the first 30 days and that this risk increases depending on how many proteins were upregulated. These results suggest that the risk score based on these 7 proteins may be used to stratify the brain-dead organ donors.

In univariate Cox regression analysis, higher donor plasma levels of moesin and lysine-specific demethylase 3A were associated with an increased risk of graft-related 1-year mortality. Moesin, a member of the ezrin-radixin-moesin family, is expressed by vascular endothelium and has a pivotal role in vascular permeability and inflammatory responses. A recent study shows that increased serum moesin contributes to the sepsis-related endothelium damages by activating the Rock1/myosin light chain and NF-κB signaling.[32] Lysine-specific demethylase 3A promotes fibrosis in cardiomyocytes and, therefore, it has been suggested as a potential pharmacological target for cardiac hypertrophy and fibrosis.[33] Donor microvascular injury may lead to inappropriate and uncontrolled activation of the coagulation cascade and thrombin formation which may lead to the early development of tissue fibrosis in transplanted organs.[34] Based on these results we suggest that the high expression of these proteins may reflect the worse overall clinical status of these donors or donor hearts, which may be partly due to increased microvascular dysfunction and cardiomyocyte damage induced by events leading to brain death.

In conclusion, we demonstrate for the first time that brain-dead donors had a unique but heterogeneous proteomic profile. We also show those donor proteins involved in endothelial dysfunction, cardiomyocyte hypoxia, and fibrosis, and vascular cell growth and arteriogenesis may play a pivotal role in graft-related outcomes. Therefore, our results suggest that systematic characterization of circulating proteins may provide a deeper understanding of the effects of donor morbidity and brain death on donor organs and identify the transplants at increased risk.

Limitations of this post-hoc analysis of a prospective, single-center study are related to the nature of the analyses and the relatively small sample size which may have an impact on data quality. The patient cohort consisted of only clinically stable multi-organ donors that were accepted for HTx. However, the median age of donors was 44 years, which is equal to the median age of heart transplant donors in Europe, compared to 31 years in North America. Depletion of the top 12 high-abundance proteins enhances the sensitivity to detect lower-abundance proteins in plasma, but it could also lead to some bias as some of the depleted proteins may have a role in the pathophysiology of brain death or prediction of the outcomes. Further mechanistic studies with a larger patient population are needed to find any biomarker or therapeutic potential of these proteins and pathways.

Author contributions

AN, KL, JL, and RR: conceptualization and research funding; AN, KL, JL, KD, and RR: research design; AN, SS, KL, SJ, MS, EJH, JL, and RK: data collection; SJ, MS, KD, JL, and RR: contributed analytic tools; KD, JL, SJ, MS: data analysis; AN, JL, KD, MS, SJ, SS, and KL: data interpretation; AN, JL, KD, SS, MS, SJ, RK, and KL: writing of the paper

Disclosure Statement

The authors have no conflicts of interest to disclose.

This study was supported by grants from the Academy of Finland, Jane and Aatos Erkko Foundation, Sigrid Juselius Foundation, Biomedicum Helsinki Foundation, Helsinki University Hospital Research Funds, Finnish Cultural Foundation, Finnish Foundation for Cardiovascular Research, Finnish Medical Association, Finnish Transplantation Society, Paavo Nurmi Foundation, Päivikki and Sakari Sohlberg Foundation and University of Helsinki.

Acknowledgments

Special thanks to the HUSLAB transplantation unit for their relentless support in collecting and storing the plasma samples. Moreover, many thanks to the transplantation coordinators for their unwavering support in managing the logistics of the study. Thanks should also go to Eeva Rouvinen for her great amount of assistance in collecting and storing the patients' samples.

Supplementary materials

Supplementary material associated with this article can be found in the online version at https://doi.org/10.1016/j.healun.2021.11.011.

References

1. Anthony DC, Couch Y, Losey P, Evans MC. The systemic response to brain injury and disease. Brain Behav Immun 2012;26:534-40. https://doi.org/10.1016/j.bbi.2011.10.011.
2. Weber DJ, Allette YM, Wilkes DS, White FA. The HMGB1-RAGE inflammatory pathway: implications for brain injury-induced pulmonary dysfunction. Antioxid Redox Signal 2015;23:1316-28. https://doi.org/10.1089/ars.2015.6299.
3. Woodcock T, Morganti-Kossmann MC. The role of markers of inflammation in traumatic brain injury. Front Neurol 2013;4:18. https://doi.org/10.3389/fneur.2013.00018. Published 2013 Mar 4.
4. Watts RP, Thom O, Fraser JF. Inflammatory signalling associated with brain dead organ donation: from brain injury to brain stem death and posttransplant ischaemia reperfusion injury. J Transplant 2013; 2013:521369. https://doi.org/10.1155/2013/521369.
5. Vorlat A, Conraads VM, Jorens PG, et al. Donor B-type natriuretic peptide predicts early cardiac performance after heart transplantation. J Heart Lung Transplant 2012;31:579-84. https://doi.org/10.1016/j.healun.2012.02.009.
6. Madan S, Saeed O, Shin J, et al. Donor troponin and survival after cardiac transplantation: an analysis of the united network of organ sharing registry. Circ Heart Fail 2016;9:e002909. https://doi.org/10.1161/CIRCHEARTFAILURE.115.002909.
7. Bontha SV, Maluf DG, Mueller TF, Mas VR. Systems biology in kidney transplantation: the application of multi-omics to a complex model. Am J Transplant 2017;17:11-21. https://doi.org/10.1111/ajt.13881.
8. Nykänen AI, Holmström EJ, Tuuminen R, et al. Donor simvastatin treatment in heart transplantation. Circulation 2019;140:627-40. https://doi.org/10.1161/CIRCULATIONAHA.119.039932.
9. Holm M, Joenväärä S, Saraswat M, et al. Plasma protein expression differs between colorectal cancer patients depending on primary tumor location. Cancer Med 2020;9:5221-34. https://doi.org/10.1002/cam4.3178.
10. Rifai N, Gillette MA, Carr SA. Protein biomarker discovery and validation: the long and uncertain path to clinical utility. Nat Biotechnol 2006;24:971-83. https://doi.org/10.1038/nbt1235.
11. Watts RP, Thom O, Fraser JF. Inflammatory signalling associated with brain dead organ donation: from brain injury to brain stem death and posttransplant ischaemia reperfusion injury. J Transplant 2013; 2013:521369. https://doi.org/10.1155/2013/521369.
12. Foley JH, Conway EM. Cross talk pathways between coagulation and inflammation. Circ Res 2016;118:1392-408. https://doi.org/10.1161/CIRCRESAHA.116.306853.
13. Amara U, Flierl MA, Rittirsch D, et al. Molecular intercommunication between the complement and coagulation systems. J Immunol 2010;185:5628-36. https://doi.org/10.4049/jimmunol.0903678.
14. Atkinson C, Floerchinger B, Qiao F, et al. Donor brain death exacerbates complement-dependent ischemia/reperfusion injury in transplanted hearts. Circulation 2013;127:1290-9. https://doi.org/10.1161/CIRCULATIONAHA.112.000784.
15. Labarrere CA, Torry RJ, Nelson DR, et al. Vascular antithrombin and clinical outcome in heart transplant patients. Am J Cardiol 2001;87:425-31. https://doi.org/10.1016/s0002-9149(00)01395-3.
16. A-Gonzalez N, Bensinger SJ, Hong C, et al. Apoptotic cells promote their own clearance and immune tolerance through activation of the nuclear receptor LXR. Immunity 2009;31:245-58. https://doi.org/10.1016/j.immuni.2009.06.018.
17. Lei P, Baysa A, Nebb HI, et al. Activation of Liver X receptors in the heart leads to accumulation of intracellular lipids and attenuation of ischemia-reperfusion injury. Basic Res Cardiol 2013;108:323. https://doi.org/10.1007/s00395-012-0323-z.
18. Xu XR, Wang Y, Adili R, et al. Apolipoprotein A-IV binds αIIbβ3 integrin and inhibits thrombosis. Nat Commun 2018;9:3608. https://doi.org/10.1038/s41467-018-05806-0. Published 2018 Sep 6.
19. Weidmann H, Heikaus L, Long AT, Naudin C, Schlüter H, Renné T. The plasma contact system, a protease cascade at the nexus of inflammation, coagulation and immunity. Biochim Biophys Acta Mol Cell Res 2017;1864:2118-27. https://doi.org/10.1016/j.bbamcr.2017.07.009.
20. Lopatko Fagerström I, Ståhl AL, Mossberg M, et al. Blockade of the kallikrein-kinin system reduces endothelial complement activation in vascular inflammation. EBioMedicine 2019;47:319-28. https://doi.org/10.1016/j.ebiom.2019.08.020.
21. Giangreco NP, Lebreton G, Restaino S, et al. Plasma kallikrein predicts primary graft dysfunction after heart transplant. J Heart Lung Transplant 2021;40:1199-211. https://doi.org/10.1016/j.healun.2021.07.001.
22. García-Heredia A, Marsillach J, Rull A, et al. Paraoxonase-1 inhibits oxidized low-density lipoprotein-induced metabolic alterations and apoptosis in endothelial cells: a nondirected metabolomic study. Mediators Inflamm 2013;2013:156053. https://doi.org/10.1155/2013/156053.
23. Wende AR, Brahma MK, McGinnis GR, Young ME. Metabolic origins of heart failure. JACC Basic Transl Sci 2017;2:297-310. https://doi.org/10.1016/j.jacbts.2016.11.009.
24. Opie LH. Myocardial ischemia—metabolic pathways and implications of increased glycolysis. Cardiovasc Drugs Ther 1990;4(suppl 4)):777-90. https://doi.org/10.1007/BF00051275.
25. Lee L, Horowitz J, Frenneaux M. Metabolic manipulation in ischaemic heart disease, a novel approach to treatment. Eur Heart J 2004;25:634-41. https://doi.org/10.1016/j.ehj.2004.02.018.
26. Kaiserova K, Tang XL, Srivastava S, Bhatnagar A. Role of nitric oxide in regulating aldose reductase activation in the ischemic heart. J Biol Chem 2008;283:9101-12. https://doi.org/10.1074/jbc.M709671200.

27. Masson F, Thicoipe M, Gin H, et al. The endocrine pancreas in brain-dead donors. A prospective study in 25 patients. Transplantation 1993;56:363-7. https://doi.org/10.1097/00007890-199308000-00022.
28. Aljiffry M, Hassanain M, Schricker T, et al. Effect of insulin therapy using hyper-insulinemic normoglycemic clamp on inflammatory response in brain dead organ donors. Exp Clin Endocrinol Diabetes 2016;124:318-23. https://doi.org/10.1055/s-0042-101240.
29. Ranasinghe AM, McCabe CJ, Quinn DW, et al. How does glucose insulin potassium improve hemodynamic performance? Evidence for altered expression of beta-adrenoreceptor and calcium handling genes. Circulation 2006;114(1 suppl):I239-44. https://doi.org/10.1161/CIRCULATIONAHA.105.000760.
30. Schumacher-Bass SM, Vesely ED, Zhang L, et al. Role for myosin-V motor proteins in the selective delivery of Kv channel isoforms to the membrane surface of cardiac myocytes. Circ Res 2014;114:982-92. https://doi.org/10.1161/CIRCRESAHA.114.302711.
31. Faries PL, Rohan DI, Wyers MC, et al. Relationship of the 20S proteasome and the proteasome activator PA28 to atherosclerosis and intimal hyperplasia in the human vascular system. Ann Vasc Surg 2001;15:628-33. https://doi.org/10.1007/s10016-001-0055-2.
32. Chen Y, Wang J, Zhang L, Zhu J, Zeng Y, Huang JA. Moesin is a novel biomarker of endothelial injury in sepsis. J Immunol Res 2021;2021:6695679. https://doi.org/10.1155/2021/6695679. Published 2021 Feb 13.
33. Zhang QJ, Tran TAT, Wang M, et al. Histone lysine dimethyl-demethylase KDM3A controls pathological cardiac hypertrophy and fibrosis. Nat Commun 2018;9:5230. https://doi.org/10.1038/s41467-018-07173-2. Published 2018 Dec 7.
34. Yamani MH, Haji SA, Starling RC, et al. Myocardial ischemic-fibrotic injury after human heart transplantation is associated with increased progression of vasculopathy, decreased cellular rejection and poor long-term outcome. J Am Coll Cardiol 2002;39:970-7. https://doi.org/10.1016/s0735-1097(02)01714-x.

SUPPLEMENTAL MATERIAL

Plasma proteome of brain-dead organ donors predicts heart transplant outcome

Lukac et al.

Figure S1. PCA for Donor Simvastatin treatment.

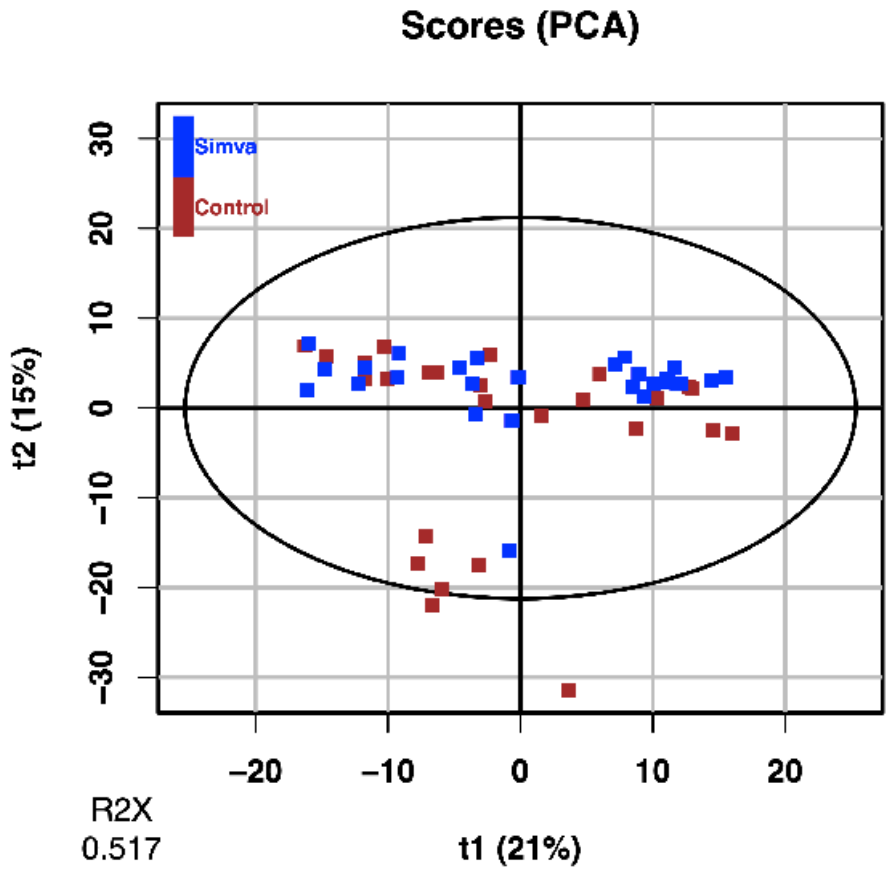

To exclude the effect of donor Simvastatin treatment on donor protein expression of 463 quantified proteins in 54 donors, PCA was performed. Examination of the PCA plot revealed that protein expression in donors did not cluster based on Simvastatin treatment. Blue: Donor Simvastatin treatment; Red: Donors without Simvastatin treatment.

Figure S2 A-F. Top pathways and enriched plasma proteins.

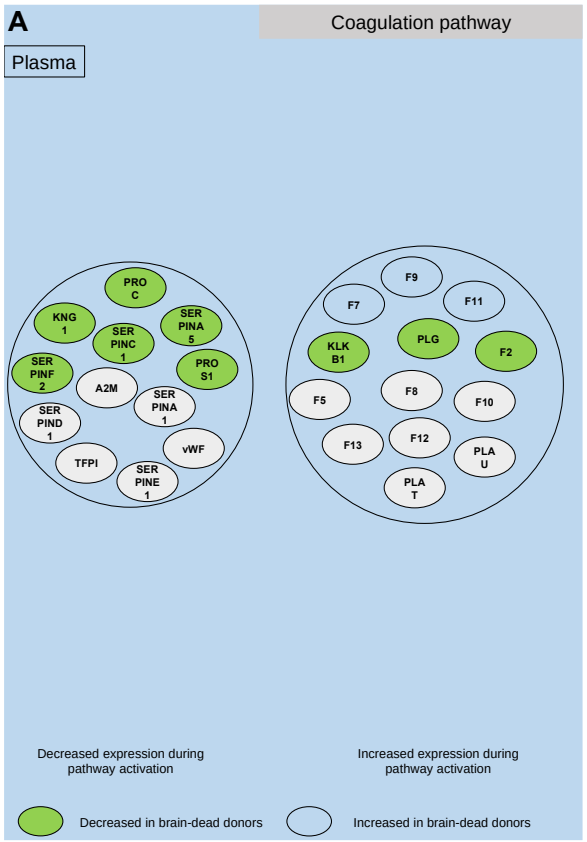

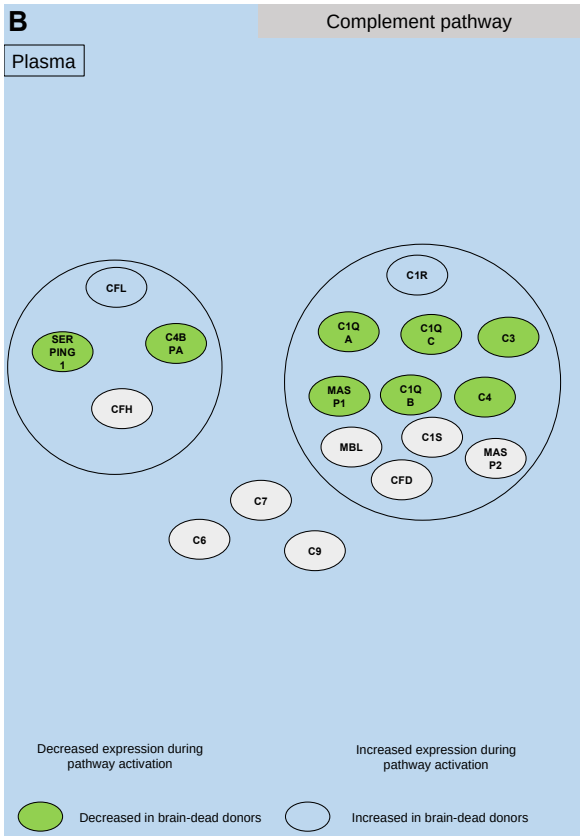
B
Complement pathway
Plasma
CFL
SER PING 1
C4B PA
CFH
C1R
C1Q A
C1Q C
C3
MAS P1
C1Q B
C4
MBL
C1S
MAS P2
CFD
C7
C6
C9
Decreased expression during pathway activation
Increased expression during pathway activation
Decreased in brain-dead donors
Increased in brain-dead donors

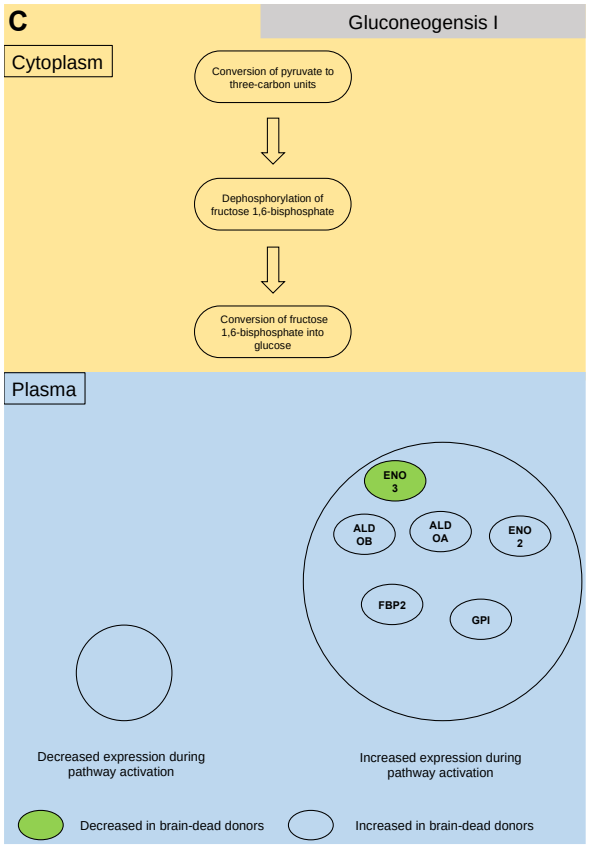
C
Gluconeogensis I
Cytoplasm
Conversion of pyruvate to three-carbon units
Dephosphorylation of fructose 1,6-bisphosphate
Conversion of fructose 1,6-bisphosphate into glucose
Plasma
ENO 3
ALD OB
ALD OA
ENO 2
FBP2
GPI
Decreased expression during pathway activation
Increased expression during pathway activation
Decreased in brain-dead donors
Increased in brain-dead donors

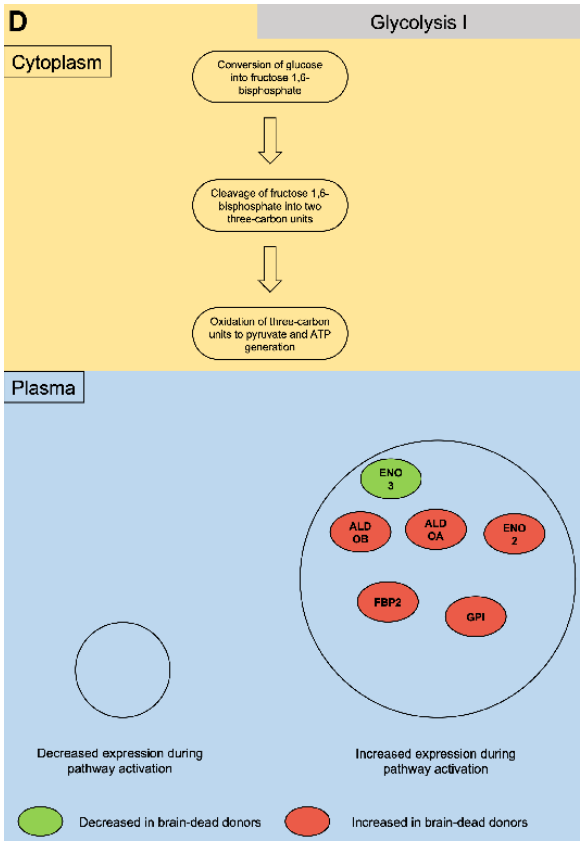
D
Glycolysis I
Cytoplasm
Conversion of glucose into fructose 1,6-bisphosphate
Cleavage of fructose 1,6-bisphosphate into two three-carbon units
Oxidation of three-carbon units to pyruvate and ATP generation
Plasma
ENO 3
ALD OB
ALD OA
ENO 2
FBP2
GPI
Decreased expression during pathway activation
Increased expression during pathway activation
Decreased in brain-dead donors
Increased in brain-dead donors

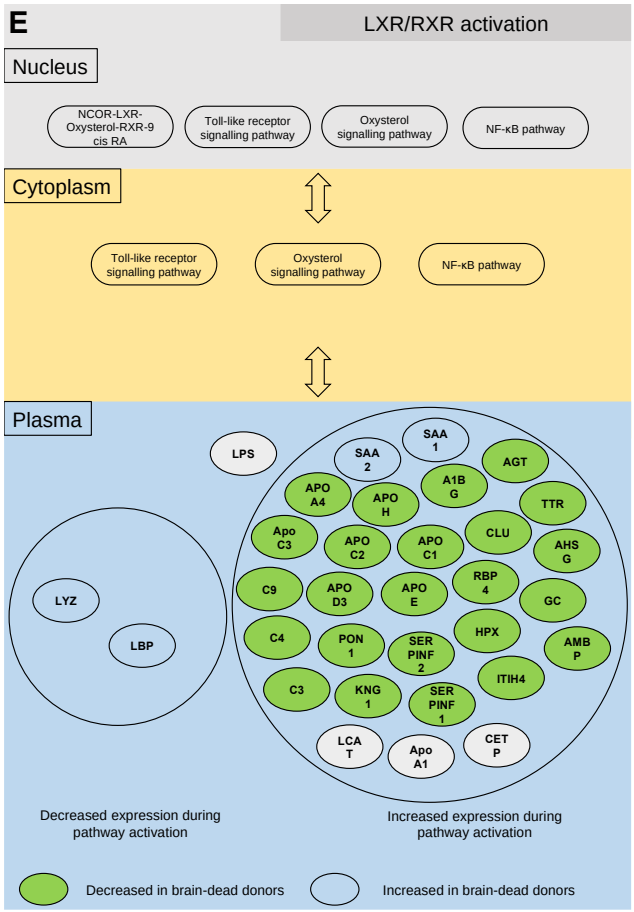
E
LXR/RXR activation
Nucleus
NCOR-LXR-Oxysterol-RXR-9 cis RA
Toll-like receptor signalling pathway
Oxysterol signalling pathway
NF-κB pathway
Cytoplasm
Toll-like receptor signalling pathway
Oxysterol signalling pathway
NF-κB pathway
Plasma
LPS
LYZ
LBP
SAA 1
SAA 2
AGT
A1BG
APO A4
APO H
TTR
Apo C3
APO C2
APO C1
CLU
AHSG
C9
APO D3
APO E
RBP 4
GC
C4
PON 1
SERPINF 2
HPX
AMBP
C3
KNG 1
SERPINF 1
ITIH4
LCAT
Apo A1
CETP
Decreased expression during pathway activation
Increased expression during pathway activation
Decreased in brain-dead donors
Increased in brain-dead donors

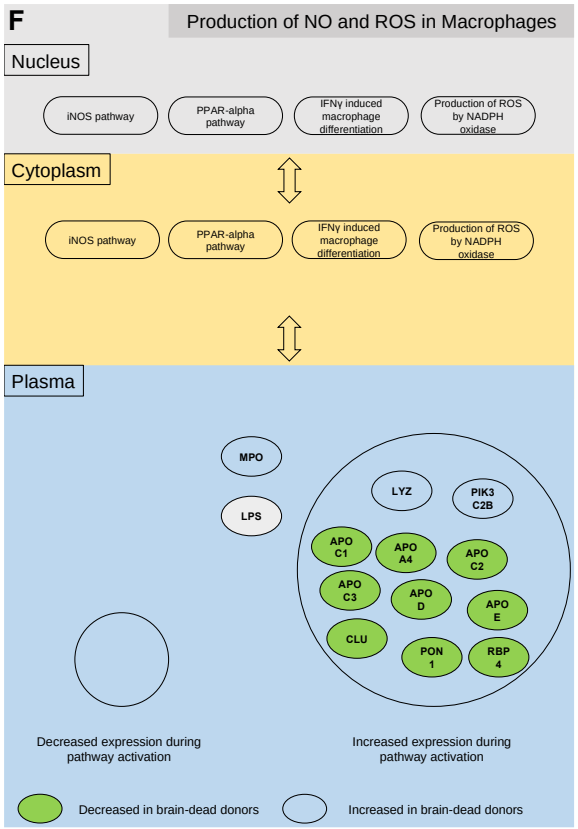

Six most significantly enriched pathways in brain-dead donors. Figure A-F pathways show key biological functions of pathways and plasma proteins that are associated with the pathways. Green: Protein with increased plasma expression in brain death and present in 237 identified proteins. Red: Protein with decreased plasma expression and present in 237 identified proteins. White: Proteins that are known to be associated with the pathway but not present among identified proteins.

Figure S3. Comparison of differentially expressed plasma proteins between subclusters of brain-dead donors.

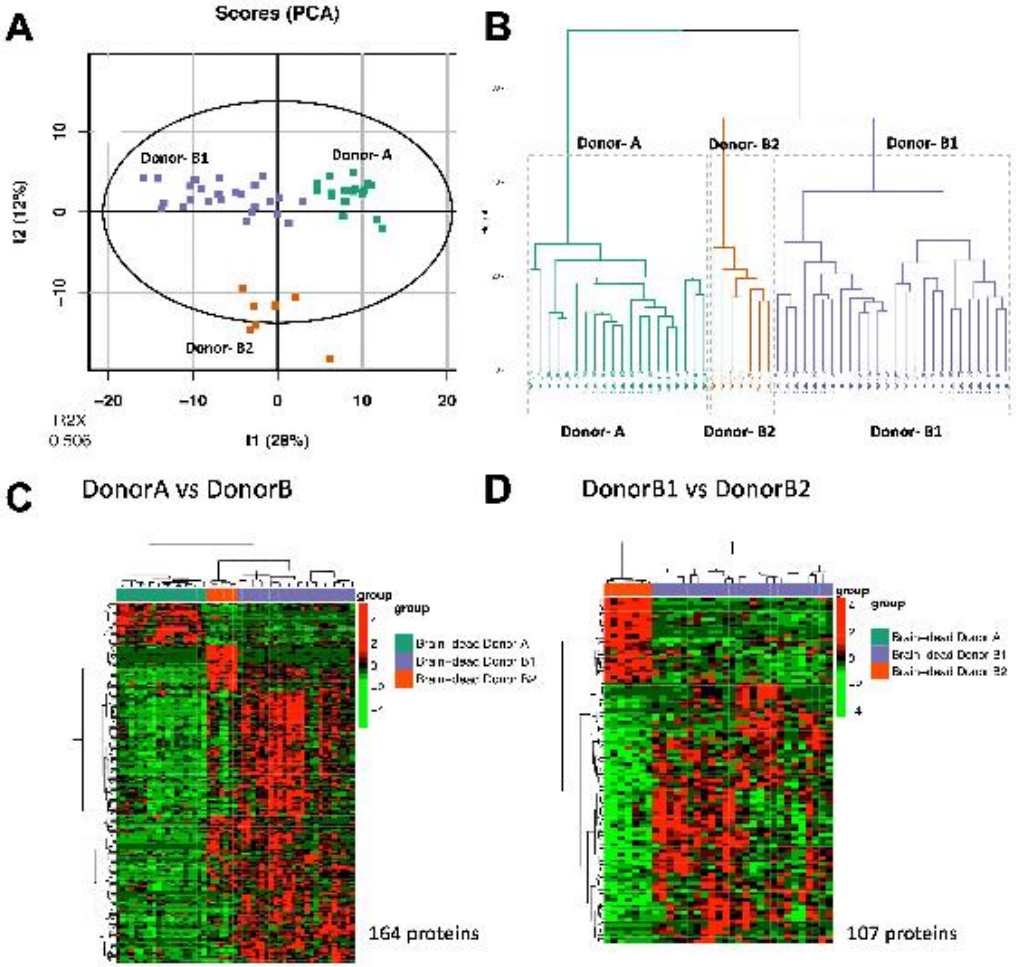

(A) PCA analyses on 53 donor plasma samples revealed 3 subclusters, donor subcluster A, B1, and B2. **(B)** Hierarchical clustering on 53 samples presents single donor samples grouping into the 3 donor subclusters A, B1, and B2. **(C)** Univariate analysis with

SOM revealed that 164 out of 237 identified proteins were significantly different between Donor A and Donor B. **(D)** SOM analysis showed that 107 out of 237 proteins were significantly different between Donor B1 and Donor B2.

Figure S4. Donor plasma proteomic immunological risk score.

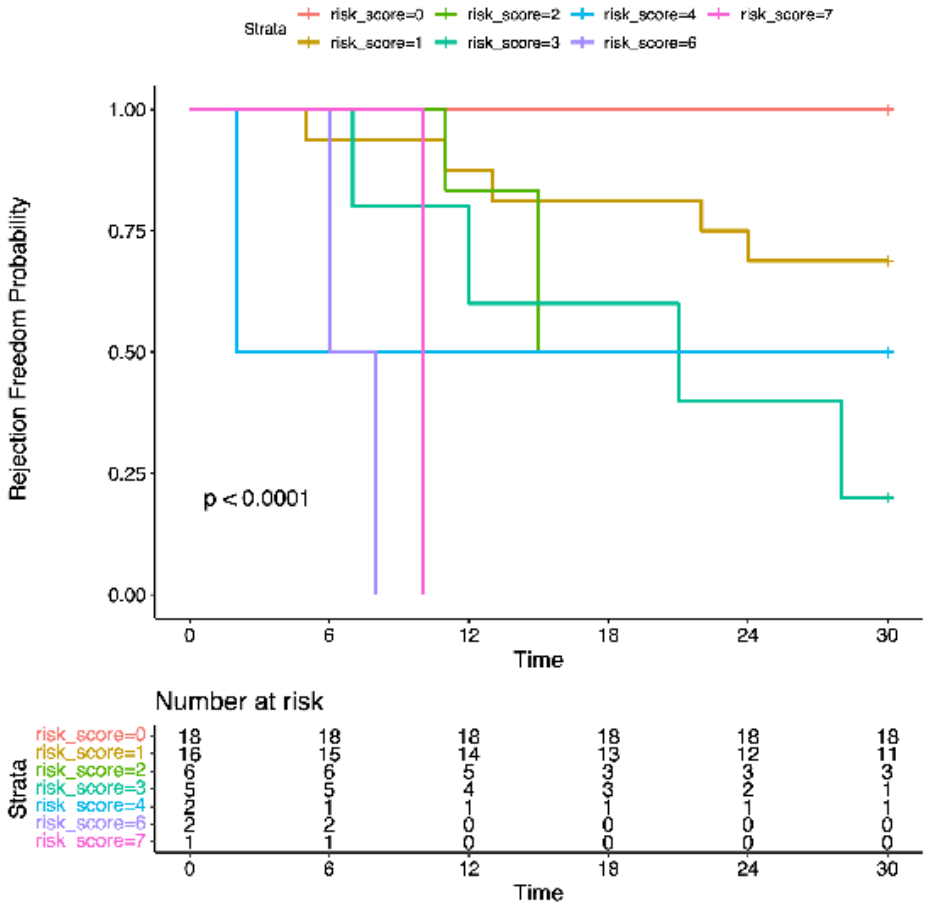

Figure S5. Multivariate Cox proportional hazards regression model for differently expressed protein levels in acute rejection with hemodynamic compromise.

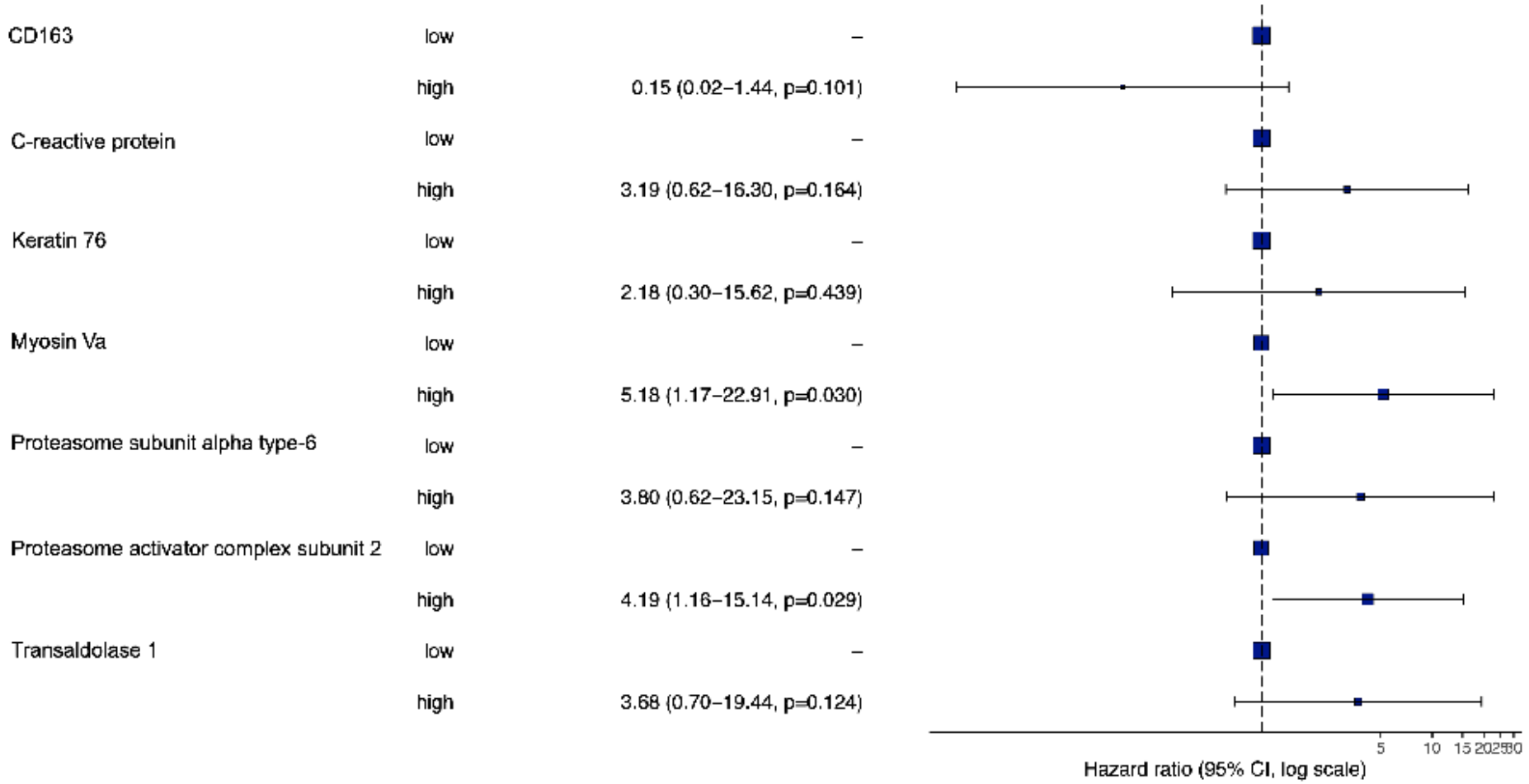

Table S1. List of 32 S-Plot proteins.

Name	Protein ID	Symbol	FDR-corrected p value	Control Mean	Donor Mean	fold change	VIPscore	AUC values
acetyl-CoA acetyltransferase 1	P24752	ACAT1	2.21E-08	47983	20018	0.42	1.56	0.68
alpha 2-HS glycoprotein	P02765	AHSG	9.88E-08	1595574	916884	0.57	1.43	0.59
Apolipoprotein A-IV	P06727	APOA4	6.69E-09	1929578	785611	0.41	1.60	0.82
apolipoprotein L3	O95236	APOL3	2.48E-08	26213	9881	0.38	1.40	0.59
complement C1q C chain	P02747	C1QC	2.41E-07	1791	11973	6.69	1.40	0.80
DEAD-box helicase 24	Q9GZR7	DDX24	1.17E-08	391010	167016	0.43	1.41	0.57
epoxide hydrolase 2	P34913	EPHX2	2.42E-08	12223	5502	0.45	1.51	0.72
extracellular matrix protein 1	Q16610	ECM1	7.79E-08	405296	184358	0.45	1.47	0.72
F-box and leucine-rich repeat protein 6	Q8N531	FBXL6	6.39E-08	18400	9828	0.53	1.45	0.61
glutathione S-transferase mu 2	P28161	GSTM2	1.03E-07	2193	934	0.43	1.48	0.55
Insulin-like growth factor-binding protein complex acid labile subunit	P35858	IGFALS	5.26E-09	195344	101311	0.52	1.57	0.50

Name	Protein ID	Symbol	FDR-corrected p value	Control Mean	Donor Mean	fold change	VIPscore	AUC values
kallikrein B1	P03952	KLKB1	1.84E-08	180135	112468	0.62	1.50	0.56
keratin 10	P13645	KRT10	7.64E-07	144102	289677	2.01	1.40	0.52
keratin 73	Q86Y46	KRT73	9.99E-09	131770	49267	0.37	1.54	0.74
kininogen 1	P01042	KNG1	1.87E-07	1285765	717267	0.56	1.46	0.68
leucine-rich alpha-2-glycoprotein 1	P02750	LRG1	3.73E-09	214535	626705	2.92	1.41	0.88
leucine-rich repeat-containing n 8 VRAC subunit C	Q8TDW0	LRRC8C	3.17E-09	46031	12211	0.27	1.71	0.72
mannan binding lectin serine peptidase 1	P48740	MASP1	1.72E-07	146910	65296	0.44	1.40	0.77
nuclear mitotic apparatus protein 1	Q14980	NUMA1	8.06E-08	19880	7942	0.40	1.45	0.69
paraoxonase 1	P27169	PON1	3.14E-08	272854	120975	0.44	1.52	0.60
plasminogen	P00747	PLG	2.02E-08	1331603	716638	0.54	1.50	0.68
protein C. inactivator of coagulation factors Va and VIIIa	P04070	PROC	1.19E-07	99945	45243	0.45	1.54	0.56
protein phosphatase 6 catalytic subunit	O00743	PPP6C	1.17E-08	25460	11375	0.45	1.57	0.51
pseudouridine synthase 7	Q96PZ0	PUS7	7.06E-09	140812	49457	0.35	1.66	0.72
quiescin sulfhydryl oxidase 1	O00391	QSOX1	6.21E-09	27085	11670	0.43	1.54	0.55

Name	Protein ID	Symbol	FDR-corrected p value	Control Mean	Donor Mean	fold change	VIPscore	AUC values
serpin family A member 4	P29622	SERPINA4	2.16E-07	311319	152482	0.49	1.46	0.58
serpin family A member 6	P08185	SERPINA6	7.05E-08	159307	72319	0.45	1.42	0.68
serpin family C member 1	P01008	SERPINC1	1.82E-08	1136537	651470	0.57	1.49	0.70
SPARC like 1	Q14515	SPARCL1	3.17E-09	142457	38149	0.27	1.70	0.67
tenascin C	P24821	TNC	5.07E-07	69637	23291	0.33	1.43	0.52
thyroid hormone receptor interactor 11	Q15643	TRIP11	6.69E-09	66661	18279	0.27	1.51	0.65
14-3-3 protein beta/alpha	P31946	YWHAB	8.07E-09	5459	2125	0.39	1.53	0.80

All the 32 S-Plot proteins passed the cut-off p(corr) [1] ±0.70 and p[1] ±0.1. Out of 32 proteins, 3 S-Plot proteins were upregulated, while 29 proteins were downregulated in brain-dead donors. MetaboAnalyst 4.0 (http://www.metaboanalyst.ca/) was used for receiver operating characteristic (ROC) analysis.

Table S2. Comparison of 463 quantified proteins with two or more unique peptides identified in brain-dead donors and healthy controls.

Protein Description	Protein Accession	Peptide count	Unique peptides	Confidence score	Donor Average	Control Average	Fold change	FDR-adjusted p value	Significant Donors vs Controls
10 kDa heat shock protein, mitochondrial OS=Homo sapiens GN=HSPE1 PE=1 SV=2	P61604	2	2	5,7	11,7	11,2	1	8,99E-01	ns.
14-3-3 protein beta/alpha OS=Homo sapiens GN=YWHAB PE=1 SV=3	P31946	5	2	35,3	2124,6	5458,5	0,4	3,31E-11	sign.
14-3-3 protein epsilon OS=Homo sapiens GN=YWHAE PE=1 SV=1	P62258	6	3	50,2	6014,9	3892,4	1,5	7,14E-02	ns.
14-3-3 protein eta OS=Homo sapiens GN=YWHAH PE=1 SV=4	Q04917	8	3	59,1	32564,2	64908,8	0,5	3,34E-02	sign.
14-3-3 protein gamma OS=Homo sapiens GN=YWHAG PE=1 SV=2	P61981	8	4	56,5	2515,5	1802,5	1,4	4,61E-03	sign.
14-3-3 protein theta OS=Homo sapiens GN=YWHAQ PE=1 SV=1	P27348	5	2	32,1	2776,6	5278,6	0,5	7,62E-05	sign.

Protein Description	Protein Accession	Peptide count	Unique peptides	Confidence score	Donor Average	Control Average	Fold change	FDR-adjusted p value	Significant Donors vs Controls
14-3-3 protein zeta/delta OS=Homo sapiens GN=YWHAZ PE=1 SV=1	P63104	13	5	80,5	2138,1	393,9	5,4	3,48E-04	sign.
4-aminobutyrate aminotransferase, mitochondrial OS=Homo sapiens GN=ABAT PE=1 SV=3	P80404	3	2	19	38,7	10,5	3,7	2,79E-01	ns.
4-hydroxyphenylpyruvate dioxygenase OS=Homo sapiens GN=HPD PE=1 SV=2	P32754	11	7	83,1	1378,6	454,3	3	1,97E-03	sign.
6-phosphogluconolactonase OS=Homo sapiens GN=PGLS PE=1 SV=2	O95336	5	2	42,3	17790,2	18928,3	0,9	8,71E-01	ns.
78 kDa glucose-regulated protein OS=Homo sapiens GN=HSPA5 PE=1 SV=2	P11021	4	2	33,9	41632,3	8500,9	4,9	7,75E-05	ns.
Acetyl-CoA acetyltransferase, mitochondrial OS=Homo sapiens GN=ACAT1 PE=1 SV=1	P24752	4	3	36,5	20017,8	47983,1	0,4	3,58E-09	sign.
Actin-depolymerizing factor OS=Homo sapiens GN=GSN PE=1 SV=1	A0A0A0MT01	108	2	898,7	4408,9	4282,6	1	8,56E-01	ns.

Protein Description	Protein Accession	Peptide count	Unique peptides	Confidence score	Donor Average	Control Average	Fold change	FDR-adjusted p value	Significant Donors vs Controls
Actin-related protein 3 OS=Homo sapiens GN=ACTR3 PE=1 SV=3	P61158	3	2	17,3	134,3	1,5	90,9	2,52E-05	sign.
Actin, cytoplasmic 1 OS=Homo sapiens GN=ACTB PE=1 SV=1	P60709	51	9	404,7	45524,9	8932,6	5,1	5,90E-06	sign.
Adiponectin OS=Homo sapiens GN=ADIPOQ PE=1 SV=1	Q15848	15	10	112,6	52407,8	10795,1	4,9	8,92E-03	ns.
Adseverin OS=Homo sapiens GN=SCIN PE=1 SV=4	Q9Y6U3	4	2	31,9	579,2	912,2	0,6	9,11E-02	ns.
Afamin OS=Homo sapiens GN=AFM PE=1 SV=1	P43652	134	85	1052,4	510833,7	796231	0,6	3,03E-08	sign.
Alanine aminotransferase 1 OS=Homo sapiens GN=GPT PE=1 SV=3	P24298	6	3	43,2	73,6	174,3	0,4	7,26E-03	sign.
Alcohol dehydrogenase 1A OS=Homo sapiens GN=ADH1A PE=1 SV=2	P07327	16	4	151,2	5515,9	135,7	40,7	5,47E-03	ns.
Alcohol dehydrogenase 1B OS=Homo sapiens GN=ADH1B PE=1 SV=2	P00325	18	4	142,6	4729,7	3601,3	1,3	1,22E-01	ns.

Protein Description	Protein Accession	Peptide count	Unique peptides	Confidence score	Donor Average	Control Average	Fold change	FDR-adjusted p value	Significant Donors vs Controls
Alcohol dehydrogenase 4 OS=Homo sapiens GN=ADH4 PE=1 SV=5	P08319	9	7	101,5	3923,5	1516,6	2,6	9,80E-02	ns.
Alcohol dehydrogenase class-3 OS=Homo sapiens GN=ADH5 PE=1 SV=4	P11766	2	2	5,8	5885,3	6024,6	1	8,46E-01	ns.
Alpha-1-acid glycoprotein 2 OS=Homo sapiens GN=ORM2 PE=1 SV=2	P19652	40	19	296,8	80573,7	80234,6	1	9,81E-01	ns.
Alpha-1-antichymotrypsin OS=Homo sapiens GN=SERPINA3 PE=1 SV=2	P01011	164	104	1150,5	1310112	725959,6	1,8	8,85E-06	sign.
Alpha-1,6-mannosylglycoprotein 6-beta-N-acetylglucosaminyltransferase A OS=Homo sapiens GN=MGAT5 PE=2 SV=1	Q09328	4	2	27,8	7188,5	12448	0,6	3,52E-02	sign.
Alpha-1B-glycoprotein OS=Homo sapiens GN=A1BG PE=1 SV=4	P04217	96	71	693	1231688,2	1429713,8	0,9	3,55E-02	sign.
Alpha-2-antiplasmin OS=Homo sapiens GN=SERPINF2 PE=1 SV=3	P08697	47	34	471,6	170813,9	219705,9	0,8	5,37E-06	sign.

Protein Description	Protein Accession	Peptide count	Unique peptides	Confidence score	Donor Average	Control Average	Fold change	FDR-adjusted p value	Significant Donors vs Controls
Alpha-2-HS-glycoprotein OS=Homo sapiens GN=AHSG PE=1 SV=1	P02765	77	55	499,4	916884,1	1595573,6	0,6	1,46E-11	sign.
Alpha-enolase OS=Homo sapiens GN=ENO1 PE=1 SV=2	P06733	32	15	220,2	58131,9	57900,7	1	9,71E-01	ns.
Alpha-protein kinase 2 OS=Homo sapiens GN=ALPK2 PE=2 SV=3	Q86TB3	13	5	81,4	37409,7	20165,1	1,9	2,83E-05	sign.
Aminopeptidase Q OS=Homo sapiens GN=LVRN PE=1 SV=4	Q6Q4G3	5	2	37,9	12518,8	16463	0,8	3,53E-01	ns.
Angiogenin OS=Homo sapiens GN=ANG PE=1 SV=1	P03950	5	3	31,4	7963,3	13044,8	0,6	1,36E-01	ns.
Angiotensinogen OS=Homo sapiens GN=AGT PE=1 SV=1	P01019	62	50	496	463777,3	592105,8	0,8	7,63E-03	sign.
Annexin A1 OS=Homo sapiens GN=ANXA1 PE=1 SV=2	P04083	28	14	214,8	184349,6	199860,7	0,9	3,34E-01	ns.

Protein Description	Protein Accession	Peptide count	Unique peptides	Confidence score	Donor Average	Control Average	Fold change	FDR-adjusted p value	Significant Donors vs Controls
Annexin A3 OS=Homo sapiens GN=ANXA3 PE=1 SV=3	P12429	5	2	27,7	48	37,9	1,3	3,25E-01	ns.
Antithrombin-III OS=Homo sapiens GN=SERPINC1 PE=1 SV=1	P01008	146	98	1141,2	651470	1136536,7	0,6	5,05E-11	sign.
Apolipoprotein A-IV OS=Homo sapiens GN=APOA4 PE=1 SV=3	P06727	120	76	1106,8	785611	1929578	0,4	6,90E-10	sign.
Apolipoprotein B receptor OS=Homo sapiens GN=APOBR PE=1 SV=2	Q0VD83	2	2	10,4	1241,9	7333,4	0,2	1,31E-01	ns.
Apolipoprotein C-I OS=Homo sapiens GN=APOC1 PE=1 SV=1	P02654	19	15	99,6	75814,7	121203,4	0,6	6,73E-03	sign.
Apolipoprotein C-II OS=Homo sapiens GN=APOC2 PE=1 SV=1	P02655	16	11	152,3	50097,7	93814,1	0,5	2,28E-03	sign.
Apolipoprotein C-III OS=Homo sapiens GN=APOC3 PE=1 SV=1	P02656	22	14	170,3	190765,9	421340,6	0,5	2,39E-03	sign.

Protein Description	Protein Accession	Peptide count	Unique peptides	Confidence score	Donor Average	Control Average	Fold change	FDR-adjusted p value	Significant Donors vs Controls
Apolipoprotein C-IV OS=Homo sapiens GN=APOC4 PE=1 SV=1	P55056	11	5	68,4	5793,6	5047,2	1,1	3,65E-01	ns.
Apolipoprotein D OS=Homo sapiens GN=APOD PE=1 SV=1	P05090	29	18	238,8	145602,7	290009,8	0,5	3,86E-06	sign.
Apolipoprotein E OS=Homo sapiens GN=APOE PE=1 SV=1	P02649	84	61	705,3	408030,2	561775	0,7	3,65E-03	sign.
Apolipoprotein F OS=Homo sapiens GN=APOF PE=1 SV=2	Q13790	5	2	22,9	4002,3	3702,8	1,1	8,26E-01	ns.
Apolipoprotein L1 OS=Homo sapiens GN=APOL1 PE=1 SV=5	O14791	32	16	203,4	16764,5	18279,2	0,9	5,00E-01	ns.
Apolipoprotein L3 OS=Homo sapiens GN=APOL3 PE=1 SV=3	O95236	3	3	17,7	9881	26212,6	0,4	1,51E-06	sign.
Apolipoprotein M OS=Homo sapiens GN=APOM PE=1 SV=2	O95445	24	10	162,9	41139,9	36618,3	1,1	1,65E-01	ns.

Protein Description	Protein Accession	Peptide count	Unique peptides	Confidence score	Donor Average	Control Average	Fold change	FDR-adjusted p value	Significant Donors vs Controls
Argininosuccinate lyase OS=Homo sapiens GN=ASL PE=1 SV=4	P04424	2	2	13,6	23141,9	56095,5	0,4	5,79E-06	sign.
Argininosuccinate synthase OS=Homo sapiens GN=ASS1 PE=1 SV=2	P00966	8	4	54,9	1616,8	1852,3	0,9	6,83E-01	ns.
Aspartate aminotransferase, cytoplasmic OS=Homo sapiens GN=GOT1 PE=1 SV=3	P17174	12	4	93,9	25	29,1	0,9	7,85E-01	ns.
ATP synthase subunit d, mitochondrial OS=Homo sapiens GN=ATP5H PE=1 SV=3	O75947	3	2	16,3	5394,7	4627,3	1,2	5,04E-01	ns.
ATP-dependent RNA helicase DDX24 OS=Homo sapiens GN=DDX24 PE=1 SV=1	Q9GZR7	8	3	48,7	11973,1	1791	6,7	4,15E-12	sign.
Attractin OS=Homo sapiens GN=ATRN PE=1 SV=2	O75882	85	45	637,6	220367,3	378144,2	0,6	8,03E-04	sign.
Band 3 anion transport protein OS=Homo sapiens GN=SLC4A1 PE=1 SV=3	P02730	5	5	24,9	153386,7	210502,7	0,7	3,64E-03	sign.

Protein Description	Protein Accession	Peptide count	Unique peptides	Confidence score	Donor Average	Control Average	Fold change	FDR-adjusted p value	Significant Donors vs Controls
Beta-2-glycoprotein 1 OS=Homo sapiens GN=APOH PE=1 SV=3	P02749	91	72	631,5	1307448,1	204492 1,7	0,6	1,00E-04	sign.
Beta-2-microglobulin OS=Homo sapiens GN=B2M PE=1 SV=1	P61769	14	8	106	13914	11064, 3	1,3	1,60E-02	sign.
Beta-actin-like protein 2 OS=Homo sapiens GN=ACTBL2 PE=1 SV=2	Q562R1	42	8	311,2	15341, 4	19553	0,8	3,13E-02	ns.
Beta-Ala-His dipeptidase OS=Homo sapiens GN=CNDP1 PE=1 SV=4	Q96KN2	40	19	321,7	102723,3	132832 ,5	0,8	5,63E-02	ns.
Beta-enolase OS=Homo sapiens GN=ENO3 PE=1 SV=5	P13929	12	3	78,2	389,4	1006,1	0,4	1,48E-04	sign.
Beta-ureidopropionase OS=Homo sapiens GN=UPB1 PE=1 SV=1	Q9UBR 1	2	2	11,8	4,6	0,4	10,8	4,11E-03	sign.
Betaine--homocysteine S-methyltransferase 1 OS=Homo sapiens GN=BHMT PE=1 SV=2	Q93088	11	4	71,6	4466,4	4551,8	1	8,27E-01	ns.

Protein Description	Protein Accession	Peptide count	Unique peptides	Confidence score	Donor Average	Control Average	Fold change	FDR-adjusted p value	Significant Donors vs Controls
Bifunctional epoxide hydrolase 2 OS=Homo sapiens GN=EPHX2 PE=1 SV=2	P34913	2	2	11,3	167016,3	391010,1	0,4	4,34E-10	sign.
Biotinidase OS=Homo sapiens GN=BTD PE=1 SV=2	P43251	27	12	170,9	17332,7	18293,8	0,9	3,16E-01	ns.
Bisphosphoglycerate mutase OS=Homo sapiens GN=BPGM PE=1 SV=2	P07738	3	2	22,2	9025,1	9057,1	1	9,89E-01	ns.
BPI fold-containing family A member 1 OS=Homo sapiens GN=BPIFA1 PE=1 SV=1	Q9NP55	2	2	15,2	86,8	34,3	2,5	2,84E-04	sign.
BPI fold-containing family B member 1 OS=Homo sapiens GN=BPIFB1 PE=1 SV=1	Q8TDL5	4	3	26,4	286,8	136	2,1	4,07E-03	sign.
BRCA1-A complex subunit RAP80 OS=Homo sapiens GN=UIMC1 PE=1 SV=2	Q96RL1	4	3	27,6	2400,5	3524	0,7	2,74E-02	sign.
C-C motif chemokine 24 OS=Homo sapiens GN=CCL24 PE=1 SV=2	O00175	3	2	17,4	1401,9	3927,3	0,4	2,43E-04	sign.

Protein Description	Protein Accession	Peptide count	Unique peptides	Confidence score	Donor Average	Control Average	Fold change	FDR-adjusted p value	Significant Donors vs Controls
C-Jun-amino-terminal kinase-interacting protein 3 OS=Homo sapiens GN=MAPK8IP3 PE=1 SV=3	Q9UPT6	5	2	46,6	21509,1	5210,7	4,1	3,82E-05	ns.
C-Jun-amino-terminal kinase-interacting protein 4 OS=Homo sapiens GN=SPAG9 PE=1 SV=4	O60271	11	4	84	784,8	340,3	2,3	2,25E-02	ns.
C-reactive protein OS=Homo sapiens GN=CRP PE=1 SV=1	P02741	29	22	171,8	319861,2	101566,9	3,1	4,02E-09	sign.
C4b-binding protein alpha chain OS=Homo sapiens GN=C4BPA PE=1 SV=2	P04003	82	51	695,5	495177,1	704148,1	0,7	2,40E-04	sign.
C4b-binding protein beta chain OS=Homo sapiens GN=C4BPB PE=1 SV=1	P20851	21	11	136,3	6807,2	7893,7	0,9	2,43E-01	ns.
Calmodulin OS=Homo sapiens GN=CALM1 PE=1 SV=2	P62158	4	2	37,3	7173,3	6136,2	1,2	9,26E-02	ns.
Calmodulin-like protein 3 OS=Homo sapiens GN=CALML3 PE=1 SV=2	P27482	5	2	42,6	14223,5	8163,5	1,7	1,13E-02	ns.

Protein Description	Protein Accession	Peptide count	Unique peptides	Confidence score	Donor Average	Control Average	Fold change	FDR-adjusted p value	Significant Donors vs Controls
Calmodulin-like protein 5 OS=Homo sapiens GN=CALML5 PE=1 SV=2	Q9NZT1	4	2	23,4	2491,9	386,7	6,4	7,05E-03	ns.
Cancer/testis antigen 2 OS=Homo sapiens GN=CTAG2 PE=1 SV=2	O75638	2	2	18,2	22898,2	32741,7	0,7	3,65E-01	ns.
Carbamoyl-phosphate synthase [ammonia], mitochondrial OS=Homo sapiens GN=CPS1 PE=1 SV=2	P31327	8	6	48,5	20295,2	12034,5	1,7	2,71E-03	sign.
Carbonic anhydrase 1 OS=Homo sapiens GN=CA1 PE=1 SV=2	P00915	27	19	245,2	44894,8	64214,3	0,7	1,97E-03	sign.
Carbonic anhydrase 2 OS=Homo sapiens GN=CA2 PE=1 SV=2	P00918	6	4	37	563,6	938,2	0,6	7,43E-02	ns.
Carbonic anhydrase 3 OS=Homo sapiens GN=CA3 PE=1 SV=3	P07451	14	8	108,6	4364,4	3397,7	1,3	3,00E-01	ns.
Carboxypeptidase B2 OS=Homo sapiens GN=CPB2 PE=1 SV=2	Q96IY4	19	8	119	23366,2	12495,4	1,9	1,82E-02	ns.

Protein Description	Protein Accession	Peptide count	Unique peptides	Confidence score	Donor Average	Control Average	Fold change	FDR-adjusted p value	Significant Donors vs Controls
Carboxypeptidase N catalytic chain OS=Homo sapiens GN=CPN1 PE=1 SV=1	P15169	34	16	249	153342	37820,5	4,1	7,59E-03	ns.
Carboxypeptidase N subunit 2 OS=Homo sapiens GN=CPN2 PE=1 SV=3	P22792	34	23	310,8	133012,9	232388,4	0,6	2,53E-05	sign.
Cartilage oligomeric matrix protein OS=Homo sapiens GN=COMP PE=1 SV=2	P49747	19	15	109,9	62044,5	69195,6	0,9	5,17E-01	ns.
Catalase OS=Homo sapiens GN=CAT PE=1 SV=3	P04040	40	24	313	17674,5	15884,1	1,1	5,14E-01	ns.
Cathepsin D OS=Homo sapiens GN=CTSD PE=1 SV=1	P07339	10	6	85,1	5997,9	11221	0,5	1,21E-05	sign.
CD5 antigen-like OS=Homo sapiens GN=CD5L PE=1 SV=1	O43866	2	2	11,3	999	659,5	1,5	1,43E-01	ns.
cDNA FLJ55673, highly similar to Complement factor B (EC 3.4.21.47) OS=Homo sapiens PE=1 SV=1	B4E1Z4	228	123	1923,4	1862796,1	163376 9,4	1,1	2,25E-02	ns.

Protein Description	Protein Accession	Peptide count	Unique peptides	Confidence score	Donor Average	Control Average	Fold change	FDR-adjusted p value	Significant Donors vs Controls
Centrosomal protein of 104 kDa OS=Homo sapiens GN=CEP104 PE=1 SV=1	O60308	12	2	72,3	8748,69	10199,9	0,9	2,55E-01	ns.
Ceruloplasmin OS=Homo sapiens GN=CP PE=1 SV=1	P00450	251	195	2128,8	2581549,1	3077861	0,8	2,78E-02	sign.
Charged multivesicular body protein 4b OS=Homo sapiens GN=CHMP4B PE=1 SV=1	Q9H444	3	2	27,5	132856,4	134761,4	1	8,60E-01	ns.
Charged multivesicular body protein 6 OS=Homo sapiens GN=CHMP6 PE=1 SV=3	Q96FZ7	2	2	19	657,7	4468	0,1	2,58E-04	sign.
Chitinase-3-like protein 1 OS=Homo sapiens GN=CHI3L1 PE=1 SV=2	P36222	18	9	110,6	8559,6	6033,7	1,4	4,79E-02	ns.
Cholinesterase OS=Homo sapiens GN=BCHE PE=1 SV=1	P06276	28	13	179,6	48698,6	133125	0,4	5,90E-06	sign.
Cingulin OS=Homo sapiens GN=CGN PE=1 SV=2	Q9P2M7	16	7	106,7	7972,3	15895,9	0,5	1,49E-06	sign.

Protein Description	Protein Accession	Peptide count	Unique peptides	Confidence score	Donor Average	Control Average	Fold change	FDR-adjusted p value	Significant Donors vs Controls
Clusterin OS=Homo sapiens GN=CLU PE=1 SV=1	P10909	69	40	608,1	316213,8	377125	0,8	4,73E-03	sign.
Coagulation factor IX OS=Homo sapiens GN=F9 PE=1 SV=2	P00740	37	24	251,1	38076,8	25913,7	1,5	1,20E-03	sign.
Coagulation factor VII OS=Homo sapiens GN=F7 PE=1 SV=1	P08709	3	2	15,6	18761,6	4288,8	4,4	8,42E-04	sign.
Coagulation factor X OS=Homo sapiens GN=F10 PE=1 SV=2	P00742	39	21	282,2	68770,9	31031,8	2,2	2,53E-02	ns.
Coagulation factor XI OS=Homo sapiens GN=F11 PE=1 SV=1	P03951	3	2	15,8	35971,7	22943,6	1,6	6,41E-04	sign.
Coagulation factor XII OS=Homo sapiens GN=F12 PE=1 SV=3	P00748	16	4	95	3384,1	4739	0,7	5,84E-02	ns.
Coiled-coil and C2 domain-containing protein 2A OS=Homo sapiens GN=CC2D2A PE=1 SV=3	Q9P2K1	3	2	16,3	2086,4	1008,3	2,1	2,38E-01	ns.

Protein Description	Protein Accession	Peptide count	Unique peptides	Confidence score	Donor Average	Control Average	Fold change	FDR-adjusted p value	Significant Donors vs Controls
Coiled-coil domain-containing protein 121 OS=Homo sapiens GN=CCDC121 PE=1 SV=1	Q6ZUS5	6	2	47,3	6302,2	956,7	6,6	1,33E-04	sign.
Coiled-coil domain-containing protein 18 OS=Homo sapiens GN=CCDC18 PE=1 SV=1	Q5T9S5	6	2	44,8	4723,2	5085,1	0,9	5,04E-01	ns.
Complement C1q subcomponent subunit A OS=Homo sapiens GN=C1QA PE=1 SV=2	P02745	5	3	36,9	12373,2	26578,6	0,5	7,50E-03	sign.
Complement C1q subcomponent subunit B OS=Homo sapiens GN=C1QB PE=1 SV=3	P02746	35	19	249,3	80131,5	134633,2	0,6	1,31E-09	sign.
Complement C1q subcomponent subunit C OS=Homo sapiens GN=C1QC PE=1 SV=3	P02747	19	12	129,7	38967,9	67113,5	0,6	4,84E-09	sign.
Complement C1r subcomponent OS=Homo sapiens GN=C1R PE=1 SV=2	P00736	84	52	713,4	353668,5	220794,5	1,6	1,12E-05	sign.
Complement C1r subcomponent-like protein OS=Homo sapiens GN=C1RL PE=1 SV=2	Q9NZP8	28	10	208,9	13593,1	13707,7	1	9,63E-01	ns.

Protein Description	Protein Accession	Peptide count	Unique peptides	Confidence score	Donor Average	Control Average	Fold change	FDR-adjusted p value	Significant Donors vs Controls
Complement C1s subcomponent OS=Homo sapiens GN=C1S PE=1 SV=1	P09871	81	55	647,9	297410,9	243239,9	1,2	2,25E-02	ns.
Complement C2 OS=Homo sapiens GN=C2 PE=1 SV=2	P06681	79	15	698,4	31268	34686,4	0,9	7,10E-02	ns.
Complement C3 OS=Homo sapiens GN=C3 PE=1 SV=2	P01024	660	498	5153,3	10547256,3	153071 80,8	0,7	1,80E-06	sign.
Complement C4-A OS=Homo sapiens GN=C4A PE=1 SV=2	P0C0L4	352	6	3040,4	39337,9	65596,4	0,6	8,90E-05	sign.
Complement C4-B OS=Homo sapiens GN=C4B PE=1 SV=2	P0C0L5	357	8	3104,3	83947,8	108888,1	0,8	2,94E-01	ns.
Complement C5 OS=Homo sapiens GN=C5 PE=1 SV=4	P01031	181	120	1551,1	513035,8	554871	0,9	2,45E-01	ns.
Complement component C6 OS=Homo sapiens GN=C6 PE=1 SV=3	P13671	89	54	735,9	101047	105774,6	1	3,88E-01	ns.

Protein Description	Protein Accession	Peptide count	Unique peptides	Confidence score	Donor Average	Control Average	Fold change	FDR-adjusted p value	Significant Donors vs Controls
Complement component C7 OS=Homo sapiens GN=C7 PE=1 SV=2	P10643	89	58	896,7	240872,5	240463,9	1	9,87E-01	ns.
Complement component C8 alpha chain OS=Homo sapiens GN=C8A PE=1 SV=2	P07357	76	51	595,8	125876,2	136175,7	0,9	2,13E-01	ns.
Complement component C8 beta chain OS=Homo sapiens GN=C8B PE=1 SV=3	P07358	73	56	668,2	267461,7	333282,3	0,8	8,22E-02	ns.
Complement component C8 gamma chain OS=Homo sapiens GN=C8G PE=1 SV=3	P07360	26	19	237	124324	151125	0,8	1,77E-02	sign.
Complement component C9 OS=Homo sapiens GN=C9 PE=1 SV=2	P02748	93	66	757,6	968224,5	1179408,8	0,8	7,97E-03	sign.
Complement factor D OS=Homo sapiens GN=CFD PE=1 SV=5	P00746	12	8	93,7	7455,7	4638,9	1,6	4,88E-02	ns.
Complement factor H OS=Homo sapiens GN=CFH PE=1 SV=4	P08603	146	78	1144,6	360528,2	411868,7	0,9	2,69E-01	ns.

Protein Description	Protein Accession	Peptide count	Unique peptides	Confidence score	Donor Average	Control Average	Fold change	FDR-adjusted p value	Significant Donors vs Controls
Complement factor H-related protein 1 OS=Homo sapiens GN=CFHR1 PE=1 SV=2	Q03591	29	3	202,9	401,1	171,8	2,3	1,97E-01	ns.
Complement factor H-related protein 2 OS=Homo sapiens GN=CFHR2 PE=1 SV=1	P36980	22	9	126,1	9168,3	7977,4	1,1	3,43E-01	ns.
Complement factor H-related protein 5 OS=Homo sapiens GN=CFHR5 PE=1 SV=1	Q9BXR6	15	5	90,4	363086,5	60262,2	6	1,12E-02	ns.
Complement factor I OS=Homo sapiens GN=CFI PE=1 SV=2	P05156	93	62	759,3	399960,2	233181,4	1,7	2,89E-05	sign.
Conserved oligomeric Golgi complex subunit 6 OS=Homo sapiens GN=COG6 PE=1 SV=2	Q9Y2V7	7	4	57,4	12370,3	21588	0,6	1,08E-03	sign.
Cornulin OS=Homo sapiens GN=CRNN PE=1 SV=1	Q9UBG3	2	2	11,7	514,4	79,3	6,5	7,29E-03	sign.
Corticosteroid-binding globulin OS=Homo sapiens GN=SERPINA6 PE=1 SV=1	P08185	30	21	229,1	72319,4	159307,1	0,5	6,66E-11	sign.

Protein Description	Protein Accession	Peptide count	Unique peptides	Confidence score	Donor Average	Control Average	Fold change	FDR-adjusted p value	Significant Donors vs Controls
COX assembly mitochondrial protein 2 homolog OS=Homo sapiens GN=CMC2 PE=1 SV=1	Q9NRP2	3	3	23,4	95636,7	83314,6	1,1	5,41E-01	ns.
Creatine kinase M-type OS=Homo sapiens GN=CKM PE=1 SV=2	P06732	35	22	257,9	55056,7	72236,2	0,8	2,90E-05	sign.
CTTNBP2 N-terminal-like protein OS=Homo sapiens GN=CTTNBP2NL PE=1 SV=2	Q9P2B4	3	2	30,1	30139,1	17667,8	1,7	4,40E-03	sign.
Cystatin-C OS=Homo sapiens GN=CST3 PE=1 SV=1	P01034	16	12	119,3	22408,5	16781,4	1,3	1,43E-01	ns.
Cystatin-SN OS=Homo sapiens GN=CST1 PE=1 SV=3	P01037	2	2	13	134,3	12,7	10,6	5,85E-02	ns.
Cysteine-rich secretory protein 3 OS=Homo sapiens GN=CRISP3 PE=1 SV=1	P54108	8	4	61,8	3290,9	1458,5	2,3	7,77E-04	sign.
Cytochrome b-c1 complex subunit 8 OS=Homo sapiens GN=UQCRQ PE=1 SV=4	O14949	3	3	21,7	2684,7	3332,6	0,8	2,44E-01	ns.
Cytochrome b5 OS=Homo sapiens GN=CYB5A PE=1 SV=2	P00167	3	2	16,9	152,9	80	1,9	3,34E-01	ns.

Protein Description	Protein Accession	Peptide count	Unique peptides	Confidence score	Donor Average	Control Average	Fold change	FDR-adjusted p value	Significant Donors vs Controls
Cytohesin-1 OS=Homo sapiens GN=CYTH1 PE=1 SV=1	Q15438	3	3	15,2	135,4	1192,5	0,1	4,56E-03	sign.
Cytoplasmic aconitate hydratase OS=Homo sapiens GN=ACO1 PE=1 SV=3	P21399	6	4	43,6	1406,8	1502,4	0,9	6,33E-01	ns.
Cytosolic 10-formyltetrahydrofolate dehydrogenase OS=Homo sapiens GN=ALDH1L1 PE=1 SV=2	O75891	2	2	10,4	4609,9	1270,5	3,6	9,82E-04	sign.
D-dopachrome decarboxylase OS=Homo sapiens GN=DDT PE=1 SV=3	P30046	3	2	22,5	762,2	102,7	7,4	2,43E-04	sign.
DDB1- and CUL4-associated factor 12-like protein 1 OS=Homo sapiens GN=DCAF12L1 PE=1 SV=1	Q5VU92	4	4	17,3	74930,5	114767	0,7	4,50E-03	sign.
Delta(3,5)-Delta(2,4)-dienoyl-CoA isomerase, mitochondrial OS=Homo sapiens GN=ECH1 PE=1 SV=2	Q13011	3	2	17,6	18156,3	5107,3	3,6	1,56E-10	sign.
DENN domain-containing protein 3 OS=Homo sapiens GN=DENND3 PE=1 SV=2	A2RUS2	19	6	113,6	17056,2	18132,3	0,9	5,06E-01	ns.

Protein Description	Protein Accession	Peptide count	Unique peptides	Confidence score	Donor Average	Control Average	Fold change	FDR-adjusted p value	Significant Donors vs Controls
Diacylglycerol kinase kappa OS=Homo sapiens GN=DGKK PE=1 SV=1	Q5KSL6	5	3	44,1	855,7	1449,8	0,6	1,34E-02	sign.
Digestive organ expansion factor homolog OS=Homo sapiens GN=DIEXF PE=1 SV=2	Q68CQ4	3	2	16,1	93	185,3	0,5	1,87E-02	sign.
DNA (cytosine-5)-methyltransferase 3-like OS=Homo sapiens PE=4 SV=1	Q9UJW3	2	2	10,4	154288,7	95376,9	1,6	2,50E-01	ns.
Dopamine beta-hydroxylase OS=Homo sapiens GN=DBH PE=1 SV=3	P09172	17	9	111,7	33618,2	32207,5	1	6,83E-01	ns.
Dual specificity protein kinase TTK OS=Homo sapiens GN=TTK PE=1 SV=2	P33981	33	12	222,5	34033,9	25021,2	1,4	2,07E-01	ns.
E3 ubiquitin-protein ligase BRE1A OS=Homo sapiens GN=RNF20 PE=1 SV=2	Q5VTR2	5	3	35,9	747,4	3552,2	0,2	1,40E-01	ns.
Early placenta insulin-like peptide OS=Homo sapiens GN=INSL4 PE=1 SV=1	Q14641	6	5	40,1	4895,2	3915,8	1,3	3,47E-01	ns.

Protein Description	Protein Accession	Peptide count	Unique peptides	Confidence score	Donor Average	Control Average	Fold change	FDR-adjusted p value	Significant Donors vs Controls
EGF-containing fibulin-like extracellular matrix protein 1 OS=Homo sapiens GN=EFEMP1 PE=1 SV=2	Q12805	20	16	156,7	13241,8	26431,6	0,5	4,72E-04	sign.
Electron transfer flavoprotein beta subunit lysine methyltransferase OS=Homo sapiens GN=ETFBKMT PE=1 SV=1	Q8IXQ9	13	3	82,2	10322,2	4125,8	2,5	1,26E-03	ns.
Endogenous retrovirus group K member 9 Pol protein OS=Homo sapiens GN=ERVK-9 PE=3 SV=3	P63128	7	3	43	5259,5	3958	1,3	1,85E-01	ns.
Envoplakin OS=Homo sapiens GN=EVPL PE=1 SV=3	Q92817	12	3	75,3	2127,5	1519,7	1,4	2,42E-01	ns.
Eomesodermin homolog OS=Homo sapiens GN=EOMES PE=1 SV=3	O95936	6	3	34,6	14449	7368,3	2	7,70E-05	sign.
Extracellular glycoprotein lacritin OS=Homo sapiens GN=LACRT PE=1 SV=1	Q9GZZ8	4	3	31,3	4037,6	4329,5	0,9	4,86E-01	ns.
Extracellular matrix protein 1 OS=Homo sapiens GN=ECM1 PE=1 SV=2	Q16610	17	12	122,5	5502,4	12222,8	0,5	1,89E-07	sign.

Protein Description	Protein Accession	Peptide count	Unique peptides	Confidence score	Donor Average	Control Average	Fold change	FDR-adjusted p value	Significant Donors vs Controls
Extracellular superoxide dismutase [Cu-Zn] OS=Homo sapiens GN=SOD3 PE=1 SV=2	P08294	8	3	56,7	16007,1	4775,9	3,4	4,57E-04	sign.
F-box only protein 33 OS=Homo sapiens GN=FBXO33 PE=1 SV=1	Q7Z6M2	6	2	33,5	105527,6	59739,7	1,8	1,72E-03	ns.
F-box only protein 6 OS=Homo sapiens GN=FBXO6 PE=1 SV=1	Q9NRD1	3	2	21,6	6233,1	6856,9	0,9	6,01E-01	ns.
F-box/LRR-repeat protein 6 OS=Homo sapiens GN=FBXL6 PE=2 SV=1	Q8N531	2	2	11,6	184358,2	405296,1	0,5	3,31E-11	sign.
Fatty acid-binding protein, epidermal OS=Homo sapiens GN=FABP5 PE=1 SV=3	Q01469	6	4	35,7	6986,1	2784,1	2,5	1,88E-03	sign.
Fatty acid-binding protein, liver OS=Homo sapiens GN=FABP1 PE=1 SV=1	P07148	4	2	33	9827,6	18398,7	0,5	1,37E-09	sign.
Fetuin-B OS=Homo sapiens GN=FETUB PE=1 SV=2	Q9UGM5	12	8	83,6	8846,6	11471,3	0,8	1,36E-01	ns.

Protein Description	Protein Accession	Peptide count	Unique peptides	Confidence score	Donor Average	Control Average	Fold change	FDR-adjusted p value	Significant Donors vs Controls
Ficolin-3 OS=Homo sapiens GN=FCN3 PE=1 SV=2	O75636	22	12	173,9	49894,5	31922,8	1,6	5,57E-02	ns.
Flavin reductase (NADPH) OS=Homo sapiens GN=BLVRB PE=1 SV=3	P30043	8	2	77,2	4926,5	957,6	5,1	4,65E-05	sign.
Follistatin-related protein 1 OS=Homo sapiens GN=FSTL1 PE=1 SV=1	Q12841	2	2	12,2	189,4	81,3	2,3	8,52E-05	sign.
Fructose-1,6-bisphosphatase 1 OS=Homo sapiens GN=FBP1 PE=1 SV=5	P09467	13	11	108	192066,3	146468,2	1,3	5,49E-02	ns.
Fructose-1,6-bisphosphatase isozyme 2 OS=Homo sapiens GN=FBP2 PE=1 SV=2	O00757	3	2	19,1	960,2	179,5	5,3	6,65E-04	sign.
Fructose-bisphosphate aldolase A OS=Homo sapiens GN=ALDOA PE=1 SV=2	P04075	23	7	187,8	36374,6	9131,9	4	1,03E-02	sign.
Fructose-bisphosphate aldolase B OS=Homo sapiens GN=ALDOB PE=1 SV=2	P05062	23	12	192,1	10022,9	5317,9	1,9	8,58E-04	sign.

Protein Description	Protein Accession	Peptide count	Unique peptides	Confidence score	Donor Average	Control Average	Fold change	FDR-adjusted p value	Significant Donors vs Controls
Fumarylacetoacetase OS=Homo sapiens GN=FAH PE=1 SV=2	P16930	8	7	69,4	4213,4	4994,5	0,8	3,25E-01	ns.
Galectin-3-binding protein OS=Homo sapiens GN=LGALS3BP PE=1 SV=1	Q08380	40	22	290,5	43228,8	50773	0,9	2,13E-01	ns.
Gamma-enolase OS=Homo sapiens GN=ENO2 PE=1 SV=3	P09104	9	3	68,3	12598,8	3888,9	3,2	4,87E-04	sign.
Gelsolin OS=Homo sapiens GN=GSN PE=1 SV=1	P06396	106	2	885,8	5904,3	7064,7	0,8	6,48E-01	ns.
Girdin OS=Homo sapiens GN=CCDC88A PE=1 SV=2	Q3V6T2	15	3	98,4	23519,4	19886,8	1,2	2,63E-01	ns.
Glucose-6-phosphate isomerase OS=Homo sapiens GN=GPI PE=1 SV=4	P06744	10	4	94,8	857,9	359,7	2,4	2,92E-04	sign.
Glucose-induced degradation protein 4 homolog OS=Homo sapiens GN=GID4 PE=2 SV=1	Q8IVV7	5	3	39,8	5127,6	1813,4	2,8	1,13E-03	ns.
Glutamate dehydrogenase 1, mitochondrial OS=Homo sapiens GN=GLUD1 PE=1 SV=2	P00367	3	2	12,2	4564,4	5154,9	0,9	3,79E-01	ns.

Protein Description	Protein Accession	Peptide count	Unique peptides	Confidence score	Donor Average	Control Average	Fold change	FDR-adjusted p value	Significant Donors vs Controls
Glutamate-rich protein 1 OS=Homo sapiens GN=ERICH1 PE=1 SV=1	Q86X53	2	2	11,7	8787,7	11723,1	0,7	2,39E-02	sign.
Glutathione peroxidase 3 OS=Homo sapiens GN=GPX3 PE=1 SV=2	P22352	29	18	277,1	84844,1	100036,9	0,8	2,48E-02	ns.
Glutathione S-transferase A1 OS=Homo sapiens GN=GSTA1 PE=1 SV=3	P08263	8	6	51,3	1292,8	500,7	2,6	2,70E-03	sign.
Glutathione S-transferase Mu 2 OS=Homo sapiens GN=GSTM2 PE=1 SV=2	P28161	4	3	20,9	933,9	2192,8	0,4	7,38E-07	sign.
Glutathione S-transferase omega-1 OS=Homo sapiens GN=GSTO1 PE=1 SV=2	P78417	6	5	42,9	2304,7	25,9	88,9	5,76E-04	sign.
Glyceraldehyde-3-phosphate dehydrogenase OS=Homo sapiens GN=GAPDH PE=1 SV=3	P04406	7	5	59,9	7733,4	2430	3,2	7,53E-02	ns.
Glycine amidinotransferase, mitochondrial OS=Homo sapiens GN=GATM PE=1 SV=1	P50440	3	2	19,8	15,4	29,2	0,5	1,43E-01	ns.

Protein Description	Protein Accession	Peptide count	Unique peptides	Confidence score	Donor Average	Control Average	Fold change	FDR-adjusted p value	Significant Donors vs Controls
Glycine N-acyltransferase OS=Homo sapiens GN=GLYAT PE=1 SV=3	Q6IB77	2	2	18	5462,2	29176	0,2	1,20E-04	sign.
Glycine N-acyltransferase-like protein 1 OS=Homo sapiens GN=GLYATL1 PE=1 SV=1	Q969I3	11	4	59,1	1812,5	730,8	2,5	1,31E-05	sign.
Glycine N-acyltransferase-like protein 2 OS=Homo sapiens GN=GLYATL2 PE=1 SV=1	Q8WU03	3	2	17,8	6472,2	7408,8	0,9	4,21E-01	ns.
Glycogen phosphorylase, brain form OS=Homo sapiens GN=PYGB PE=1 SV=5	P11216	2	2	10	828,3	863,3	1	8,65E-01	ns.
Glycogen phosphorylase, liver form OS=Homo sapiens GN=PYGL PE=1 SV=4	P06737	5	4	33	50,8	11,3	4,5	9,65E-02	ns.
Glyoxylate reductase/hydroxypyruvate reductase OS=Homo sapiens GN=GRHPR PE=1 SV=1	Q9UBQ7	3	2	16,7	51,8	36,4	1,4	2,47E-01	ns.
Golgi apparatus membrane protein TVP23 homolog C OS=Homo sapiens GN=TVP23C PE=1 SV=3	Q96ET8	6	2	32,8	620,1	800,6	0,8	5,43E-01	ns.

Protein Description	Protein Accession	Peptide count	Unique peptides	Confidence score	Donor Average	Control Average	Fold change	FDR-adjusted p value	Significant Donors vs Controls
Golgin subfamily A member 8M OS=Homo sapiens GN=GOLGA8M PE=3 SV=1	H3BSY2	6	3	47,7	200,6	537,7	0,4	1,26E-01	ns.
GRIP and coiled-coil domain-containing protein 2 OS=Homo sapiens GN=GCC2 PE=1 SV=4	Q8IWJ2	17	5	99,9	6163,6	12643,3	0,5	6,25E-07	sign.
Guanine nucleotide exchange factor DBS OS=Homo sapiens GN=MCF2L PE=1 SV=2	O15068	20	8	139,7	18961,7	30409,6	0,6	4,44E-02	sign.
Haptoglobin-related protein OS=Homo sapiens GN=HPR PE=2 SV=2	P00739	59	7	569	71642,6	117007,6	0,6	6,56E-02	ns.
Heat shock 70 kDa protein 6 OS=Homo sapiens GN=HSPA6 PE=1 SV=2	P17066	6	2	33,7	64,2	3,9	16,5	1,56E-01	ns.
Heat shock cognate 71 kDa protein OS=Homo sapiens GN=HSPA8 PE=1 SV=1	P11142	13	5	83,7	37033,1	66214,8	0,6	2,78E-03	sign.
Hemoglobin subunit alpha OS=Homo sapiens GN=HBA1 PE=1 SV=2	P69905	84	64	435,1	61723,5	54808,1	1,1	1,21E-01	ns.

Protein Description	Protein Accession	Peptide count	Unique peptides	Confidence score	Donor Average	Control Average	Fold change	FDR-adjusted p value	Significant Donors vs Controls
Hemoglobin subunit beta OS=Homo sapiens GN=HBB PE=1 SV=2	P68871	120	60	495	119970,1	127458,4	0,9	3,74E-01	ns.
Hemoglobin subunit delta OS=Homo sapiens GN=HBD PE=1 SV=2	P02042	76	12	372,6	7218,6	10854,2	0,7	2,43E-04	sign.
Hemoglobin subunit epsilon OS=Homo sapiens GN=HBE1 PE=1 SV=2	P02100	15	3	85,7	29233,9	10030,9	2,9	2,76E-09	sign.
Hemoglobin subunit gamma-2 OS=Homo sapiens GN=HBG2 PE=1 SV=2	P69892	23	2	180,5	5147,3	7963,6	0,6	3,06E-08	sign.
Hemoglobin subunit zeta OS=Homo sapiens GN=HBZ PE=1 SV=2	P02008	12	8	95,9	25986,5	68727,9	0,4	5,91E-04	sign.
Hemopexin OS=Homo sapiens GN=HPX PE=1 SV=2	P02790	157	111	1095	2178826,9	3039299,2	0,7	1,02E-03	sign.
Heparin cofactor 2 OS=Homo sapiens GN=SERPIND1 PE=1 SV=3	P05546	79	48	681,6	370363,5	299508,9	1,2	4,62E-01	ns.

Protein Description	Protein Accession	Peptide count	Unique peptides	Confidence score	Donor Average	Control Average	Fold change	FDR-adjusted p value	Significant Donors vs Controls
Hepatocyte growth factor activator OS=Homo sapiens GN=HGFAC PE=1 SV=1	Q04756	19	9	120,3	4681	5696,7	0,8	1,78E-02	sign.
Hepatocyte growth factor-like protein OS=Homo sapiens GN=MST1 PE=1 SV=2	P26927	24	12	154,2	19291,6	17914,5	1,1	4,66E-01	ns.
High mobility group nucleosome-binding domain-containing protein 5 OS=Homo sapiens GN=HMGN5 PE=1 SV=1	P82970	8	4	44,5	9332,8	1416,9	6,6	7,66E-03	ns.
Histidine protein methyltransferase 1 homolog OS=Homo sapiens GN=METTL18 PE=1 SV=1	O95568	19	5	111,8	2921,3	13245	0,2	8,91E-05	sign.
Histidine-rich glycoprotein OS=Homo sapiens GN=HRG PE=1 SV=1	P04196	71	49	492,8	415981	563961	0,7	6,30E-02	ns.
Histone acetyltransferase KAT2B OS=Homo sapiens GN=KAT2B PE=1 SV=3	Q92831	5	2	40,2	82107,6	142356,2	0,6	3,33E-10	sign.
Histone acetyltransferase KAT7 OS=Homo sapiens GN=KAT7 PE=1 SV=1	O95251	16	6	104,5	9812,9	17312,3	0,6	3,05E-01	ns.

Protein Description	Protein Accession	Peptide count	Unique peptides	Confidence score	Donor Average	Control Average	Fold change	FDR-adjusted p value	Significant Donors vs Controls
Histone H2B type 1-K OS=Homo sapiens GN=HIST1H2BK PE=1 SV=3	O60814	7	5	52,5	380	84,1	4,5	2,48E-02	sign.
Histone H4 OS=Homo sapiens GN=HIST1H4A PE=1 SV=2	P62805	7	6	73,3	4322,8	4329	1	9,88E-01	ns.
HIV Tat-specific factor 1 OS=Homo sapiens GN=HTATSF1 PE=1 SV=1	O43719	13	6	74,7	7718	23820,2	0,3	5,46E-05	sign.
Hyaluronan-binding protein 2 OS=Homo sapiens GN=HABP2 PE=1 SV=1	Q14520	33	21	224,9	83710,4	125222,3	0,7	8,49E-06	sign.
Ig kappa chain C region OS=Homo sapiens GN=IGKC PE=1 SV=1	P01834	14	9	154,2	26978,3	49872,7	0,5	6,25E-03	sign.
Immunoglobulin heavy variable 3-21 OS=Homo sapiens GN=IGHV3-21 PE=1 SV=1	A0A0B4J1V1	6	2	35,7	1024,9	1585,2	0,6	6,00E-02	ns.
Immunoglobulin J chain OS=Homo sapiens GN=JCHAIN PE=1 SV=4	P01591	7	6	54,5	6121,3	8258,7	0,7	2,56E-01	ns.

Protein Description	Protein Accession	Peptide count	Unique peptides	Confidence score	Donor Average	Control Average	Fold change	FDR-adjusted p value	Significant Donors vs Controls
Immunoglobulin lambda-like polypeptide 5 OS=Homo sapiens GN=IGLL5 PE=2 SV=2	Q6PL24	22	4	177,8	548,1	2081,9	0,3	2,63E-03	sign.
Indoleamine 2,3-dioxygenase 1 OS=Homo sapiens GN=IDO1 PE=1 SV=1	P14902	4	2	15,7	1128,7	843,5	1,3	1,57E-01	ns.
Insulin-like growth factor II OS=Homo sapiens GN=IGF2 PE=1 SV=1	P01344	6	3	34,8	11572,1	11448,4	1	9,65E-01	ns.
Insulin-like growth factor-binding protein 1 OS=Homo sapiens GN=IGFBP1 PE=1 SV=1	P08833	3	3	18	713,3	2233,9	0,3	2,52E-04	sign.
Insulin-like growth factor-binding protein 2 OS=Homo sapiens GN=IGFBP2 PE=1 SV=2	P18065	18	12	122,7	35168,3	17562,7	2	6,28E-09	sign.
Insulin-like growth factor-binding protein 3 OS=Homo sapiens GN=IGFBP3 PE=1 SV=2	P17936	20	12	127,7	5834,7	9951	0,6	4,78E-05	sign.
Insulin-like growth factor-binding protein 4 OS=Homo sapiens GN=IGFBP4 PE=1 SV=2	P22692	4	2	28,9	6031,5	6831,5	0,9	2,52E-01	ns.

Protein Description	Protein Accession	Peptide count	Unique peptides	Confidence score	Donor Average	Control Average	Fold change	FDR-adjusted p value	Significant Donors vs Controls
Insulin-like growth factor-binding protein complex acid labile subunit OS=Homo sapiens GN=IGFALS PE=1 SV=1	P35858	41	29	389,4	101310,7	195344,4	0,5	1,96E-11	sign.
Inter-alpha-trypsin inhibitor heavy chain H1 OS=Homo sapiens GN=ITIH1 PE=1 SV=3	P19827	108	65	990,8	696848,2	1089474,6	0,6	1,11E-05	sign.
Inter-alpha-trypsin inhibitor heavy chain H2 OS=Homo sapiens GN=ITIH2 PE=1 SV=2	P19823	146	88	1130,5	878019,1	1291365,6	0,7	5,75E-09	sign.
Inter-alpha-trypsin inhibitor heavy chain H3 OS=Homo sapiens GN=ITIH3 PE=1 SV=2	Q06033	74	41	567,6	128589,2	81487,1	1,6	1,19E-07	sign.
Inter-alpha-trypsin inhibitor heavy chain H4 OS=Homo sapiens GN=ITIH4 PE=1 SV=4	Q14624	168	117	1414,9	948612,1	1357404,4	0,7	3,27E-05	sign.
Interleukin enhancer-binding factor 3 OS=Homo sapiens GN=ILF3 PE=1 SV=3	Q12906	4	3	23,5	98017,5	133598,7	0,7	2,37E-02	sign.
Isocitrate dehydrogenase [NADP] cytoplasmic OS=Homo sapiens GN=IDH1 PE=1 SV=2	O75874	15	10	113,6	36387,1	45092,1	0,8	1,77E-02	sign.

Protein Description	Protein Accession	Peptide count	Unique peptides	Confidence score	Donor Average	Control Average	Fold change	FDR-adjusted p value	Significant Donors vs Controls
Izumo sperm-egg fusion protein 2 OS=Homo sapiens GN=IZUMO2 PE=2 SV=1	Q6UXV1	3	2	23,5	616,4	981,6	0,6	1,15E-02	sign.
Kallistatin OS=Homo sapiens GN=SERPINA4 PE=1 SV=3	P29622	52	39	449,5	152482,4	311319,1	0,5	3,83E-08	sign.
Kanadaptin OS=Homo sapiens GN=SLC4A1AP PE=1 SV=1	Q9BWU0	5	2	32,7	37364,4	19849,5	1,9	1,27E-05	sign.
KAT8 regulatory NSL complex subunit 3 OS=Homo sapiens GN=KANSL3 PE=1 SV=2	Q9P2N6	5	2	43,8	1934,3	5191,1	0,4	3,00E-01	ns.
Keratin-associated protein 2-3 OS=Homo sapiens GN=KRTAP2-3 PE=1 SV=2	P0C7H8	2	2	20,8	235,5	263,8	0,9	8,91E-01	ns.
Keratin-associated protein 4-3 OS=Homo sapiens GN=KRTAP4-3 PE=2 SV=2	Q9BYR4	2	2	13	37,9	7,9	4,8	1,78E-02	ns.
Keratin, type I cuticular Ha3-I OS=Homo sapiens GN=KRT33A PE=2 SV=2	O76009	15	2	110,1	3983,9	3423,1	1,2	4,00E-01	ns.

Protein Description	Protein Accession	Peptide count	Unique peptides	Confidence score	Donor Average	Control Average	Fold change	FDR-adjusted p value	Significant Donors vs Controls
Keratin, type I cuticular Ha5 OS=Homo sapiens GN=KRT35 PE=2 SV=5	Q92764	9	6	51	2026	944,4	2,1	4,86E-02	ns.
Keratin, type I cytoskeletal 10 OS=Homo sapiens GN=KRT10 PE=1 SV=6	P13645	43	25	429,6	289677,2	144101,7	2	2,73E-08	sign.
Keratin, type I cytoskeletal 12 OS=Homo sapiens GN=KRT12 PE=1 SV=1	Q99456	14	3	93,9	11963,3	5811,6	2,1	1,37E-05	sign.
Keratin, type I cytoskeletal 13 OS=Homo sapiens GN=KRT13 PE=1 SV=4	P13646	30	13	241,8	12839,4	9317,1	1,4	4,56E-03	sign.
Keratin, type I cytoskeletal 14 OS=Homo sapiens GN=KRT14 PE=1 SV=4	P02533	46	10	385,7	10080,9	8802,8	1,1	6,40E-01	ns.
Keratin, type I cytoskeletal 15 OS=Homo sapiens GN=KRT15 PE=1 SV=3	P19012	32	7	222,7	17502,7	24305,8	0,7	7,44E-03	sign.
Keratin, type I cytoskeletal 16 OS=Homo sapiens GN=KRT16 PE=1 SV=4	P08779	50	21	436,5	25430,7	45085	0,6	7,70E-05	sign.

Protein Description	Protein Accession	Peptide count	Unique peptides	Confidence score	Donor Average	Control Average	Fold change	FDR-adjusted p value	Significant Donors vs Controls
Keratin, type I cytoskeletal 17 OS=Homo sapiens GN=KRT17 PE=1 SV=2	Q04695	34	9	245,2	54364,5	47060	1,2	3,07E-01	ns.
Keratin, type I cytoskeletal 18 OS=Homo sapiens GN=KRT18 PE=1 SV=2	P05783	16	8	85,4	5036,8	6920,4	0,7	1,54E-02	sign.
Keratin, type I cytoskeletal 19 OS=Homo sapiens GN=KRT19 PE=1 SV=4	P08727	20	4	144,6	208,5	26,9	7,8	1,52E-01	ns.
Keratin, type I cytoskeletal 9 OS=Homo sapiens GN=KRT9 PE=1 SV=3	P35527	76	41	694,9	105511	89194,9	1,2	4,82E-01	ns.
Keratin, type II cuticular Hb2 OS=Homo sapiens GN=KRT82 PE=3 SV=3	Q9NSB4	9	3	64,4	266,8	231,1	1,2	7,85E-01	ns.
Keratin, type II cuticular Hb5 OS=Homo sapiens GN=KRT85 PE=1 SV=1	P78386	22	6	178,3	70816,9	84241,2	0,8	1,57E-01	ns.
Keratin, type II cuticular Hb6 OS=Homo sapiens GN=KRT86 PE=1 SV=1	O43790	22	2	149,8	192,9	31,9	6	9,11E-05	sign.

Protein Description	Protein Accession	Peptide count	Unique peptides	Confidence score	Donor Average	Control Average	Fold change	FDR-adjusted p value	Significant Donors vs Controls
Keratin, type II cytoskeletal 1 OS=Homo sapiens GN=KRT1 PE=1 SV=6	P04264	100	52	913,9	613562,8	171567,2	3,6	2,02E-03	sign.
Keratin, type II cytoskeletal 1b OS=Homo sapiens GN=KRT77 PE=2 SV=3	Q7Z794	54	24	433	39477,3	67438,6	0,6	1,16E-05	sign.
Keratin, type II cytoskeletal 2 epidermal OS=Homo sapiens GN=KRT2 PE=1 SV=2	P35908	60	28	462,8	156214,7	121559,7	1,3	2,92E-01	ns.
Keratin, type II cytoskeletal 2 oral OS=Homo sapiens GN=KRT76 PE=1 SV=2	Q01546	32	10	224,1	9762,2	15308,1	0,6	5,30E-03	sign.
Keratin, type II cytoskeletal 4 OS=Homo sapiens GN=KRT4 PE=1 SV=4	P19013	28	11	245,5	143409	1759,6	8,1	3,59E-05	sign.
Keratin, type II cytoskeletal 5 OS=Homo sapiens GN=KRT5 PE=1 SV=3	P13647	35	6	281,4	145082	12300,7	1,2	3,33E-01	ns.
Keratin, type II cytoskeletal 6A OS=Homo sapiens GN=KRT6A PE=1 SV=3	P02538	36	4	304,1	3577	13648,7	0,3	5,48E-04	sign.

Protein Description	Protein Accession	Peptide count	Unique peptides	Confidence score	Donor Average	Control Average	Fold change	FDR-adjusted p value	Significant Donors vs Controls
Keratin, type II cytoskeletal 6B OS=Homo sapiens GN=KRT6B PE=1 SV=5	P04259	50	12	388,9	97522,6	84808,2	1,1	2,36E-01	ns.
Keratin, type II cytoskeletal 7 OS=Homo sapiens GN=KRT7 PE=1 SV=5	P08729	22	2	168,5	4031,6	3940,5	1	9,38E-01	ns.
Keratin, type II cytoskeletal 73 OS=Homo sapiens GN=KRT73 PE=1 SV=1	Q86Y46	10	2	88,6	49266,6	131769,7	0,4	1,11E-10	sign.
Keratin, type II cytoskeletal 74 OS=Homo sapiens GN=KRT74 PE=1 SV=2	Q7RTS7	14	2	79,7	2426,2	2902,9	0,8	2,53E-01	ns.
Keratin, type II cytoskeletal 78 OS=Homo sapiens GN=KRT78 PE=2 SV=2	Q8N1N4	3	2	21,6	21128,2	28864,8	0,7	1,26E-03	sign.
Keratin, type II cytoskeletal 79 OS=Homo sapiens GN=KRT79 PE=1 SV=2	Q5XKE5	13	3	74,5	4957,5	7224,6	0,7	1,73E-03	sign.
Kinesin heavy chain isoform 5A OS=Homo sapiens GN=KIF5A PE=1 SV=2	Q12840	5	2	36,5	8052,4	292,3	27,6	6,85E-05	sign.

Protein Description	Protein Accession	Peptide count	Unique peptides	Confidence score	Donor Average	Control Average	Fold change	FDR-adjusted p value	Significant Donors vs Controls
Kinetochore protein Spc24 OS=Homo sapiens GN=SPC24 PE=1 SV=2	Q8NBT2	4	2	34,1	68693,1	6203,4	11,1	4,86E-04	sign.
Kininogen-1 OS=Homo sapiens GN=KNG1 PE=1 SV=2	P01042	95	66	783,9	717267,4	1285765,5	0,6	2,31E-08	sign.
L-lactate dehydrogenase A chain OS=Homo sapiens GN=LDHA PE=1 SV=2	P00338	17	9	143,7	3626,8	2835,1	1,3	1,33E-01	ns.
L-lactate dehydrogenase B chain OS=Homo sapiens GN=LDHB PE=1 SV=2	P07195	29	13	248,9	18719,6	18975,6	1	8,98E-01	ns.
L-lactate dehydrogenase C chain OS=Homo sapiens GN=LDHC PE=1 SV=4	P07864	14	3	99,8	5219,2	1898,2	2,7	4,68E-03	ns.
L-xylulose reductase OS=Homo sapiens GN=DCXR PE=1 SV=2	Q7Z4W1	3	3	21,1	67,5	4	16,7	2,75E-02	sign.
Lactotransferrin OS=Homo sapiens GN=LTF PE=1 SV=6	P02788	23	16	182,6	2297,1	1363,5	1,7	6,74E-02	ns.

Protein Description	Protein Accession	Peptide count	Unique peptides	Confidence score	Donor Average	Control Average	Fold change	FDR-adjusted p value	Significant Donors vs Controls
Leucine-rich alpha-2-glycoprotein OS=Homo sapiens GN=LRG1 PE=1 SV=2	P02750	62	45	530,8	626705,1	214534,5	2,9	1,50E-14	sign.
Leucine-rich PPR motif-containing protein, mitochondrial OS=Homo sapiens GN=LRPPRC PE=1 SV=3	P42704	8	2	58	1834,1	1736,6	1,1	6,26E-01	ns.
Leucine-rich repeat-containing protein 74A OS=Homo sapiens GN=LRRC74A PE=2 SV=2	Q0VAA2	7	2	58,6	2292,7	1576,8	1,5	1,60E-02	ns.
Leucine-rich single-pass membrane protein 1 OS=Homo sapiens GN=LSMEM1 PE=1 SV=1	Q8N8F7	4	2	36,2	461,9	55,9	8,3	1,50E-02	sign.
Lipocalin-1 OS=Homo sapiens GN=LCN1 PE=1 SV=1	P31025	9	5	67,4	582	177,2	3,3	2,51E-03	ns.
Lipopolysaccharide-binding protein OS=Homo sapiens GN=LBP PE=1 SV=3	P18428	19	11	150,3	48582,9	9971,1	4,9	1,46E-11	sign.
Long-chain fatty acid transport protein 6 OS=Homo sapiens GN=SLC27A6 PE=2 SV=1	Q9Y2P4	10	4	62,5	9042,2	19698,8	0,5	5,56E-02	ns.

Protein Description	Protein Accession	Peptide count	Unique peptides	Confidence score	Donor Average	Control Average	Fold change	FDR-adjusted p value	Significant Donors vs Controls
Lumican OS=Homo sapiens GN=LUM PE=1 SV=2	P51884	37	22	308,5	81739,7	141901,4	0,6	9,58E-07	sign.
Lutropin subunit beta OS=Homo sapiens GN=LHB PE=1 SV=3	P01229	2	2	11,5	11326,6	10917,2	1	8,37E-01	ns.
Lymphatic vessel endothelial hyaluronic acid receptor 1 OS=Homo sapiens GN=LYVE1 PE=1 SV=2	Q9Y5Y7	3	3	15,2	1247,6	3028,6	0,4	2,49E-06	sign.
Lysine-specific demethylase 3A OS=Homo sapiens GN=KDM3A PE=1 SV=4	Q9Y4C1	5	2	31,6	1739	3280,3	0,5	1,45E-02	sign.
Lysosome-associated membrane glycoprotein 5 OS=Homo sapiens GN=LAMP5 PE=1 SV=1	Q9UJQ1	2	2	13,7	18041,2	54,3	332	6,23E-02	ns.
Lysozyme C OS=Homo sapiens GN=LYZ PE=1 SV=1	P61626	15	8	145,9	37343,6	29523,3	1,3	2,27E-03	sign.
Malate dehydrogenase, cytoplasmic OS=Homo sapiens GN=MDH1 PE=1 SV=4	P40925	22	12	167,7	18147,7	20097,2	0,9	2,14E-01	ns.

Protein Description	Protein Accession	Peptide count	Unique peptides	Confidence score	Donor Average	Control Average	Fold change	FDR-adjusted p value	Significant Donors vs Controls
Malate dehydrogenase, mitochondrial OS=Homo sapiens GN=MDH2 PE=1 SV=3	P40926	3	3	21,3	18,1	9,3	1,9	1,58E-01	ns.
Mammaglobin-B OS=Homo sapiens GN=SCGB2A1 PE=1 SV=1	O75556	3	3	24,7	625	389,6	1,6	2,12E-01	ns.
Mannan-binding lectin serine protease 1 OS=Homo sapiens GN=MASP1 PE=1 SV=3	P48740	25	13	217,7	65296,4	146910,1	0,4	1,32E-09	sign.
Matrix metalloproteinase-9 OS=Homo sapiens GN=MMP9 PE=1 SV=3	P14780	2	2	12,3	231,8	158,6	1,5	1,01E-01	ns.
Metalloproteinase inhibitor 1 OS=Homo sapiens GN=TIMP1 PE=1 SV=1	P01033	14	6	121,3	10594,8	13709,2	0,8	2,16E-02	sign.
Microtubule-associated serine/threonine-protein kinase 2 OS=Homo sapiens GN=MAST2 PE=1 SV=2	Q6P0Q8	7	2	42,3	637,8	113,2	5,6	3,71E-01	ns.
Mitogen-activated protein kinase kinase kinase 15 OS=Homo sapiens GN=MAP3K15 PE=1 SV=2	Q6ZN16	15	5	107,9	4794,8	5669,5	0,8	9,56E-02	ns.

Protein Description	Protein Accession	Peptide count	Unique peptides	Confidence score	Donor Average	Control Average	Fold change	FDR-adjusted p value	Significant Donors vs Controls
MOB kinase activator 2 OS=Homo sapiens GN=MOB2 PE=1 SV=1	Q70IA6	2	2	18,2	15552,4	4597,3	3,4	3,30E-03	ns.
Moesin OS=Homo sapiens GN=MSN PE=1 SV=3	P26038	8	4	55,2	4076,5	10249,8	0,4	8,04E-03	sign.
Monocarboxylate transporter 4 OS=Homo sapiens GN=SLC16A3 PE=1 SV=1	O15427	4	4	22,7	6025,3	3574,2	1,7	1,50E-02	ns.
Monocyte differentiation antigen CD14 OS=Homo sapiens GN=CD14 PE=1 SV=2	P08571	21	11	174,2	6530,8	8969,2	0,7	9,10E-02	ns.
MORC family CW-type zinc finger protein 2 OS=Homo sapiens GN=MORC2 PE=1 SV=2	Q9Y6X9	12	3	67,9	6778,7	5611,1	1,2	1,89E-02	sign.
Myeloperoxidase OS=Homo sapiens GN=MPO PE=1 SV=1	P05164	18	13	135	9697,3	3953,1	2,5	5,75E-09	sign.
Myoglobin OS=Homo sapiens GN=MB PE=1 SV=2	P02144	34	26	210	67948,7	68140	1	9,81E-01	ns.

Protein Description	Protein Accession	Peptide count	Unique peptides	Confidence score	Donor Average	Control Average	Fold change	FDR-adjusted p value	Significant Donors vs Controls
Myosin light chain 5 OS=Homo sapiens GN=MYL5 PE=2 SV=1	Q02045	7	4	48,1	10651,8	12039,1	0,9	1,57E-01	ns.
Myosin-10 OS=Homo sapiens GN=MYH10 PE=1 SV=3	P35580	11	2	73,2	24871,3	7686,3	3,2	5,41E-04	sign.
N-acetylmuramoyl-L-alanine amidase OS=Homo sapiens GN=PGLYRP2 PE=1 SV=1	Q96PD5	58	41	519,9	320942,5	515633,1	0,6	3,60E-06	sign.
Neugrin OS=Homo sapiens GN=NGRN PE=1 SV=2	Q9NPE2	5	3	37,1	7769	7887,7	1	9,42E-01	ns.
Neutrophil defensin 1 OS=Homo sapiens GN=DEFA1 PE=1 SV=1	P59665	5	5	46,3	2191,2	1513,6	1,4	1,29E-01	ns.
Nicolin-1 OS=Homo sapiens GN=NICN1 PE=2 SV=1	Q9BSH3	2	2	11,4	18967,1	9170,5	2,1	8,96E-04	sign.
Nuclear mitotic apparatus protein 1 OS=Homo sapiens GN=NUMA1 PE=1 SV=2	Q14980	7	3	46,9	7942,3	19879,5	0,4	4,12E-08	sign.

Protein Description	Protein Accession	Peptide count	Unique peptides	Confidence score	Donor Average	Control Average	Fold change	FDR-adjusted p value	Significant Donors vs Controls
Opiorphin prepropeptide OS=Homo sapiens GN=OPRPN PE=1 SV=2	Q99935	2	2	11,8	10,6	6,5	1,6	7,48E-01	ns.
Pantothenate kinase 2, mitochondrial OS=Homo sapiens GN=PANK2 PE=1 SV=3	Q9BZ23	2	2	18,4	19325,6	24668,6	0,8	6,37E-01	ns.
Peflin OS=Homo sapiens GN=PEF1 PE=1 SV=1	Q9UBV8	6	5	56,7	230755,1	233532,1	1	9,67E-01	ns.
Pentraxin-related protein PTX3 OS=Homo sapiens GN=PTX3 PE=1 SV=3	P26022	13	8	95,2	37866,1	5329,3	7,1	1,37E-05	sign.
Peptidase inhibitor 16 OS=Homo sapiens GN=PI16 PE=1 SV=1	Q6UXB8	3	2	17,1	320,9	443,7	0,7	4,96E-01	ns.
Peptidyl-prolyl cis-trans isomerase A OS=Homo sapiens GN=PPIA PE=1 SV=2	P62937	8	4	53,1	4813,8	886,4	5,4	7,03E-06	sign.
Peripheral-type benzodiazepine receptor-associated protein 1 OS=Homo sapiens GN=TSPOAP1 PE=1 SV=2	O95153	7	3	57,1	16001,4	37657,4	0,4	9,57E-05	sign.

Protein Description	Protein Accession	Peptide count	Unique peptides	Confidence score	Donor Average	Control Average	Fold change	FDR-adjusted p value	Significant Donors vs Controls
Peroxiredoxin-1 OS=Homo sapiens GN=PRDX1 PE=1 SV=1	Q06830	12	6	83,3	9849	6697,6	1,5	1,87E-03	sign.
Peroxiredoxin-2 OS=Homo sapiens GN=PRDX2 PE=1 SV=5	P32119	25	16	245,8	5674,1	3236,3	1,8	1,86E-04	sign.
Peroxiredoxin-6 OS=Homo sapiens GN=PRDX6 PE=1 SV=3	P30041	6	4	40,5	10581,3	11344,1	0,9	4,94E-01	ns.
Phosphatidylcholine-sterol acyltransferase OS=Homo sapiens GN=LCAT PE=1 SV=1	P04180	11	5	65,3	4150,1	1971,2	2,1	8,04E-03	ns.
Phosphatidylethanolamine-binding protein 1 OS=Homo sapiens GN=PEBP1 PE=1 SV=3	P30086	5	4	33,7	4634,2	2847	1,6	1,64E-02	ns.
Phosphatidylinositol 4-phosphate 3-kinase C2 domain-containing subunit beta OS=Homo sapiens GN=PIK3C2B PE=1 SV=2	O00750	6	2	44,1	8658,6	5300,5	1,6	1,40E-02	sign.

Protein Description	Protein Accession	Peptide count	Unique peptides	Confidence score	Donor Average	Control Average	Fold change	FDR-adjusted p value	Significant Donors vs Controls
Phosphatidylinositol 4,5-bisphosphate 3-kinase catalytic subunit alpha isoform OS=Homo sapiens GN=PIK3CA PE=1 SV=2	P42336	8	2	49	2988,3	2971,9	1	9,81E-01	ns.
Phosphatidylinositol 5-phosphate 4-kinase type-2 gamma OS=Homo sapiens GN=PIP4K2C PE=1 SV=3	Q8TBX8	19	7	131,9	7973,3	16563,4	0,5	1,70E-09	sign.
Phosphatidylinositol-glycan-specific phospholipase D OS=Homo sapiens GN=GPLD1 PE=1 SV=3	P80108	18	8	123,8	89700,4	75395,5	1,2	2,33E-01	ns.
Phosphoglucomutase-1 OS=Homo sapiens GN=PGM1 PE=1 SV=3	P36871	5	4	31,1	1200,7	421,3	2,8	7,02E-04	sign.
Phosphoglycerate kinase 1 OS=Homo sapiens GN=PGK1 PE=1 SV=3	P00558	13	9	97,6	26656,3	30445,2	0,9	1,84E-01	ns.
Pigment epithelium-derived factor OS=Homo sapiens GN=SERPINF1 PE=1 SV=4	P36955	55	30	460,3	235869,3	315935,8	0,7	1,57E-05	sign.
Plasma kallikrein OS=Homo sapiens GN=KLKB1 PE=1 SV=1	P03952	85	55	737,7	112468,1	180134,6	0,6	5,47E-10	sign.

Protein Description	Protein Accession	Peptide count	Unique peptides	Confidence score	Donor Average	Control Average	Fold change	FDR-adjusted p value	Significant Donors vs Controls
Plasma protease C1 inhibitor OS=Homo sapiens GN=SERPING1 PE=1 SV=2	P05155	115	82	879,8	622295,1	890167,6	0,7	3,11E-04	sign.
Plasma serine protease inhibitor OS=Homo sapiens GN=SERPINA5 PE=1 SV=3	P05154	11	5	81	2096,3	4242,6	0,5	2,87E-10	sign.
Plasminogen activator inhibitor 1 OS=Homo sapiens GN=SERPINE1 PE=1 SV=1	P05121	9	8	59,6	242,2	108,7	2,2	2,48E-01	ns.
Plasminogen OS=Homo sapiens GN=PLG PE=1 SV=2	P00747	147	92	1407,5	716638,3	1331602,7	0,5	2,50E-10	sign.
Plasminogen-like protein B OS=Homo sapiens GN=PLGLB1 PE=3 SV=1	Q02325	12	2	134,6	270	50,5	5,3	9,48E-06	sign.
Plastin-2 OS=Homo sapiens GN=LCP1 PE=1 SV=6	P13796	28	15	209,3	104777,1	116027,2	0,9	4,86E-01	ns.
Platelet basic protein OS=Homo sapiens GN=PPBP PE=1 SV=3	P02775	9	3	56,5	1414,8	1440,3	1	9,36E-01	ns.

Protein Description	Protein Accession	Peptide count	Unique peptides	Confidence score	Donor Average	Control Average	Fold change	FDR-adjusted p value	Significant Donors vs Controls
Platelet factor 4 OS=Homo sapiens GN=PF4 PE=1 SV=2	P02776	4	3	25,8	3173,3	5364	0,6	1,54E-02	sign.
Platelet-activating factor acetylhydrolase IB subunit gamma OS=Homo sapiens GN=PAFAH1B3 PE=1 SV=1	Q15102	5	5	29,7	33302,3	22596,1	1,5	3,45E-01	ns.
Polymeric immunoglobulin receptor OS=Homo sapiens GN=PIGR PE=1 SV=4	P01833	15	12	121,6	3348,4	2414,6	1,4	1,94E-01	ns.
POTE ankyrin domain family member E OS=Homo sapiens GN=POTEE PE=2 SV=3	Q6S8J3	104	5	768,8	69170,3	45548,5	1,5	8,14E-05	sign.
POTE ankyrin domain family member F OS=Homo sapiens GN=POTEF PE=1 SV=2	A5A3E0	116	3	849	1551,3	1130,9	1,4	3,44E-01	ns.
POTE ankyrin domain family member I OS=Homo sapiens GN=POTEI PE=3 SV=1	P0CG38	74	2	527,3	210658,7	319594,2	0,7	7,03E-06	sign.
POTE ankyrin domain family member J OS=Homo sapiens GN=POTEJ PE=3 SV=1	P0CG39	77	2	540,4	6312,6	8471,6	0,7	8,30E-02	ns.

Protein Description	Protein Accession	Peptide count	Unique peptides	Confidence score	Donor Average	Control Average	Fold change	FDR-adjusted p value	Significant Donors vs Controls
Pregnancy zone protein OS=Homo sapiens GN=PZP PE=1 SV=4	P20742	88	39	641,4	72038,5	106148,5	0,7	5,80E-04	sign.
Profilin-1 OS=Homo sapiens GN=PFN1 PE=1 SV=2	P07737	5	2	38,4	1125	776,1	1,4	1,15E-01	ns.
Prolactin-inducible protein OS=Homo sapiens GN=PIP PE=1 SV=1	P12273	8	6	64,3	1318,7	606,3	2,2	1,15E-01	ns.
Proline-rich protein 4 OS=Homo sapiens GN=PRR4 PE=1 SV=3	Q16378	4	2	15,4	135,7	19,7	6,9	7,10E-02	ns.
Properdin OS=Homo sapiens GN=CFP PE=1 SV=2	P27918	27	18	184,5	110308	173271,7	0,6	6,71E-05	sign.
Prosaposin OS=Homo sapiens GN=PSAP PE=1 SV=2	P07602	6	3	34,7	10153,4	15172,1	0,7	2,10E-03	sign.
Prostaglandin reductase 1 OS=Homo sapiens GN=PTGR1 PE=1 SV=2	Q14914	5	3	35,1	1152,1	3881,6	0,3	1,49E-06	sign.
Prostaglandin-H2 D-isomerase OS=Homo sapiens GN=PTGDS PE=1 SV=1	P41222	5	3	41,9	20836	22347,9	0,9	3,25E-01	ns.

Protein Description	Protein Accession	Peptide count	Unique peptides	Confidence score	Donor Average	Control Average	Fold change	FDR-adjusted p value	Significant Donors vs Controls
Proteasome activator complex subunit 2 OS=Homo sapiens GN=PSME2 PE=1 SV=4	Q9UL46	2	2	11,4	97,4	298,3	0,3	1,49E-06	sign.
Proteasome subunit alpha type-6 OS=Homo sapiens GN=PSMA6 PE=1 SV=1	P60900	2	2	11,7	670,3	237,3	2,8	3,85E-03	sign.
Proteasome subunit beta type-8 OS=Homo sapiens GN=PSMB8 PE=1 SV=3	P28062	8	3	46	3751,2	3708	1	9,81E-01	ns.
Protein ABHD14A-ACY1 (Fragment) OS=Homo sapiens GN=ABHD14A-ACY1 PE=4 SV=1	A0A1B0GW23	8	5	57,6	77007,1	61902,1	1,2	2,78E-02	ns.
Protein AMBP OS=Homo sapiens GN=AMBP PE=1 SV=1	P02760	68	48	629,5	398536,8	626878,9	0,6	4,57E-07	sign.
Protein C1orf194 OS=Homo sapiens GN=C1orf194 PE=2 SV=1	Q5T5A4	3	2	28,9	1014,1	4014	0,3	6,13E-02	ns.
Protein Daple OS=Homo sapiens GN=CCDC88C PE=1 SV=3	Q9P219	6	2	47,5	43705,7	37700,9	1,2	1,95E-01	ns.

Protein Description	Protein Accession	Peptide count	Unique peptides	Confidence score	Donor Average	Control Average	Fold change	FDR-adjusted p value	Significant Donors vs Controls
Protein deglycase DJ-1 OS=Homo sapiens GN=PARK7 PE=1 SV=2	Q99497	3	2	24	611,1	987	0,6	2,92E-01	ns.
Protein FAM161A OS=Homo sapiens GN=FAM161A PE=1 SV=2	Q3B820	8	2	53,9	53177,5	45343	1,2	3,47E-01	ns.
Protein FAM193A OS=Homo sapiens GN=FAM193A PE=1 SV=2	P78312	3	2	32,9	9713,8	15801,1	0,6	7,02E-04	sign.
Protein GLYATL1P3 OS=Homo sapiens GN=GLYATL1P3 PE=4 SV=1	A0A0U1RQE8	9	5	55,4	9307,6	3064,6	3	8,59E-04	sign.
Protein LINC00238 OS=Homo sapiens GN=LINC00238 PE=4 SV=1	A0A1B0GTZ2	4	2	39,7	237,7	1152,1	0,2	1,07E-02	sign.
Protein LOC105371267 OS=Homo sapiens GN=LOC105371267 PE=4 SV=1	A0A1B0GV96	2	2	11,1	12918,2	5	2584,1	1,72E-01	ns.
Protein PALM2-AKAP2 (Fragment) OS=Homo sapiens GN=PALM2-AKAP2 PE=1 SV=1	B1ALY0	2	2	16,7	8273,8	7464,6	1,1	3,74E-01	ns.

Protein Description	Protein Accession	Peptide count	Unique peptides	Confidence score	Donor Average	Control Average	Fold change	FDR-adjusted p value	Significant Donors vs Controls
Protein SAA2-SAA4 OS=Homo sapiens GN=SAA2-SAA4 PE=4 SV=1	A0A096LPE2	61	23	439,6	199052,6	175042,1	1,1	9,30E-03	sign.
Protein TRAJ56 (Fragment) OS=Homo sapiens GN=TRAJ56 PE=1 SV=1	A0A075B6Z2	5	2	44,3	3438,6	3911,2	0,9	1,09E-01	ns.
Protein unc-45 homolog A OS=Homo sapiens GN=UNC45A PE=1 SV=1	Q9H3U1	6	2	41,9	171,5	28,6	6	1,34E-03	sign.
Protein WWC2 OS=Homo sapiens GN=WWC2 PE=1 SV=2	Q6AWC2	5	2	42,6	12522,8	20732,8	0,6	1,01E-06	sign.
Protein Z-dependent protease inhibitor OS=Homo sapiens GN=SERPINA10 PE=1 SV=1	Q9UK55	29	16	190,1	44765,5	47152,8	0,9	5,70E-01	ns.
Protein ZNF816-ZNF321P OS=Homo sapiens GN=ZNF816-ZNF321P PE=4 SV=1	A0A0X1KG74	6	3	40,7	37372,7	20070,6	1,9	1,38E-01	ns.
Proteoglycan 4 OS=Homo sapiens GN=PRG4 PE=1 SV=2	Q92954	15	8	101,2	9421,7	5928,4	1,6	1,25E-03	sign.

Protein Description	Protein Accession	Peptide count	Unique peptides	Confidence score	Donor Average	Control Average	Fold change	FDR-adjusted p value	Significant Donors vs Controls
Prothrombin OS=Homo sapiens GN=F2 PE=1 SV=2	P00734	139	98	1142	1027280,7	1702975,3	0,6	6,43E-08	sign.
Pseudouridylate synthase 7 homolog OS=Homo sapiens GN=PUS7 PE=1 SV=2	Q96PZ0	5	2	54,6	49456,9	140812,5	0,4	1,37E-09	sign.
PTB domain-containing engulfment adapter protein 1 OS=Homo sapiens GN=GULP1 PE=1 SV=1	Q9UBP9	4	2	24,3	10135,3	5832,2	1,7	5,61E-03	ns.
Putative beta-actin-like protein 3 OS=Homo sapiens GN=POTEKP PE=5 SV=1	Q9BYX7	12	2	91	7904,1	9603,6	0,8	3,33E-01	ns.
Putative keratin-87 protein OS=Homo sapiens GN=KRT87P PE=5 SV=4	A6NCN2	12	2	98,2	65,9	69,2	1	9,36E-01	ns.
Pyruvate kinase PKM OS=Homo sapiens GN=PKM PE=1 SV=4	P14618	7	4	54,2	78825,7	89911,7	0,9	3,53E-01	ns.
Rab GDP dissociation inhibitor beta OS=Homo sapiens GN=GDI2 PE=1 SV=2	P50395	4	2	24,7	615,4	886,9	0,7	1,15E-02	sign.

Protein Description	Protein Accession	Peptide count	Unique peptides	Confidence score	Donor Average	Control Average	Fold change	FDR-adjusted p value	Significant Donors vs Controls
Rabenosyn-5 OS=Homo sapiens GN=RBSN PE=1 SV=2	Q9H1K0	6	2	55,7	1835,2	2849,3	0,6	9,39E-03	sign.
Ras-related GTP-binding protein A OS=Homo sapiens GN=RRAGA PE=1 SV=1	Q7L523	16	2	115,3	1299,8	1166,8	1,1	3,88E-01	ns.
Ras-related GTP-binding protein B OS=Homo sapiens GN=RRAGB PE=1 SV=1	Q5VZM2	24	10	178	39650,4	26506	1,5	2,09E-05	sign.
Retinal dehydrogenase 1 OS=Homo sapiens GN=ALDH1A1 PE=1 SV=2	P00352	16	8	137,5	1618,4	500,7	3,2	3,30E-03	sign.
Retinol-binding protein 4 OS=Homo sapiens GN=RBP4 PE=1 SV=3	P02753	52	32	393,9	162649,8	250541,9	0,6	8,69E-05	sign.
Ribonuclease pancreatic OS=Homo sapiens GN=RNASE1 PE=1 SV=4	P07998	10	6	60,8	3205,7	214,9	14,9	4,18E-02	sign.
Ribonuclease UK114 OS=Homo sapiens GN=HRSP12 PE=1 SV=1	P52758	3	2	32,5	144,7	250,5	0,6	2,88E-02	sign.

Protein Description	Protein Accession	Peptide count	Unique peptides	Confidence score	Donor Average	Control Average	Fold change	FDR-adjusted p value	Significant Donors vs Controls
Ribosomal RNA processing protein 1 homolog A OS=Homo sapiens GN=RRP1 PE=1 SV=1	P56182	7	4	44,2	21016,4	167993,1	0,1	5,95E-04	sign.
RNA-binding motif protein, X chromosome OS=Homo sapiens GN=RBMX PE=1 SV=3	P38159	7	5	40,1	11551,3	14832,6	0,8	1,90E-02	sign.
RNA-binding protein Raly OS=Homo sapiens GN=RALY PE=1 SV=1	Q9UKM9	2	2	16,6	12682,4	12695,8	1	9,96E-01	ns.
Rootletin OS=Homo sapiens GN=CROCC PE=1 SV=1	Q5TZA2	13	3	92,6	290273,2	328868	0,9	2,84E-01	ns.
S phase cyclin A-associated protein in the endoplasmic reticulum OS=Homo sapiens GN=SCAPER PE=1 SV=2	Q9BY12	3	2	16,4	2034,1	1995,7	1	9,15E-01	ns.
S-formylglutathione hydrolase OS=Homo sapiens GN=ESD PE=1 SV=2	P10768	2	2	11,8	5,4	12	0,5	3,77E-01	ns.
Scavenger receptor cysteine-rich type 1 protein M130 OS=Homo sapiens GN=CD163 PE=1 SV=2	Q86VB7	10	4	67,1	25330,9	11008,4	2,3	1,31E-07	sign.

Protein Description	Protein Accession	Peptide count	Unique peptides	Confidence score	Donor Average	Control Average	Fold change	FDR-adjusted p value	Significant Donors vs Controls
Selenium-binding protein 1 OS=Homo sapiens GN=SELENBP1 PE=1 SV=2	Q13228	10	6	66,4	11409	27683,5	0,4	7,86E-06	sign.
Selenoprotein P OS=Homo sapiens GN=SELENOP PE=1 SV=3	P49908	12	5	90,6	6837,6	6424,3	1,1	7,39E-01	ns.
Semaphorin-4B OS=Homo sapiens GN=SEMA4B PE=1 SV=3	Q9NPR2	11	2	79,8	4261,8	1699,5	2,5	2,40E-04	sign.
Serine/threonine-protein phosphatase 4 regulatory subunit 2 OS=Homo sapiens GN=PPP4R2 PE=1 SV=3	Q9NY27	3	2	16	8140,8	4591,9	1,8	1,94E-02	ns.
Serine/threonine-protein phosphatase 6 catalytic subunit OS=Homo sapiens GN=PPP6C PE=1 SV=1	O00743	4	3	22,4	11375	25459,9	0,4	6,54E-10	sign.
Serum amyloid A-1 protein OS=Homo sapiens GN=SAA1 PE=1 SV=1	P0DJI8	60	22	372,6	593439,1	44116,8	13,5	7,32E-12	sign.
Serum amyloid A-2 protein OS=Homo sapiens GN=SAA2 PE=1 SV=1	P0DJI9	49	12	309,8	350494	13829	25,3	4,70E-10	sign.

Protein Description	Protein Accession	Peptide count	Unique peptides	Confidence score	Donor Average	Control Average	Fold change	FDR-adjusted p value	Significant Donors vs Controls
Serum amyloid P-component OS=Homo sapiens GN=APCS PE=1 SV=2	P02743	21	12	209,6	241952	274890,3	0,9	2,34E-01	ns.
Serum paraoxonase/arylesterase 1 OS=Homo sapiens GN=PON1 PE=1 SV=3	P27169	41	28	392,6	120974,8	272854,4	0,4	6,66E-11	sign.
Seryl-tRNA synthetase OS=Homo sapiens PE=4 SV=1	M0R2C6	4	2	22,2	605,5	34,6	17,5	2,69E-01	ns.
Sex hormone-binding globulin OS=Homo sapiens GN=SHBG PE=1 SV=2	P04278	19	10	125	6882,5	14029,1	0,5	1,87E-03	sign.
Signal-induced proliferation-associated 1-like protein 1 OS=Homo sapiens GN=SIPA1L1 PE=1 SV=4	O43166	5	2	20,3	8092,1	10774,5	0,8	7,78E-02	ns.
Signal-regulatory protein beta-2 OS=Homo sapiens GN=SIRPB2 PE=2 SV=1	Q5JXA9	2	2	20	5363,7	7822,9	0,7	9,32E-02	ns.
Single-pass membrane and coiled-coil domain-containing protein 2 OS=Homo sapiens GN=SMCO2 PE=2 SV=2	A6NFE2	3	2	14	793,2	1287,2	0,6	1,25E-01	ns.

Protein Description	Protein Accession	Peptide count	Unique peptides	Confidence score	Donor Average	Control Average	Fold change	FDR-adjusted p value	Significant Donors vs Controls
Somatotropin OS=Homo sapiens GN=GH1 PE=1 SV=2	P01241	2	2	11,9	1193,2	717,8	1,7	3,22E-03	ns.
Sorbitol dehydrogenase OS=Homo sapiens GN=SORD PE=1 SV=4	Q00796	2	2	12,3	44,5	3,8	11,8	3,12E-01	ns.
Sorting nexin-20 OS=Homo sapiens GN=SNX20 PE=1 SV=1	Q7Z614	6	2	47,9	4238,4	4958,2	0,9	3,86E-01	ns.
SPARC-like protein 1 OS=Homo sapiens GN=SPARCL1 PE=1 SV=2	Q14515	38	26	249,4	38148,9	142456,6	0,3	2,76E-09	sign.
Spectrin beta chain, erythrocytic OS=Homo sapiens GN=SPTB PE=1 SV=5	P11277	7	2	35,7	1599,1	1893,1	0,8	2,88E-01	ns.
Structural maintenance of chromosomes protein 1B OS=Homo sapiens GN=SMC1B PE=2 SV=2	Q8NDV3	5	3	26,5	13335,5	15043,7	0,9	6,83E-01	ns.
Sulfhydryl oxidase 1 OS=Homo sapiens GN=QSOX1 PE=1 SV=3	O00391	9	4	54,1	11670,4	27085,2	0,4	6,71E-12	sign.
Superoxide dismutase [Cu-Zn] OS=Homo sapiens GN=SOD1 PE=1 SV=2	P00441	7	5	57,5	28098,3	2678,6	10,5	7,38E-03	sign.

Protein Description	Protein Accession	Peptide count	Unique peptides	Confidence score	Donor Average	Control Average	Fold change	FDR-adjusted p value	Significant Donors vs Controls
T-complex protein 1 subunit epsilon OS=Homo sapiens GN=CCT5 PE=1 SV=1	P48643	9	3	62,2	10546,9	20369,2	0,5	1,09E-06	sign.
Tenascin OS=Homo sapiens GN=TNC PE=1 SV=3	P24821	10	8	69,2	23290,8	69636,7	0,3	2,79E-06	sign.
Testis- and ovary-specific PAZ domain-containing protein 1 OS=Homo sapiens GN=TOPAZ1 PE=2 SV=3	Q8N9V7	11	4	73,7	14364,3	58233,4	0,2	8,90E-05	sign.
Tetranectin OS=Homo sapiens GN=CLEC3B PE=1 SV=3	P05452	37	22	332,4	72980	79693,1	0,9	3,70E-01	ns.
Thrombospondin-1 OS=Homo sapiens GN=THBS1 PE=1 SV=2	P07996	19	12	156	7330,4	11196,9	0,7	2,35E-03	sign.
Thyroid receptor-interacting protein 11 OS=Homo sapiens GN=TRIP11 PE=1 SV=3	Q15643	15	3	80	18279,2	66661,3	0,3	8,53E-08	sign.
Thyroxine-binding globulin OS=Homo sapiens GN=SERPINA7 PE=1 SV=2	P05543	36	25	296,3	390660,8	90004,9	4,3	7,81E-03	ns.

Protein Description	Protein Accession	Peptide count	Unique peptides	Confidence score	Donor Average	Control Average	Fold change	FDR-adjusted p value	Significant Donors vs Controls
TLD domain-containing protein 2 OS=Homo sapiens GN=TLDC2 PE=2 SV=1	A0PJX2	2	2	11,2	9031	8946	1	9,63E-01	ns.
Transaldolase OS=Homo sapiens GN=TALDO1 PE=1 SV=2	P37837	4	3	26,8	8203,2	2868,5	2,9	4,15E-12	sign.
Transforming growth factor-beta-induced protein ig-h3 OS=Homo sapiens GN=TGFBI PE=1 SV=1	Q15582	14	6	87,4	2762,1	1316,9	2,1	7,95E-05	sign.
Transient receptor potential cation channel subfamily M member 6 OS=Homo sapiens GN=TRPM6 PE=1 SV=2	Q9BX84	11	5	60,4	4205,3	3975,6	1,1	7,85E-01	ns.
Transketolase OS=Homo sapiens GN=TKT PE=1 SV=3	P29401	11	8	84,3	779,8	357,3	2,2	1,00E-04	sign.
Transmembrane protein 56 OS=Homo sapiens GN=TMEM56 PE=1 SV=1	Q96MV1	2	2	11,3	22978,4	16230	1,4	2,17E-04	sign.
Transthyretin OS=Homo sapiens GN=TTR PE=1 SV=1	P02766	42	28	361,7	751166,2	1192105	0,6	2,09E-07	sign.

Protein Description	Protein Accession	Peptide count	Unique peptides	Confidence score	Donor Average	Control Average	Fold change	FDR-adjusted p value	Significant Donors vs Controls
Triokinase/FMN cyclase OS=Homo sapiens GN=TKFC PE=1 SV=2	Q3LXA3	6	4	33,8	112,4	0,3	379,5	2,23E-02	sign.
Triosephosphate isomerase OS=Homo sapiens GN=TPI1 PE=1 SV=3	P60174	15	11	132,4	10004	8714,2	1,1	2,13E-01	ns.
Tripartite motif-containing protein 15 OS=Homo sapiens GN=TRIM15 PE=1 SV=1	Q9C019	3	2	17,8	421,4	1223,6	0,3	7,66E-03	sign.
Trypsin-3 OS=Homo sapiens GN=PRSS3 PE=1 SV=2	P35030	3	2	23,3	4743,8	3071,7	1,5	1,59E-01	ns.
Tudor domain-containing protein 6 OS=Homo sapiens GN=TDRD6 PE=2 SV=2	O60522	3	2	22,7	1183,8	2202,5	0,5	1,69E-02	sign.
Tumor necrosis factor receptor superfamily member 6 OS=Homo sapiens GN=FAS PE=1 SV=1	P25445	5	3	40	1495,1	253,8	5,9	7,69E-09	sign.
Uncharacterized protein (Fragment) OS=Homo sapiens PE=1 SV=3	H0YJW9	20	2	175,7	360,2	186,8	1,9	2,33E-01	ns.
Uncharacterized protein C4orf32 OS=Homo sapiens GN=C4orf32 PE=2 SV=2	Q8N8J7	2	2	16,6	3679,1	14823	0,2	1,40E-01	ns.

Protein Description	Protein Accession	Peptide count	Unique peptides	Confidence score	Donor Average	Control Average	Fold change	FDR-adjusted p value	Significant Donors vs Controls
Uncharacterized protein KIAA0825 OS=Homo sapiens GN=KIAA0825 PE=2 SV=2	Q8IV33	12	3	68,5	1606,9	1388,9	1,2	6,11E-01	ns.
Uncharacterized protein OS=Homo sapiens PE=4 SV=2	A0A087X1X8	2	2	17,2	12991,4	3744,5	3,5	1,58E-04	sign.
Unconventional myosin-Ih OS=Homo sapiens GN=MYO1H PE=1 SV=2	Q8N1T3	7	2	56,8	9078,1	5479,1	1,7	1,30E-02	ns.
Unconventional myosin-Va OS=Homo sapiens GN=MYO5A PE=1 SV=2	Q9Y4I1	7	2	48,3	1696,8	2370,7	0,7	3,51E-02	sign.
UTP--glucose-1-phosphate uridylyltransferase OS=Homo sapiens GN=UGP2 PE=1 SV=5	Q16851	11	7	79,7	9532,7	465,6	20,5	1,69E-02	sign.
Vitamin D-binding protein OS=Homo sapiens GN=GC PE=1 SV=1	P02774	207	159	1534,5	2492573,7	3333948	0,7	3,95E-05	sign.
Vitamin K-dependent protein C OS=Homo sapiens GN=PROC PE=1 SV=1	P04070	17	10	136,6	45242,7	99945,3	0,5	2,75E-07	sign.

Protein Description	Protein Accession	Peptide count	Unique peptides	Confidence score	Donor Average	Control Average	Fold change	FDR-adjusted p value	Significant Donors vs Controls
Vitamin K-dependent protein S OS=Homo sapiens GN=PROS1 PE=1 SV=1	P07225	63	36	465,5	130378,4	160796,5	0,8	8,08E-04	sign.
Vitronectin OS=Homo sapiens GN=VTN PE=1 SV=1	P04004	83	42	611,3	583196,1	638521,5	0,9	2,88E-01	ns.
Volume-regulated anion channel subunit LRRC8C OS=Homo sapiens GN=LRRC8C PE=1 SV=2	Q8TDW0	6	2	38,3	12210,9	46031,1	0,3	8,11E-10	sign.
WD repeat-containing protein 60 OS=Homo sapiens GN=WDR60 PE=1 SV=3	Q8WVS4	4	2	21,2	2526,8	2583,3	1	8,65E-01	ns.
WD repeat-containing protein 92 OS=Homo sapiens GN=WDR92 PE=1 SV=1	Q96MX6	4	2	23,7	473,1	561,9	0,8	6,81E-01	ns.
Xaa-Pro dipeptidase OS=Homo sapiens GN=PEPD PE=1 SV=3	P12955	3	2	14,7	263	555,6	0,5	1,20E-03	sign.
Xenotropic and polytropic retrovirus receptor 1 OS=Homo sapiens GN=XPR1 PE=1 SV=1	Q9UBH6	7	3	36,6	6810	8052	0,8	3,25E-01	ns.

Protein Description	Protein Accession	Peptide count	Unique peptides	Confidence score	Donor Average	Control Average	Fold change	FDR-adjusted p value	Significant Donors vs Controls
Zinc finger protein 827 OS=Homo sapiens GN=ZNF827 PE=1 SV=1	Q17R98	24	8	142,2	17906,1	17106,4	1	6,05E-01	ns.
Zinc finger protein 831 OS=Homo sapiens GN=ZNF831 PE=2 SV=4	Q5JPB2	6	3	50,4	16226,1	22084,1	0,7	4,59E-03	sign.
Zinc-alpha-2-glycoprotein OS=Homo sapiens GN=AZGP1 PE=1 SV=2	P25311	74	59	658,6	888441	1168738,4	0,8	1,59E-03	sign.
Zona pellucida-binding protein 1 OS=Homo sapiens GN=ZPBP PE=2 SV=1	Q9BS86	3	2	25,1	42607,5	46786,4	0,9	3,88E-01	ns.

463 quantified proteins with two or more unique peptides were compared between brain-dead donors and healthy controls. Based on the FDR-corrected p value, there were 237 differentially expressed proteins between brain-dead donors and healthy controls. These 237 significant proteins are labeled as “sign.” in the right-most column.

Table S3. Effect of log2 fold change on significantly enriched IPA pathways in brain-dead donors.

Pathway	**log2fold change ND (237 proteins)**	**log2(fold change) ≥1 (118 proteins)**	**log2(fold change) ≥1.5 (66 proteins)**	**Identified proteins**
14-3-3-mediated Signaling	x			PIK3C2B,YWHAB,YWHAG,YWHAH,YWHAQ,YWHAZ
Actin Cytoskeleton Signaling	x	x	x	ACTB,ACTR3,F2,KNG1,LBP,MSN,MYH10,PIK3C2B
Acute Phase Response Signaling	x	x	x	AGT,AHSG,AMBP,APOH,C1QA,C1QB,C1QC,C1R,C3, C4A/C4B,C4BPA,C9,CP,CRP,F2,HPX,ITIH2,ITIH3,ITIH 4,KLKB1,LBP,PLG,RBP4,SAA1,SAA2,SAA2SAA4,SER PINA3,SERPINF1,SERPINF2,SERPING1,TR
Agranulocyte Adhesion and Diapedesis				ACTB,CCL24,MSN,MYH10
Airway Pathology in Chronic Obstructive Pulmonary Disease	x			AMBP,APOD,C8G,MPO,RBP4
Alanine Biosynthesis II		x		GPT
Alanine Degradation III		x		GPT
Apelin Adipocyte Signaling Pathway	x	x		GSTA1,GSTM2,SOD1
Apelin Liver Signaling Pathway	x			AGT,FAS

Pathway	log2fold change ND (237 proteins)	log2(fold change) ≥1 (118 proteins)	log2(fold change) ≥1.5 (66 proteins)	Identified proteins
Arsenate Detoxification I (Glutaredoxin)			x	GSTO1
Aryl Hydrocarbon Receptor Signaling	x	x	x	ALDH1A1,ALDH1L1,CTSD,FAS,GSTA1,GSTM2,GSTO1,TRIP11
Ascorbate Recycling (Cytosolic)			x	GSTO1
Atherosclerosis Signaling	x			APOA4,APOC1,APOC2,APOC3,APOD,APOE,CLU,LYZ,PON1,RBP4
BAG2 Signaling Pathway	x			HSPA8,PSMA6,PSME2
Cell Cycle: G2/M DNA Damage Checkpoint Regulation	x			KAT2B,YWHAB,YWHAG,YWHAH,YWHAQ,YWHAZ
Clathrin-mediated Endocytosis Signaling	x			ACTB,ACTR3,APOA4,APOC1,APOC2,APOC3,APOD,APOE,CLU,F2,HSPA8,LYZ,PIK3C2B,PON1,RBP4
Coagulation System	x	x		F11,F2,F7,F9,KLKB1,KNG1,PLG,PROC,PROS1,SERPINA5,SERPINC1,SERPINF2

Pathway	**log2fold change ND (237 proteins)**	**log2(fold change) ≥1 (118 proteins)**	**log2(fold change) ≥1.5 (66 proteins)**	**Identified proteins**
Colanic Acid Building Blocks Biosynthesis	x	x	x	GPI,UGP2
Complement System	x	x		C1QA,C1QB,C1QC,C1R,C3,C4A/C4B,C4BPA,C8G,C9 ,CFI,MASP1,SERPING1
Crosstalk between Dendritic Cells and Natural Killer Cells			x	ACTB,FAS
D-glucuronate Degradation I		x	x	DCXR
Death Receptor Signaling			x	ACTB,FAS
Epithelial Adherens Junction Signaling		x	x	ACTB,ACTR3,MYH10
ERK/MAPK Signaling	x			PIK3C2B,YWHAB,YWHAG,YWHAH,YWHAQ,YWHAZ
ERK5 Signaling	x	x		YWHAB, YWHA G, YWH AH,YWHAQ,YWHAZ
Erythropoietin Signaling Pathway	x			HBD,HBE1,HBG2,HBZ,PIK3C2B
Eumelanin Biosynthesis			x	DDT

Pathway	**log2fold change ND (237 proteins)**	**log2(fold change) ≥1 (118 proteins)**	**log2(fold change) ≥1.5 (66 proteins)**	**Identified proteins**
Extrinsic Prothrombin Activation Pathway	x	x	x	F2,F7,PROC,PROS1,SERPINC1
Fcγ Receptor-mediated Phagocytosis in Macrophages and Monocytes			x	ACTB,ACTR3
FXR/RXR Activation	x	x	x	A1BG,AGT,AHSG,AMBP,APOA4,APOC1,APOC2,APOC3,APOD,APOE,APOH,C3,C4A/C4B,C9,CLU,GC,HPX,ITIH4,KNG1,PON1,RBP4,SAA1,SAA2,SERPINF1,SERPINF2,TTR
GDP-glucose Biosynthesis			x	PGM1
Glioma Invasiveness Signaling	x			PIK3C2B,PLG,TIMP1
Glucocorticoid Receptor Signaling	x	x	x	ACTB,AGT,B2M,CD163,HSPA8,KAT2B,KRT1,KRT10,KRT12,KRT13,KRT15,KRT16,KRT18,KRT4,KRT6A,KRT73,KRT76,KRT77,KRT78,KRT79,KRT86,PIK3C2B,YWHAH

Pathway	log2fold change ND (237 proteins)	log2(fold change) ≥1 (118 proteins)	log2(fold change) ≥1.5 (66 proteins)	Identified proteins
Glucose and Glucose-1-phosphate Degradation				PGM1
Gluconeogenesis I	x	x	x	ALDOA,ALDOB,ENO2,ENO3,FBP2,GPI
Glutaryl-CoA Degradation	x			Glutaryl-CoA Degradation
Glutathione Redox Reactions I	x	x		GSTA1,GSTM2
Glutathione-mediated Detoxification	x	x		GSTA1,GSTM2,GSTO1
Glycogen Biosynthesis II (from UDP-D-Glucose)			x	UGP2
Glycogen Degradation II			x	PGM1
Glycogen Degradation III			x	PGM1
Glycolysis I	x	x	x	ALDOA,ALDOB,ENO2,ENO3,FBP2,GPI
Growth Hormone Signaling	x			IGFALS,IGFBP3,PIK3C2B
Heme Degradation		x	x	BLVRB
Hepatic Fibrosis / Hepatic Stellate Cell Activation	x		x	AGT,FAS,IGFBP3,LBP,MYH10,TIMP1

Pathway	log2fold change ND (237 proteins)	log2(fold change) ≥1 (118 proteins)	log2(fold change) ≥1.5 (66 proteins)	Identified proteins
HIPPO signaling	x			YWHAB, YWH, YWHA H,YWHAQ,YWHAZ
IGF-1 Signaling	x	x	x	IGFBP1,IGFBP2,IGFBP3,PIK3C2B,YWHAB,YWHAG,YWHAH,YWHAQ,YWHAZ
IL-10 Signaling		x	x	BLVRB,LBP
IL-6 Signaling			x	CRP,LBP
IL-12 Signaling and Production in Macrophages	x	x		APOA4,APOC1,APOC2,APOC3,APOD,APOE,CLU,LYZ,PIK3C2B,PON1,RBP4
Inhibition of ARE-Mediated mRNA Degradation Pathway	x	x		PSMA6,PSME2,YWHAB,YWHAG,YWHAH,YWHAQ,YWHAZ
Intrinsic Prothrombin Activation Pathway	x			F11,F2,F9,KLKB1,KNG1,PROC,PROS1,SERPINC1
Iron homeostasis signaling pathway	x	x		CD163,CP,HBD,HBE1,HBG2,HBZ,HPX
LPS/IL-1 Mediated Inhibition of RXR Function	x	x	x	ALDH1A1,ALDH1L1,APOC1,APOC2,APOE,FABP1,FABP5,GSTA1,GSTM2,GSTO1,LBP,SOD3

Pathway	log2fold change ND (237 proteins)	log2(fold change) ≥1 (118 proteins)	log2(fold change) ≥1.5 (66 proteins)	Identified proteins
LXR/RXR Activation	x	x	x	A1BG,AGT,AHSG,AMBP,APOA4,APOC1,APOC2,APOC3,APOD,APOE,APOH,C3,C4A/C4B,C9,CLU,GC,HPX,ITIH4,KNG1,LBP,LYZ,PON1,RBP4,SAA1,SAA2,SERPINF1,SERPINF2,TTR
Maturity Onset Diabetes of Young (MODY) Signaling	x	x		ALDOB,APOA4,APOC1,APOC2,APOC3,APOD,APOE,APOH,APOL3,FABP1
Mechanisms of Viral Exit from Host Cells		x	x	ACTB,CHMP6
Melatonin Degradation III		x		MPO
MSP-RON Signaling In Cancer Cells Pathway	x			F11,HGFAC,KLKB1,PIK3C2B,YWHAB,YWHAG,YWHAH,YWHAQ,YWHAZ
MSP-RON Signaling Pathway	x			ACTB,F11,KLKB1,PIK3C2B
Neuroprotective Role of THOP1 in Alzheimer's Disease	x			AGT,C1R,F11,F7,HGFAC,KNG1,MASP1,PLG,SERPINA3

Pathway	log2fold change ND (237 proteins)	log2(fold change) ≥1 (118 proteins)	log2(fold change) ≥1.5 (66 proteins)	Identified proteins
NRF2-mediated Oxidative Stress Response	x	x	x	ACTB,GSTA1,GSTM2,GSTO1,PIK3C2B,PRDX1,SOD1,SOD3
p53 Signaling	x			FAS,KAT2B,PIK3C2B,THBS1
p70S6K Signaling	x			AGT,F2,PIK3C2B,YWHAB,YWHAG,YWHAH,YWHAQ,YWHAZ
PEDF Signaling	x			FAS,PIK3C2B,SERPINF1
Pentose Phosphate Pathway	x	x		TALDO1,TKT
Pentose Phosphate Pathway (Non-oxidative Branch)	x	x	x	TALDO1,TKT
PFKFB4 Signaling Pathway	x	x		FBP2,GPI,TKT
Phagosome Maturation	x			B2M,CTSD,MPO,PRDX1,PRDX2
PI3K/AKT Signaling	x			YWHA B, YW H AG, Y WHAH,YWHAQ,YWHAZ
Production of Nitric Oxide and Reactive Oxygen Species in Macrophages	x	x		APOA4,APOC1,APOC2,APOC3,APOD,APOE,CLU,LYZ,MPO,PIK3C2B,PON1,RBP4

Pathway	log2fold change ND (237 proteins)	log2(fold change) ≥1 (118 proteins)	log2(fold change) ≥1.5 (66 proteins)	Identified proteins
PXR/RXR Activation	x	x	x	ALDH1A1,GSTA1,GSTM2,IGFBP1
Rac Signaling	x			ACTR3,MCF2L,PIK3C2B,PIP4K2C
RAR Activation	x			ACTB,ALDH1A1,IGFBP3,KAT2B,RBP4
Regulation of Actin-based Motility by Rho		x	x	ACTB,ACTR3,PIP4K2C
Remodeling of Epithelial Adherens Junctions		x	x	ACTB,ACTR3
RhoA Signaling	x	x	x	ACTB,ACTR3,MSN,PIP4K2C
RhoGDI Signaling		x	x	ACTB,ACTR3,MSN,MYH10,PIP4K2C
Role of Pattern Recognition Receptors in Recognition of Bacteria and Viruses	x			C1QA,C1QB,C1QC,C3,PIK3C2B,PTX3
Sucrose Degradation V (Mammalian)	x	x	x	ALDOA,ALDOB,TKFC
Superoxide Radicals Degradation	x	x	x	SOD1,SOD3
Thymine Degradation		x	x	UPB1

Pathway	log2fold change ND (237 proteins)	log2(fold change) ≥1 (118 proteins)	log2(fold change) ≥1.5 (66 proteins)	Identified proteins
Tumoricidal Function of Hepatic Natural KillCellslls	x			FAS,LYVE1
Tyrosine Degradation I			x	HPD
Uracil Degradation II (Reductive)		x	x	UPB1
Urea Cycle	x			ASL,CPS1
Vitamin-C Transport	x	x	x	GSTO1,LRRC8C
Xenobiotic Metabolism AHR Signaling Pathway	x	x	x	ALDH1A1,ALDH1L1,GSTA1,GSTM2,GSTO1,PON1
Xenobiotic Metabolism CAR Signaling Pathway	x	x	x	ALDH1A1,ALDH1L1,GSTA1,GSTM2,GSTO1,SOD3
Xenobiotic Metabolism General Signaling Pathway	x	x		GSTA1,GSTM2,GSTO1,PIK3C2B
Xenobiotic Metabolism PXR Signaling Pathway	x	x	x	ALDH1A1,ALDH1L1,GSTA1,GSTM2,GSTO1

Pathway	log2fold change ND (237 proteins)	log2(fold change) ≥1 (118 proteins)	log2(fold change) ≥1.5 (66 proteins)	Identified proteins
Xenobiotic Metabolism Signaling	x	x	x	ALDH1A1,ALDH1L1,GSTA1,GSTM2,GSTO1,PIK3C2B, SOD3

IPA enrichment analysis pathways with a -log(p value) of >1.3 (p value <0.05) without taking z-score into account. Identified proteins enriched into significant pathways are presented.

Table S4. List of enriched pathways comparing Donor A and Donor B.

Ingenuity Canonical Pathways	-log(p value)	z-score	Identified proteins
Acute Phase Response Signaling	26	-1,265	AGT,AMBP,APOH,C1QA,C1QB,C1QC,C1R,C3,C4A/C4B,C4BPA,C9,CP,CRP,F2,HPX,ITIH2,ITIH4,KLKB1,PLG,RBP4,SAA1,SAA2,SERPINA3,SERPINF2,SERPING1,TTR
LXR/RXR Activation	21,3	-3,13	AGT,AMBP,APOA4,APOC1,APOD,APOE,APOH,C3,C4A/C4B,C9,HPX,I

Ingenuity Canonical Pathways	-log(p value)	z-score	Identified proteins
FXR/RXR Activation	19,6	NA	TIH4,KNG1,LYZ,PON1,RBP4,SAA1, SAA2,SERPINF2,TTR AGT,AMBP,APOA4,APOC1,APOD, APOE,APOH,C3,C4A/C4B,C9,HPX,I
Complement System	16,9	-1,265	TIH4,KNG1,PON1,RBP4,SAA1,SAA 2,SERPINF2,TTR C1QA,C1QB,C1QC,C1R,C3,C4A/C 4B,C4BPA,C8G,C9,CFI,MASP1,SE RPING1
Coagulation System	10,1	0	F2,F9,KLKB1,KNG1,PLG,PROS1,S ERPINC1,SERPINF2
Intrinsic Prothrombin Activation Pathway	6,37	-0,447	F2,F9,KLKB1,KNG1,PROS1,SERPI NC1
Glycolysis I	6,06	-2,236	ALDOA,ENO2,ENO3,FBP2,GPI
Gluconeogenesis I	6,06	-2,236	ALDOA,ENO2,ENO3,FBP2,GPI
Clathrin-mediated Endocytosis Signaling	6,01	NA	ACTR3,APOA4,APOC1,APOD,APO E,F2,LYZ,PIK3C2B,PON1,RBP4

Ingenuity Canonical Pathways	-log(p value)	z-score	Identified proteins
Maturity Onset Diabetes of Young (MODY) Signaling	5,94	NA	APOA4,APOC1,APOD,APOE,APOH ,APOL3,FABP1
IL-12 Signaling and Production in Macrophages	5,32	NA	APOA4,APOC1,APOD,APOE,LYZ,P IK3C2B,PON1,RBP4
Production of Nitric Oxide and Reactive Oxygen Species in Macrophages	5,12	-2,121	APOA4,APOC1,APOD,APOE,LYZ, MPO,PIK3C2B,PON1,RBP4
Glucocorticoid Receptor Signaling	4,89	NA	AGT,B2M,CD163,KAT2B,KRT1,KRT 10,KRT15,KRT16,KRT18,KRT4,KR T73,KRT76,KRT77,KRT78,PIK3C2B
Atherosclerosis Signaling	4,47	NA	APOA4,APOC1,APOD,APOE,LYZ,P ON1,RBP4
IGF-1 Signaling	4,07	NA	IGFBP1,IGFBP3,PIK3C2B,YWHAB, YWHAQ,YWHAZ
Extrinsic Prothrombin Activation Pathway	3,77	NA	F2,PROS1,SERPINC1
Neuroprotective Role of THOP1 in Alzheimer's Disease	3,76	0	AGT,C1R,KNG1,MASP1,PLG,SERP INA3

Ingenuity Canonical Pathways	-log(p value)	z-score	Identified proteins
p70S6K Signaling	3,5	NA	AGT,F2,PIK3C2B,YWHAB,YWHAQ, YWHAZ
Cell Cycle: G2/M DNA Damage Checkpoint Regulation	3,4	NA	KAT2B,YWHAB,YWHAQ,YWHAZ
Pentose Phosphate Pathway (Non-oxidative Branch)	3,16	NA	TALDO1,TKT
Role of Pattern Recognition Receptors in Recognition of Bacteria and Viruses	3,12	-1,342	C1QA,C1QB,C1QC,C3,PIK3C2B,PTX3
Aryl Hydrocarbon Receptor Signaling	3,07	NA	CTSD,FAS,GSTA1,GSTM2,GSTO1, TRIP11
Airway Pathology in Chronic Obstructive Pulmonary Disease	2,86	NA	AMBP,APOD,C8G,MPO,RBP4
Glutathione-mediated Detoxification	2,82	NA	GSTA1,GSTM2,GSTO1
Pentose Phosphate Pathway	2,69	NA	TALDO1,TKT
MSP-RON Signaling In Cancer Cells Pathway	2,56	-1,342	KLKB1,PIK3C2B,YWHAB,YWHAQ, YWHAZ

Ingenuity Canonical Pathways	-log(p value)	z-score	Identified proteins
Xenobiotic Metabolism AHR Signaling Pathway	2,5	-2	GSTA1,GSTM2,GSTO1,PON1
PFKFB4 Signaling Pathway	2,4	NA	FBP2,GPI,TKT
Colanic Acid Building Blocks Biosynthesis	2,39	NA	GPI,UGP2
Phagosome Maturation	2,3	NA	B2M,CTSD,MPO,PRDX1,PRDX2
Glutaryl-CoA Degradation	2,22	NA	ACAT1,CA1
NRF2-mediated Oxidative Stress Response	2,21	NA	GSTA1,GSTM2,GSTO1,PIK3C2B,PRDX1,SOD1
Melatonin Degradation III	2,16	NA	MPO
Actin Cytoskeleton Signaling	2,14	-0,447	ACTR3,F2,KNG1,MSN,MYH10,PIK3C2B
LPS/IL-1 Mediated Inhibition of RXR Function	2,08	NA	APOC1,APOE,FABP1,GSTA1,GSTM2,GSTO1
PXR/RXR Activation	1,99	NA	GSTA1,GSTM2,IGFBP1
14-3-3-mediated Signaling	1,93	-1	PIK3C2B,YWHAB,YWHAQ,YWHAZ
Tumoricidal Function of Hepatic Natural Killer Cells	1,93	NA	FAS,LYVE1

Ingenuity Canonical Pathways	-log(p value)	z-score	Identified proteins
Tryptophan Degradation III (Eukaryotic)	1,93	NA	ACAT1,CA1
Vitamin-C Transport	1,93	NA	GSTO1,LRRC8C
Glutathione Redox Reactions I	1,89	NA	GSTA1,GSTM2
Growth Hormone Signaling	1,88	NA	IGFALS,IGFBP3,PIK3C2B
ERK5 Signaling	1,87	NA	YWHAB,YWHAQ,YWHAZ
Apelin Liver Signaling Pathway	1,86	NA	AGT,FAS
Rac Signaling	1,81	-1	ACTR3,MCF2L,PIK3C2B,PIP4K2C
Iron homeostasis signaling pathway	1,8	NA	CD163,CP,HBG2,HPX
Xenobiotic Metabolism General Signaling Pathway	1,76	-1	GSTA1,GSTM2,GSTO1,PIK3C2B
Thyroid Hormone Biosynthesis	1,69	NA	CTSD
HIPPO signaling	1,68	NA	YWHAB,YWHAQ,YWHAZ
Apelin Adipocyte Signaling Pathway	1,66	NA	GSTA1,GSTM2,SOD1
Ascorbate Recycling (Cytosolic)	1,56	NA	GSTO1
p53 Signaling	1,52	NA	FAS,KAT2B,PIK3C2B
Arsenate Detoxification I (Glutaredoxin)	1,47	NA	GSTO1

Ingenuity Canonical Pathways	-log(p value)	z-score	Identified proteins
Creatine-phosphate Biosynthesis	1,47	NA	CKM
Citrulline-Nitric Oxide Cycle	1,47	NA	ASL
Tyrosine Degradation I	1,47	NA	HPD
Arginine Biosynthesis IV	1,39	NA	ASL
Urea Cycle	1,39	NA	ASL
GDP-mannose Biosynthesis	1,39	NA	GPI
Hepatic Fibrosis / Hepatic Stellate Cell Activation	1,34	NA	AGT,FAS,IGFBP3,MYH10
Glycogen Biosynthesis II (from UDP-D-Glucose)	1,32	NA	UGP2

An activation z-score is calculated by IPA. The z-score makes predictions about potential inhibition or activation of identified pathways. A -log(p value) of >3.0 corresponds to a p value of <0.001, while -log(p value) of >1.3 corresponds to a p value of <0.05. Identified proteins enriched into significant pathways are presented.

Table S5. Enriched pathways comparing Donor B1 and Donor B2.

Ingenuity Canonical Pathways	-log(p value)	z-score	Identified proteins
Acute Phase Response Signaling	10,6	NA	AHSG,APOH,C1QA,C1QC,C4BPA, C9,ITIH2,ITIH3,ITIH4,KLKB1,LBP,S ERPINF1
LXR/RXR Activation	8,38	3	AHSG,APOH,C9,CLU,GC,ITIH4,KN G1,LBP,SERPINF1
Coagulation System	8,15	0	F11,F7,KLKB1,KNG1,PROS1,SERP INA5
FXR/RXR Activation	6,92	NA	AHSG,APOH,C9,CLU,GC,ITIH4,KN G1,SERPINF1
IGF-1 Signaling	6,48	NA	IGFBP2,IGFBP3,PIK3C2B,YWHAB, YWHAG,YWHAQ,YWHAZ
Complement System	6,27	1	C1QA,C1QC,C4BPA,C9,MASP1
MSP-RON Signaling In Cancer Cells Pathway	5,71	0,378	F11,KLKB1,PIK3C2B,YWHAB,YWH AG,YWHAQ,YWHAZ
Intrinsic Prothrombin Activation Pathway	4,49	NA	F11,KLKB1,KNG1,PROS1

Ingenuity Canonical Pathways	-log(p value)	z-score	Identified proteins
Cell Cycle: G2/M DNA Damage Checkpoint Regulation	4,23	NA	YWHAB,YWHAG,YWHAQ,YWHAZ
MSP-RON Signaling Pathway	3,95	NA	ACTB,F11,KLKB1,PIK3C2B
14-3-3-mediated Signaling	3,66	0,447	PIK3C2B,YWHAB,YWHAG,YWHAQ ,YWHAZ
ERK5 Signaling	3,59	0	YWHAB,YWHAG,YWHAQ,YWHAZ
p70S6K Signaling	3,53	NA	PIK3C2B,YWHAB,YWHAG,YWHAQ ,YWHAZ
HIPPO signaling	3,32	0	YWHAB,YWHAG,YWHAQ,YWHAZ
Iron homeostasis signaling pathway	3,31	NA	CD163,HBD,HBE1,HBG2,HBZ
NRF2-mediated Oxidative Stress Response	3,3	NA	ACTB,GSTM2,PIK3C2B,PRDX1,SO D1,SOD3
Glycolysis I	3,13	NA	ALDOA,ENO2,FBP2
Superoxide Radicals Degradation	3,11	NA	SOD1,SOD3
Glucocorticoid Receptor Signaling	3,06	NA	ACTB,CD163,HSPA8,KRT1,KRT16, KRT6A,KRT73,KRT79,PIK3C2B
Gluconeogenesis I	2,99	NA	ALDOA,ENO2,FBP2
Erythropoietin Signaling Pathway	2,97	2,236	HBD,HBE1,HBG2,HBZ,PIK3C2B

Ingenuity Canonical Pathways	-log(p value)	z-score	Identified proteins
Neuroprotective Role of THOP1 in Alzheimer's Disease	2,73	NA	F11,F7,KNG1,MASP1
ERK/MAPK Signaling	2,64	NA	PIK3C2B,YWHAB,YWHAG,YWHAQ,YWHAZ
Extrinsic Prothrombin Activation Pathway	2,59	NA	F7,PROS1
Role of Pattern Recognition Receptors in Recognition of Bacteria and Viruses	2,37	NA	C1QA,C1QC,PIK3C2B,PTX3
LPS/IL-1 Mediated Inhibition of RXR Function	2,33	NA	ALDH1L1,FABP5,GSTM2,LBP,SOD3
Inhibition of ARE-Mediated mRNA Degradation Pathway	2,32	0	YWHAB,YWHAG,YWHAQ,YWHAZ
Glutaryl-CoA Degradation	2,21	NA	ACAT1,CA1
Clathrin-mediated Endocytosis Signaling	2,02	NA	ACTB,CLU,HSPA8,PIK3C2B
PI3K/AKT Signaling	1,96	0	YWHAB,YWHAG,YWHAQ,YWHAZ

Ingenuity Canonical Pathways	-log(p value)	z-score	Identified proteins
Mechanisms of Viral Exit from Host Cells	1,89	NA	ACTB,CHMP6
MSP-RON Signaling In Macrophages Pathway	1,85	NA	F11,KLKB1,PIK3C2B
Docosahexaenoic Acid (DHA) Signaling	1,83	NA	PIK3C2B,SERPINF1
Tryptophan Degradation III (Eukaryotic)	1,74	NA	ACAT1,CA1
Actin Cytoskeleton Signaling	1,68	NA	ACTB,KNG1,LBP,PIK3C2B
Alanine Degradation III	1,6	NA	GPT
Alanine Biosynthesis II	1,6	NA	GPT
Xenobiotic Metabolism Signaling	1,46	NA	ALDH1L1,GSTM2,PIK3C2B,SOD3
eNOS Signaling	1,44	NA	HSPA8,KNG1,PIK3C2B
Creatine-phosphate Biosynthesis	1,43	NA	CKM
Lactose Degradation III	1,43	NA	PSAP
Glioma Invasiveness Signaling	1,41	NA	PIK3C2B,TIMP1
Growth Hormone Signaling	1,4	NA	IGFBP3,PIK3C2B

Ingenuity Canonical Pathways	-log(p value)	z-score	Identified proteins
Xenobiotic Metabolism CAR Signaling Pathway	1,34	NA	ALDH1L1,GSTM2,SOD3
PEDF Signaling	1,31	NA	PIK3C2B,SERPINF1

An activation z-score is calculated by IPA. The z-score makes predictions about potential inhibition or activation of identified pathways. A -log(p value) of >3.0 corresponds to a p value of <0.001, while -log(p value) of >1.3 corresponds to a p value of <0.05. Identified proteins enriched into significant pathways are presented.

Table S6. Clinical characteristics of donors with primary graft dysfunction (PGD) after transplantation.

Donor characteristics	All donors (N=53)	Donors without any grade of PGD (N=36)	Donors with any grade of PGD (N=17)	Donors with severe PGD (N=6)
Age, y	44 (33-51)	42 (30.25-51)	49 (37-52)	44 (35.5-50.25)
Female sex, No. (%)	10 (18.9)	8 (22.2)	2 (11.8)	0 (0.0)
Body mass Index, kg/m^2	25.2±4.8	25±2.9	25.7±7.5	24.1±11.3
Donor Simvastatin treatment, No. (%)	27 (51)	19 (52.8)	8 (37.5)	3 (50)
Previous medical history, No. (%)*				

Donor characteristics	**All donors (N=53)**	**Donors without any grade of PGD (N=36)**	**Donors with any grade of PGD (N=17)**	**Donors with severe PGD (N=6)**
Hypertension	6 (11)	4 (11.1)	2 (16.7)	0 (0.0)
Smoking, No. (%)				
Current	23 (43)	16 (44.4)	7 (41.2)	2 (33.3)
Former	4 (8)	3 (8.3)	1 (5.9)	1 (16.7)
Never	15 (28)	8 (22.2)	7 (41.2)	1 (16.7)
Unknown	11 (21)	9 (25)	2 (11.8)	2 (33.3)
CMV-positive, No. (%)	44 (83)	32 (88.9)	12 (70.6)	3 (50)
Donor cause of death, No. (%)				
Intracranial hemorrhage	26 (49.1)	18 (50)	8 (47.1)	2 (33.3)
Traumatic brain injury	19 (35.8)	14 (38.9)	5 (29.4)	2 (33.3)
Cerebral infarction	6 (11.3)	2 (5.6)	4 (23.5)	2 (33.3)
Cerebral anoxia after cardiorespiratory arrest	0 (0.0)	0 (0.0)	0 (0.0)	0 (0.0)
Other	2 (3.8)	2 (5.6)	0 (0.0)	0 (0.0)
Donor P-troponin I, ng/l	47 (9-207)	78 (8.78-238.25)	28 (13-56)	18 (5.8-447.8)
Donor P-troponin T, ng/l	21 (9-55)	21.3 (10-60)	14 (8-63)	10 (7.5-50.25)

Donor characteristics	All donors (N=53)	Donors without any grade of PGD (N=36)	Donors with any grade of PGD (N=17)	Donors with severe PGD (N=6)
Hemoglobin, g/L	121±23	119±18.8	127±21	144±33.6
CRP, mg/L	82±87	84±91	68±73.3	80±86.6
Thrombocytes, E9/L	186±80	183±78.6	196±78.1	177±53.5
Total P-cholesterol, mmol/l	2.7±0.9	2.7±0.9	2.8±0.9	2.7±1
P-HDL, mmol/l	1±0.4	1±0.4	0.9±0.3	0.8±0.1
P-LDL, mmol/l	1.2±0.7	1.2±0.7	1.3±0.7	1.3±0.7
P-triglycerides, mmol/l	0.9±0.5	0.8±0.4	1±0.6	1.2±0.9
Donor echocardiogram				
Left ventricle ejection fraction, %	62 (59-65)	63 (60-65)	62 (54-67)	61 (51-67)
Presence of regional wall motion abnormality, No. (%)	6 (11)	5 (13.9)	1 (5.9)	0 (0.0)
Diastolic posterior wall thickness, mm	11 (9-12)	10 (9-12)	11 (10-13)	11 (10-13)
Diastolic septum thickness, mm	11 (10-12)	11 (10-11)	11 (10-12)	11 (10-13)

Donor characteristics	All donors (N=53)	Donors without any grade of PGD (N=36)	Donors with any grade of PGD (N=17)	Donors with severe PGD (N=6)
Donor coronary angiography†				
Performed, No. (%)	30 (57)	18 (50)	12 (70.6)	3 (50)
Abnormal finding angiography, No. (%)	6 (11.3)	3 (8.3)	3 (17.6)	1 (16.7)
Donor ionotropic support, No. (%)	37 (70)	23 (63.9)	14 (82.4)	5 (83.3)
Donor resuscitation, No. (%)	9 (17)	6 (16.7)	3 (17.6)	1 (16.7
Time of ROSC for resuscitated donors, min	17±13	12±6	21±10	26±0
Time between declaration of brain death and organ procurement, h	15±4	15±4	14±3	15±4
Organ Retrieval from Donors, No. (%)				
Heart	53 (100)	36 (100)	17 (100)	6 (100)
Lung	17 (32)	12 (33.3)	5 (29.4)	1 (16.7)

Donor characteristics	All donors (N=53)	Donors without any grade of PGD (N=36)	Donors with any grade of PGD (N=17)	Donors with severe PGD (N=6)
Liver	36 (68)	25 (69.4)	11 (64.7)	4 (66.7)
Kidneys	86 (90.6)	55 (86.1)	21 (100)	11 (100)
Pancreas	31 (58)	22 (61.1)	9 (52.9)	2 (33.3)

Plus-minus values are mean ±SD; values with range in parentheses are median (interquartile range). CMV indicates cytomegalovirus; HDL, high-density lipoprotein; LDL, low-density lipoprotein; ROSC, return of spontaneous circulation; and Tx, transplantation. *In the previous medical history of the donors there was no coronary artery disease, chronic obstructive pulmonary disease, peripheral vascular disease, previous malignancy, prior stroke, and no history of sternotomy. †Donor coronary angiography was performed for donors with >40 years of age, strong family history for coronary disease or smoking.

Table S7. Transplant outcome and clinical characteristics of recipients with primary graft dysfunction (PGD) after transplantation.

Recipient characteristics	All recipients (N=53)	Recipients without any PGD (N=36)	Recipients with any PGD (N=17)	Recipients with severe PGD (N=6)
Recipient characteristics				
Age, y	58 (46.5-61)	58 (45-61.75)	57 (53-60.5)	58 (52.75-63.5)

Recipient characteristics	All recipients (N=53)	Recipients without any PGD (N=36)	Recipients with any PGD (N=17)	Recipients with severe PGD (N=6)
Female sex, No. (%)	13 (24.5)	10 (27.8)	3 (17.6)	0 (0.0)
Body mass index, kg/m^2	26±4.4	25±4.3	26±4.4	25±1.8
Previous medical history, No. (%)				
Hypertension	8 (15.1)	6 (16.7)	2 (11.8)	1 (16.7)
Chronic obstructive pulmonary disease	2 (3.8)	1 (2.8)	1 (5.9)	0 (0.0)
Coronary artery disease	11 (20.8)	8 (22.2)	3 (17.6)	1 (16.7)
Diabetes	7 (13.2)	3 (8.3)	4 (23.5)	0 (0.0)
Previous malignancy	5 (9.4)	5 (13.9)	0 (0.0)	0 (0.0)
Prior stroke	7 (13.2)	5 (13.9)	2 (11.8)	1 (16.7)
Amiodarone <6 months prior to transplantation, No. (%)	14 (26.4)	9 (25)	5 (29.4)	2 (33.3)
History of sternotomy	15 (28.3)	10 (27.8)	5 (29.4)	1 (16.7)
Primary disease, No. (%)				
Endstage coronary disease	12 (22.6)	8 (22.2)	4 (23.5)	1 (16.7)
Dilatative cardiomyopathy	26 (49)	19 (52.8)	7 (41.2)	3 (50)
Congenital	4 (7.6)	3 (8.3)	1 (5.9)	0 (0.0)

Recipient characteristics	**All recipients (N=53)**	**Recipients without any PGD (N=36)**	**Recipients with any PGD (N=17)**	**Recipients with severe PGD (N=6)**
Myocarditis	3 (5.7)	0 (0.0)	3 (17.6)	1 (16.7)
Other	8 (15.1)	5 (13.9)	3 (17.6)	1 (16.7)
Donor-recipient gender mismatch	6 (11.3)	5 (13.9)	1 (11.8)	0 (0.0)
Mechanical circulatory support prior to HTx, No. (%)	13 (24.5)	9 (25)	4 (23.5)	2 (33.3)
ECMO, No. (%)	6 (11.3)	5 (13.9)	1 (5.9)	1 (16.7)
LVAD, No. (%)	7 (13.2)	4 (11.1)	3 (17.6)	1 (16.7)
Days on waiting list	190 (41.8-352.5)	120 (39.5-270)	350 (30-400)	240 (21-690)
Graft ischemia time, min				
Cold	97±50.1	101±50.9	88±45.3	126±9.3
Warm	80±20.2	78±17.4	84±24.2	85.4±18.2
Total	173±54.1	174±54.7	171±51	**203±22***
Organ functions before transplantation				
PVR, Woods units	3±1.3	3±1.3	2.2±0.9	2±0.7
TPG, mmHg	10 (7-12)	10 (7-13)	8.5 (6-12)	11 (5-14)
SPAP, mmHg	43±12.8	43±12.6	43±12.6	39±14.3

Recipient characteristics	**All recipients (N=53)**	**Recipients without any PGD (N=36)**	**Recipients with any PGD (N=17)**	**Recipients with severe PGD (N=6)**
P-bilirubin, µmol	13 (10-19)	12 (10-21.25)	13 (8.5-19)	15 (9-25)
Glomerular filtration rate, mL/min per 1.73 square meters	55.7 (45-73)	55.5 (45-75)	55.7 (47.5-69)	55.4 (50-59.25)
NT-proBNP, ng/L	3171 (1075-5686)	3100 (1028-6327)	3178 (1232-4755)	3024 (1996-4697)
Immunosuppressive therapy				
Induction therapy				
Antithymocyte globulin	21 (39.6)	11 (30.6)	10 (58.8)	3 (50)
Maintenance therapy				
Cyclosporine A	10 (18.9)	6 (16.7)	4 (23.5)	2 (33.3)
Tacrolimus	39 (73.6)	29 (80.6)	10 (58.8)	2 (33.3)
Azathioprine	2 (3.8)	1 (2.8)	1 (5.9)	1 (16.7)
Mycophenolic acid	46 (86.8)	34 (94.4)	12 (70.6)	2 (33.3)
Prednisolone	53 (100)	36 (100)	17 (100)	6 (100)
Recipient outcome				
Intubation time, h	42 (20-125)	30 (20-94)	80 (44-312)	**528 (312-738)***
Time on ICU, h	216 (144-480)	192 (120-374)	324 (180-684)	**708 (570-954)***
Hospital Length of Stay	44±29	37±21	**61±36****	**94±30.3*****

Recipient characteristics	All recipients (N=53)	Recipients without any PGD (N=36)	Recipients with any PGD (N=17)	Recipients with severe PGD (N=6)
Inotropic support, No. (%)	47 (88.7)	30 (83.3)	17 (100)	6 (100)
30-day survival, No. (%)	50 (94.3)	36 (100)	14 (82.4)	4 (66.7)
1-year survival, No. (%)	46 (86.8)	32 (88.9)	14 (82.4)	4 (66.7)
Primary graft dysfunction, No. (%)				
Any PGD	17 (32.1)	0 (0.0)	17 (100)	6 (100)
Severe PGD	6 (11.3)	0 (0.0)	6 (35.3)	6 (100)
ProBNP, ng/l				
ProBNP, 7d	28686±21718	31062±21984	23300±20086	**12832±6619****
ProBNP, 14d	32369±24176	35085±25635	26162±19053	**16778±6115****
ProBNP, 21d	27411±24724	25779±24851	37846±31490	23583±10145
ProBNP,1m	18156±21232	15667±20159	24556±22543	25022±13425
ProBNP, 3m	7793±15397	3668±20159	**17813±24441****	**23697±25790****
ProBNP, 6m	25745±11366	1203±5509	**104479±18760***	**19605±29128****
ProBNP, 1y	2660±6893	1006±1381	**7389±12084****	**14747±17852****
Left ventricle ejection fraction (LVEF), %				
LVEF, 7d	59±9	60±9	56±10	50±13
LVEF, 14d	61±7	62±7	61±8	58±10

Recipient characteristics	All recipients (N=53)	Recipients without any PGD (N=36)	Recipients with any PGD (N=17)	Recipients with severe PGD (N=6)
LVEF, 21d	61±9	62±9	60±7	60±7
LVEF, 1m	62±8	63±8	61±8	59±6
LVEF, 3m	60±9	62±8	54±9	57±13
LVEF, 6m	59±9	60±8	57±11	54±14
LVEF, 1y	60±8	61±8	55±8	53±5
Recipient P-troponin I, ng/l				
1h	12648 (8440-29998)	12277 (7728-18857)	25321 (9572-42289)	39568 (24102-60829)
6h	86310 (40072-169213)	61996 (28080-109491)	**149187 (62328-400274)***	**400275 (255774-500000)****
12h	95188 (41617-213709)	62367(39306-135643)	**181665 (64322-379414)***	**340220 (236980)****
24h	49437 (32797-107456)	44574 (28687-101849)	**112557 (57794-246513)***	**246513 (162564-436723)***
Recipient P-troponin T, ng/l				
1h	3587 (2189-5681)	2982 (1877-4502)	**5645 (2599- 9191)***	8594 (5478-12292)
6h	8940 (4602-17440)	7329 (4034-12675)	**18630 (8003-30330)****	**30330 (22475-39638)****
12h	7947 (4354-14658)	6015 (3548-12443)	**14745 (7657-26228)****	**24000 (18160-37810)***
24h	5918 (3192-9291)	4597 (2326-8226)	**8780 (4983-18970)***	**18970 (9615-30010)***
Lactate, mmol/l				
1h	3.1±1.3	3±1.2	3.4±1.5	3.7±2

Recipient characteristics	All recipients (N=53)	Recipients without any PGD (N=36)	Recipients with any PGD (N=17)	Recipients with severe PGD (N=6)
6h	8.5±4.4	7.5±3.3	**10.7±5.6***	**15±6.4***
12h	6.2±3.8	4.9±2.6	**8.8±4.7****	**13.8±3.6****
24h	2.7±2.3	2.1±1.4	**4.2±3.2***	**7.1±3***
Leukocytes, E9/l				
1h	14±5.2	14.3±5	13.4±3.4	12.8±4.9
6h	14±5.1	14.4±5.5	13±3.9	10.7±3.1
12h	13.1±5.3	13.1±5.7	13±4.3	8.8±3.1
24h	17.3±6.7	18.5±7	14.8±5.1	10.8±3.4
hsCRP, mg/L				
1h	2.8 (1.9-7)	2.6 (1.8-7.2)	3.1 (2-6)	3.6 (2-7.6)
6h	5.6 (3.8-12.6)	5.9 (3.8-13)	5.2 (3.5-12.6)	4.9 (3-9.6)
12h	26.2 (16.2-44.8)	25.3 (16-49.4)	28.5 (16.1-36.3)	26.7 (13.3-31.6)
24h	87.1 (61.4-123.1)	85 (61.4-123.1)	96.1 (61-125)	78 (61.1–94.7)

Plus-minus values are mean ±SD; values with range in parentheses are median (interquartile range). CMV indicates cytomegalovirus; HDL, high-density lipoprotein; LDL, low-density lipoprotein; ROSC, return of spontaneous circulation; Tx, transplantation. In this study cohort, we did not see any cases of antibody-mediated rejection within 30 days and 1 year. P-values are marked as asterisks (*P<0.05. **P<0.01. ***P<0.001).

Table S8. Donor plasma proteins correlate with PGD in heart transplant recipients.

PGD	Protein	Correlation (r)	Confint value	P value
Any Grade of PGD (n=17)	Beta-ureidopropionase	0.28	(0,011-0,51)	0.0417
	Nicolin 1	-0.28	(-0,51-0,012)	0.0415
	Lysine-specific demethylase 3A	0.4	(0,15-0,61)	0.00298
	Insulin-like growth factor-binding protein 2	-0.27	(-0,5-0,00088)	0.0496
	Retinol-binding protein 4	-0.27	(-0,51-0,0026)	0.0482
Severe PGD (n=6)	Proteasome subunit alpha type-6	0.39	(0,14-0,6)	0.00372
	Moesin	0.34	(0,076-0,56)	0.0129
	Apolipoprotein L3	0.28	(0,016-0,52)	0.0388
	Lysine-specific demethylase 3A	0.42	(0,17-0,62)	0.00158
	Eomesodermin	-0.28	(-0,51--0,0085)	0.0437
	Keratin 76	0.31	(0,044-0,54)	0.0237

Table S9. Cause of deaths in heart transplant recipients within 5-years after transplantation.

Donor Tx number	Survival days	Graft-related cause of death	Cause of death	TX urgency	Donor Age	Donor Sex
9	53	Yes	Primary graft failure	High	52	Male
38	9	Yes	Primary graft failure	Normal	54	Female
42	3	Yes	Primary graft dysfunction	Normal	34	Male
43	168	Yes	Acute rejection	Normal	57	Male
47	9	Yes	Primary graft failure	Normal	37	Male
77	304	Yes	Acute rejection	High	46	Male
81	740	Yes	Chronic rejection	Normal	53	Male
5	524	No	CMV pneumonia	Normal	43	Male
22	1407	No	B-Cell lymphoma	Normal	51	Male
50	1429	No	Bleeding	Normal	50	Male

Table S10. Clinical characteristics of donors with acute rejection with hemodynamic compromise during first 30 days after transplantation.

Donor characteristics	**All donors (N=50)**	**Donors without acute rejection with hemodynamic compromise (N=34)**	**Donors with acute rejection with hemodynamic compromise (N=16)**
Age, y	45 (33-51)	45 (34-51)	45 (32.5-51)
Female sex, No. (%)	9 (18)	7 (20.6)	2 (12.5)
Body mass Index, kg/m^2	25±4.7	24.8±2.8	25.3±7.4
Donor Simvastatin treatment, No. (%)	26 (52)	20 (58.8)	6 (37.5)
Previous medical history, No. (%)*			
Hypertension	6 (12)	3 (8.8)	3 (18.8)
Smoking, No. (%)			
Current	21 (42)	14 (41.2)	7 (43.8)
Former	4 (8)	3 (8.8)	1 (6.3)
Never	15 (30)	8 (23.5)	7 (43.8)
Unknown	10 (20)	9 (26.5)	1 (6.3)
CMV-positive, No. (%)	43 (86)	30 (88.2)	13 (81.3)
Donor cause of death, No. (%)			
Intracranial hemorrhage	25 (50)	18 (53)	7 (43.8)

Donor characteristics	**All donors (N=50)**	**Donors without acute rejection with hemodynamic compromise (N=34)**	**Donors with acute rejection with hemodynamic compromise (N=16)**
Traumatic brain injury	16 (32)	11 (32.4)	5 (31.3)
Cerebral infarction	5 (10)	3 (8.8)	2 (12.5)
Cerebral anoxia after cardiorespiratory arrest	0 (0.0)	0 (0.0)	0 (0.0)
Other	4 (8)	2 (5.6)	2 (12.5)
Donor P-troponin I, ng/l	48 (10-207)	56 (12-207)	38 (6-265)
Donor P-troponin T, ng/l	21 (9-55)	21 (10-50)	19 (8-63)
Hemoglobin, g/L	119±20	117±19	123±21
CRP, mg/L	79±87	83±92	70±77
Thrombocytes, E9/L	187±80	185±89	199±61
Total P-cholesterol, mmol/l	2.7±0.9	2.7±1	2.6±0.8
P-HDL, mmol/l	0.9±0.4	1±0.4	0.9±0.4
P-LDL, mmol/l	1.2±0.7	1.2±0.8	1.2±0.6
P-triglycerides, mmol/l	0.8±0.4	0.9±0.4	0.7±0.4
Donor echocardiogram			
Left ventricle ejection fraction, %	62 (59-65)	63 (60-66)	60 (57-65)

Donor characteristics	All donors (N=50)	Donors without acute rejection with hemodynamic compromise (N=34)	Donors with acute rejection with hemodynamic compromise (N=16)
Presence of regional wall motion abnormality, No. (%)	5 (10)	5 (14.7)	0 (0.0)
Diastolic posterior wall thickness, mm	11 (9-12)	11 (9-12)	11 (10-13)
Diastolic septum thickness, mm	11 (10-12)	11 (10-11)	11 (10-12)
Donor coronary angiography†			
Performed, No. (%)	28 (56)	16 (47.1)	12 (75)
Abnormal finding angiography, No. (%)	6 (12)	4 (11.8)	2 (12.5)
Donor ionotropic support, No. (%)	34 (68)	22 (64.7)	12 (75)
Donor resuscitation, No. (%)	6 (12)	3 (8.8)	3 (18.8)
Time of ROSC for resuscitated donors, min	16.6±12.5	18.3±1	14.8±1
The time between the declaration of brain death and organ procurement, h	14.5±4	14.9±4.3	13.7±3.1
Organ Retrieval from Donors, No. (%)			
Heart	50 (100)	34 (100)	16 (100)
Lung	17 (34)	10 (29.4)	7 (43.8)
Liver	32 (64)	22 (64.7)	10 (72.7)
Kidneys	45 (90)	30 (88.2)	15 (93.8)

Donor characteristics	All donors (N=50)	Donors without acute rejection with hemodynamic compromise (N=34)	Donors with acute rejection with hemodynamic compromise (N=16)
Pancreas	28 (56)	18 (53)	10 (62.5)

Plus-minus values are mean ±SD; values with range in parentheses are median (interquartile range). CMV, indicates cytomegalovirus; HDL, high-density lipoprotein; LDL, low-density lipoprotein; ROSC, return of spontaneous circulation; and Tx, transplantation. *In the previous medical history of the donors there was no coronary artery disease, chronic obstructive pulmonary disease, peripheral vascular disease, previous malignancy, prior stroke, and no history of sternotomy. †Donor coronary angiography was performed for donors with >40 years of age, strong family history for coronary disease or smoking.

Table S11. Transplant outcome and Clinical Characteristics of recipients with acute rejection with hemodynamic compromise within first 30 days after transplantation.

Recipient characteristics	**All recipients (N=50)**	**Recipients without acute rejection with hemodynamic compromise (N=34)**	**Recipients with acute rejection with hemodynamic compromise (N=16)**
Recipient characteristics			
Age, y	58 (46.5-61)	58 (46-61.75)	57 (49.75-61)
Female sex, No. (%)	12 (24)	7 (20.6)	5 (31.3)
Body mass index, kg/m^2	26±4.6	26±4.8	25.7±4.3
Previous medical history, No. (%)			
Chronic obstructive pulmonary disease	2 (4)	2 (5.9)	0 (0)
Coronary artery disease	10 (20)	7 (20.6)	3 (18.8)
Diabetes	7 (14)	6 (17.6)	1 (6.3)
Previous malignancy	5 (10)	3 (8.8)	2 (12.5)
Prior stroke	7 (14)	5 (14.7)	2 (12.5)
Amiodarone <6 months prior to transplantation, No. (%)	13 (26)	10 (29.4)	3 (18.8)
History of sternotomy	14 (28)	9 (26.5)	5 (31.3)

Recipient characteristics	**All recipients (N=50)**	**Recipients without acute rejection with hemodynamic compromise (N=34)**	**Recipients with acute rejection with hemodynamic compromise (N=16)**
Primary disease, No. (%)			
Endstage coronary disease	11 (22)	8 (23.5)	3 (18.8)
Dilatative cardiomyopathy	25 (50)	16 (47.1)	9 (56.3)
Congenital	4 (8)	4 (11.8)	0 (0)
Myocarditis	3 (6)	2 (5.9)	1 (6.3)
Other	7 (14)	4 (11.8)	3 (18.8)
Donor-recipient gender mismatch	5 (10)	2 (5.9)	3 (18.8)
Mechanical circulatory support prior to	12 (24)	6 (17.6)	6 (37.5)
HTx, No. (%)			
ECMO, No. (%)	6 (12)	3 (8.8)	3 (18.8)
LVAD, No. (%)	6 (12)	3 (8.8)	3 (18.8)
Days on waiting list	180 (44-330)	157 (51.8-330)	200 (31-365)
Graft ischemia time, min			
Cold	98±50.1	93±53.3	106±43.6
Warm	79±20.1	75±19.9	87±19.1
Total	173±54.6	164±58.1	193±41.3

Recipient characteristics	All recipients (N=50)	Recipients without acute rejection with hemodynamic compromise (N=34)	Recipients with acute rejection with hemodynamic compromise (N=16)
Organ functions before transplantation			
PVR, Woods units	3±1.3	3±1.2	3±1.7
TPG, mmHg	10 (7-12)	10 (8-13)	8 (7-10.3)
SPAP, mmHg	42±12.3	41±15.6	43±8.9
P-bilirubin, µmol	11 (9.3-21.3)	11 (9.3-15)	15 (9.8-23.3)
Glomerular filtration rate, mL/min per 1.73 square meters	56 (45-74.5)	55.5 (40.8-67.8)	55.5 (40.8-67.8)
NT-proBNP, ng/L	3164 (1028-5942)	2591 (1028-5601)	3241 (1397-7715.8)
Immunosuppressive therapy			
Induction therapy			
Antithymocyte globulin	20 (40)	13 (38.2)	7 (43.8)
Maintenance therapy			
Cyclosporine A	10 (20)	7 (20.6)	3 (18.8)
Tacrolimus	39 (78)	26 (76.5)	13 (81.3)
Azathioprine	2 (4)	2 (5.9)	0 (0)
Mycophenolic acid	46 (92)	31 (91.2)	15 (93.8)

Recipient characteristics	**All recipients (N=50)**	**Recipients without acute rejection with hemodynamic compromise (N=34)**	**Recipients with acute rejection with hemodynamic compromise (N=16)**
Prednisolone	50 (100)	34 (100)	16 (100)
Recipient outcome			
Intubation time	42 (20-125)	30 (19.3-76.5)	105 (28.5-264)
Time on ICU	216 (144-480)	192 (120-336)	**444 (180-666)***
Hospital Length of Stay	44±29	38±24	**56±35***
Inotropic support, No. (%)	44 (88)	30 (88.2)	14 (87.5)
30-day survival, No. (%)	50 (100)	34 (100)	16 (100)
1-year survival, No. (%)	46 (92)	31 (91.2)	15 (93.8)
Primary graft dysfunction, No. (%)			
Any PGD	14 (28)	8 (23.5)	6 (37.5)
Severe PGD	4 (8)	1 (2.9)	3 (18.8)
ProBNP, ng/l			
ProBNP, 7d	28143±21438	27090±17671	30628±29123
ProBNP, 14d	32369±24443	30383±25520	36909±21983
ProBNP, 21d	27411±24980	22807±24356	37846±23937
ProBNP,1m	18156±21448	13574±18655	**27893±24257***

Recipient characteristics	**All recipients (N=50)**	**Recipients without acute rejection with hemodynamic compromise (N=34)**	**Recipients with acute rejection with hemodynamic compromise (N=16)**
ProBNP, 3m	7794±15560	4600±12473	**14181±19282***
ProBNP, 6m	4089±11495	1344±1161	**9578±18965***
ProBNP, 1y	2761±7137	1358±2340	5367±11446
Left ventricle ejection fraction (LVEF), %			
LVEF, 7d	59±9	60±9	55±10
LVEF, 14d	61±8	62±7	60±8
LVEF, 21d	61±9	63±9	58±8
LVEF, 1m	62±8	64±8	**59±7***
LVEF, 3m	60±9	60±8	59±10
LVEF, 6m	59±9	59±8	59±11
LVEF, 1y	60±9	61±8	58±10
Recipient P-troponin I, ng/l			
1h	12644 (8436-29393)	11652 (8165-22035)	18857 (9572-42289)
6h	82842 (39946-148051)	71159 (36734-130672)	90343 (47616-279326)
12h	95188 (41617-184090)	81698 (40886-141063)	128078(48928-316671)
24h	52434 (32740-106006)	48340 (32740-101849)	**85947 (32987-205895)***

Recipient characteristics	All recipients (N=50)	Recipients without acute rejection with hemodynamic compromise (N=34)	Recipients with acute rejection with hemodynamic compromise (N=16)
Recipient P-troponin T, ng/l			
1h	3035 (2160-5610)	2915 (2092-4941)	4502 (2683- 6677)
6h	8769 (4585-16523)	7595 (4305-12955)	12070 (5381-19205)
12h	8460 (4354-14318)	7686 (4354-13585)	**12390 (4780-19473)***
24h	5361 (3156-9043)	4371 (3156-8226)	**7712 (4114-11275)***
Lactate, mmol/l			
1h	3.1±1.2	3.2±1.2	2.8±1.2
6h	8.1±3.5	8±3.3	8.1±4
12h	5.7±3.3	5.4±2.8	6.5±4.1
24h	2.5±2	2.1±1	**3.38±3.1***
Leukocytes, E9/l			
1h	13.8±5.3	13.8±5	13.8±6
6h	14±5.2	13.7±5	14.6±5.7
12h	13.1±5.3	12.4±4.3	14.6±7
24h	17.5±6.8	17.4±5.7	17.7±8.5
hsCRP, mg/L			

Recipient characteristics	All recipients (N=50)	Recipients without acute rejection with hemodynamic compromise (N=34)	Recipients with acute rejection with hemodynamic compromise (N=16)
1h	12.2±33	11.5±36	13.61±27
6h	13.2±19.6	12.4±18.3	15±22.4
12h	36.3±34.2	37±36.2	35±30.8
24h	96.6±45.8	100.7±40.8	88.1±55.4

Plus-minus values are mean ±SD; values with range in parentheses are median (interquartile range). CMV indicates cytomegalovirus; HDL, high-density lipoprotein; LDL, low-density lipoprotein; ROSC, return of spontaneous circulation; Tx, transplantation. P-values are marked as asterisks (*P<0.05. **P<0.01. ***P<0.001).

Table S12. The possible biological role of key proteins predicting heart transplant outcomes.

	Protein	Expression level in donors with worse heart transplant outcome	Possible biological role in cardiac pathophysiology
Any PGD	Beta-ureidopropionase	High	*Unknown*
	Nicolin 1	Low	*Unknown*
	Lysine-specific demethylase 3A	High	Fibrosis of cardiomyocytes
	Insulin-like growth factor binding protein 2	Low	Angiogenesis and antiapoptosis
	Retinol-binding protein 4	Low	Insulin resistance and cardiomyocyte hypertrophy
Severe PGD	Proteasome subunit alpha type-6	High	Angiogenesis and arteriogenesis
	Moesin	High	Endothelial dysfunction
	Apolipoprotein L3	High	Angiogenesis and endothelial dysfunction
	Eomesodermin	Low	Leukocyte activation
Acute rejection with hemodynamic compromise	Keratin 76	High	Hypoxia in cardiomyocytes
	CD163	High	Leukocyte activation
	CRP	High	Endothelial dysfunction
	Keratin 76	High	Hypoxia in cardiomyocytes
	Myosin Va	High	Channel trafficking in cardiomyocytes
	Proteasome subunit alpha type-6	High	Angiogenesis and arteriogenesis

	Protein	Expression level in donors with worse heart transplant outcome	Possible biological role in cardiac pathophysiology
within 30 days	Proteasome activator subunit 2	High	Angiogenesis and arteriogenesis
	Transaldolase 1	High	Endothelial dysfunction and oxidative stress
1-year survival	D-dopachrome decarboxylase	Low	Fibrosis and angiogenesis
	Leucine-rich alpha-2-glycoprotein 1	Low	Angiogenesis and cardiac remodeling
	Lysine-specific demethylase 3A	High	Fibrosis of cardiomyocytes
	Moesin	High	Endothelial dysfunction
	Keratin 79	Low	*Unknown*

METHODS

Plasma sample processing and trypsin digestion

Plasma samples were drawn into 10ml heparin tubes coated with lithium and centrifuged at 1600×g at RT for 10 min. Subsequently, samples were cooled down to -20 °C and moved to -80 °C until further processing.[1] The analysis of low-abundant proteins is complicated by the presence of high concentrations of proteins such as albumin and IgG. Therefore, the removal of these proteins is essential for the study.

The protein amount of the depleted plasma was measured with BRADFORD MX reagent (EXPEDION) and an equal amount of protein per sample was dried and resuspended in 50 mM Tris buffer containing 6 M urea (pH 7.8). Dithiothreitol was added to a final concentration of 10 mM and samples were shaken at RT for 1 hour. Iodoacetamide was added to a final concentration of 40 mM and samples were shaken at RT for 1 hour. Dithiothreitol (40 mM) was used to quench excess iodoacetamide at RT for 1 hour. Trypsin was added to the protein mixtures at a trypsin:protein ratio by weight of 1:50 and the samples were incubated at 37 °C overnight. For trypsin digestion one missed cleavage was allowed. The resulting tryptic peptides were cleaned with C18 spin columns. Tryptic peptides were desalted and isolated by C18 spin columns (Pierce, ThermoFisher). Peptides were dissolved to achieve a final

concentration of 1.4µg/4µL in 0.1% formic acid. 12.5 fmol/µL of Hi3 spike-in standard peptides (Waters, MA, USA) were included to enable the quantification. Auto error tolerances for fragment and precursor were used. Minimum one ion fragment per peptide, minimum three fragments per protein, and minimum one peptide per protein were marked as “required” for ion matching. Peptide abundances were normalized with Hi3 spiked standard and relative quantitation was performed with the non-conflicting peptides found.

Nano Ultra Performance Liquid Chromatography and quantification of Label-Free Ultra-definition mass spectrometry (UPLC-MS/MS)

We performed UPLC-MS/MS as described.[2] Samples of 4 µL (equivalent to ~1.4µg total protein) were injected into a nanoAcquity UPLC-system (Waters Corporation, MA, USA). As a separating device before the mass spectrometer, we used TRIZAIC nanoTile 85µm x 100 mm HSS-T3u wTRAP. Buffers were made from UPLC-grade chemicals (Sigma-Aldrich, MO, USA). Data was acquired in a data-independent acquisition mode (UDMSE) with a Synapt G2-S HDMS (Waters Corporation, MA, USA) in resolution mode. Progenesis QI for proteomics software (Nonlinear Dynamics, Newcastle, UK) was used for protein identification with an FDR of less than 2%. The peptide identification was done against Uniprot human FASTA sequences (UniprotKB Release 2015_09, 20205 sequence entries) which included ClpB protein sequence (CLPB_ECOLI (P63285)) for label-free quantification. The quantified protein amounts equaled the total protein contents of the analyzed samples.

Univariate and multivariate analysis for finding differentially expressed proteins

Multivariate analysis was carried out with OPLS-DA modeling to further discriminate between the 2 groups. OPLS-DA modeling allows us to find variables that are driving the separation between 2 groups and proteins associated with it. ROC analysis generates a plot of the true positive rate against the false-positive rate. The area under the ROC curve (AUC) is an objective and statistically valid technique for biomarker performance evaluation and allows interpretation for disease classification from healthy subjects.

Enrichment pathway analysis on differentially expressed proteins in brain-dead donors

QIAGEN Ingenuity Pathway Analysis (IPA; Ingenuity Systems, Redwood City, CA, USA) is a commercially available web-based bioinformatics application. IPA implements the manually expert-curated QIAGEN Knowledge Base which retrieves relevant scientific and clinical information from the literature and public databases. In pathway analysis, IPA identifies significant pathways by calculating a -log(p value). A -log(p value) value of >1.3 is corresponding to a p value of <0.05 and is generally considered as a cut-off for significant pathways. Moreover, IPA calculates an activation z-score. The z-score makes predictions about potential inhibition or activation of identified pathways.

To interrogate the biological importance of S-Plot proteins, proteins were separately matched to the top biological pathways with a p value of <0.001 and an absolute value of z-score greater than 1, and to the information retrieved from literature research. By

summarizing the protein-specific characteristics, we filtered S-Plot proteins that were taking part in the most important biological pathways of protein set enrichment analyses, and out of S-Plot proteins, these proteins and their associated pathways were further discussed.

Clinical outcome analysis

The diagnostic criteria for PGD were established in a consensus statement by ISHLT in 2014.[3] Correlation analysis provides a correlation coefficient (r-value) which ranges from 0 to 1. The diagnosis and treatment of acute rejection with hemodynamic compromise were based on clinical decisions such as a clinically significant decrease in ventricular function increase, increase in ventricular wall thickness, and/or arrhythmias. The diagnose of acute rejection with hemodynamic compromise always required treatment with high dose of intravenous pulse steroids, and/or anti-thymocyte globulin. We did not consider any other acute rejections equal to or greater than grade 2R based on ISHLT criteria or any other endpoints for acute rejection due to the low incidence of these rejections in our study cohort.[4]

Statistical analysis of demographics

In statistical analysis of baseline demographic and clinical characteristics, we used the Kolmogorov-Smirnov test to determine the normality of distributions. For 2-group comparisons, the independent samples t-test or Mann-Whitney U-test was used for parametric

and non-parametric variables, respectively. For categorical comparisons, Fisher's exact test was applied. P <0.05 was considered statistically significant.

Results

Study population and demographic data

The final study population consisted of 53 multi-organ donors for HTx, and 23 age and sex-matched healthy blood donors. The median age of the donors was 44 years (interquartile range: 33-51), and 10 (18.9%) were female. In healthy controls, the median age was 46 years (37-54), and 6 (21.1%) were female. Causes of donor brain death were intracranial hemorrhage (49.1%), traumatic brain injury (35.8%), cerebral infarction (11.3%), and other (3.8%). The mean time between the declaration of brain death and organ procurement was 14.9±4 hours, an approximate time for plasma collection for proteomics (**Table 1**).

Specific treatment for acute rejection with hemodynamic compromise

Out of 16 recipients with acute rejection with hemodynamic compromise, 9 recipients received methylprednisolone 500mg/day for 3 days, 2 patients received methylprednisolone 500mg/day for 2 days, and 1 patient methylprednisolone 250mg/day for 3 days. 3

patients received first methylprednisolone 500mg/day for 3 days and then anti-thymocyte globulin once daily for 3 days. One patient received only anti-thymocyte globulin once daily for 3 days.

Proteome profile discriminated 3 subclusters within brain-dead donors

We carried out separate PCA analysis and hierarchical clustering including only brain-dead donors. This analysis confirmed that there were 2 main clusters of donors (Donor A and Donor B), and the Donor B cluster was grouped into 2 subclusters Donor B1 and B2 (**Figure S3A, B**)**.** In donor characteristics, cerebral infarction as a donor cause of death was significantly more prominent in Donor A group, while traumatic brain injury was more prominent in the Donor B group. All the donors with hypertension in their medical history (18.2%) belonged to the Donor B1 group. Donor B2 subcluster had significantly reduced levels of thrombocytes and plasma LDL when compared to the Donor B1 group. When comparing the recipient outcomes between Donor A and Donor B groups, none of the recipients from Donor A was treated with LVAD, whereas 21.2% of recipients from Donor B were bridged with LVAD. However, transplants from the Donor B2 group showed a better left-ventricle ejection fraction at 7 days, lower hsTnI and hsTnT at 6h, 12h, and 24h, and lower high sensitivity CRP at 24h after transplantation (**Table 1, Table 3**). Univariate analysis on the 3 subclusters of donors showed that out of 237 proteins, 164 proteins were significantly different between Donor A and Donor B (**Figure S3C**), and 107 proteins significantly differed between Donor B1 and Donor B2 (**Figure 3D**). Pathway enrichment analysis on differentially expressed

proteins between Donor A and B subcluster (N=164), and Donor B1 and B2 subclusters (N=107) showed that most of the enriched pathways were overlapping between the donor subclusters (**Table S4 and S5**).

DISCUSSION

Generally, acute brain injury results in systemic acute phase response, a coordinated series of neuroendocrinological, physiological, and metabolic changes initiated after tissue injury as a repair and regeneration process. Out of 31 identified proteins belonging to acute phase response signaling, 23 downregulated proteins belonged to complement and coagulation pathways. Considering the nature of brain injury and brain death, it is possible that these proteins were consumed during the activation of these pathways during these incidents. Even though the acute phase response signaling pathway did not show an activation pattern based on z-score, our results suggest that acute phase response was present in brain-dead donors.

Beta-ureidopropionase, Nicolin 1, insulin-like growth factor binding protein 2, and retinol-binding protein 4 were correlated with any PGD grade. Beta-ureidopropionase functions as an enzyme in pyrimidine graduation.[5] Pyrimidines are important regulators of the central nervous system and alterations of pyrimidine are linked to neurological disorders.[6] However, the potential function of beta-

ureidopropionase in brain-dead organ donors remains to be elucidated. Nicolin 1 may be mostly expressed by the liver while expression levels depend on the metabolic state of the liver.[7] However, more research is warranted to elucidate the biological function of Nicolin 1. Insulin-like growth factor binding protein 2 has been suggested as a strong diagnostic and prognostic biomarker for heart failure which may have higher accuracy than brain natriuretic peptide.[8] Under hypoxic conditions and oxidative stress, insulin-like growth factor binding protein 2 enhances VEGF expression which mediates anti-apoptosis and angiogenesis.[9,10] In lung transplant recipients, pretransplant VEGF levels predict primary graft dysfunction.[11] Retinol-binding protein 4 a has been suggested as a prognostic biomarker for heart failure as well.[12] Retinol-binding protein 4 activates the pro-inflammatory TLR4/MyD88 pathway by which it promotes insulin resistance and hypertrophy in cardiomyocytes.[13]

Moreover, apolipoprotein L3 and eomesodermin were correlated to severe PGD. Apolipoprotein L3 modulates MAPK and FAK signaling pathways in endothelial cells and contributes to inflammation-mediated angiogenesis and endothelial dysfunction.[14] Eomesodermin, also known as eomes, is involved in CD4(+) T-cell differentiation, and CD4(+) eomes T-cells accumulate in inflamed tissues of patients with proinflammatory diseases.[15,16,17] In acute ischemia-reperfusion injury, CD4(+) T-cells mediate the infiltration of neutrophils and chemokine production.[18] Therefore, we hypothesize that eomes may play a role in CD4(+) mediated ischemia-reperfusion injury which is inherently connected to the development of primary graft dysfunction.

Transaldolase 1 was significantly associated with acute rejection with hemodynamic compromise. Transaldolase 1 is a key enzyme of the nonoxidative pentose-phosphate pathway. The pentose-phosphate pathway plays a pivotal role in cardiac anaerobic glucose metabolism, and pathway activity is enhanced by hyperglycemia and aggravates endothelial dysfunction and oxidative stress in failing hearts.[19,20] CD163 is a high-affinity scavenger receptor for the hemoglobin-haptoglobin complex but also a macrophage activation marker.[21] CD163 has been introduced as an immune-related biomarker for the severity of heart failure.[22] CRP may affect NO bioavailability and induce endothelial dysfunction.[23] High CRP levels in brain-dead donors are associated with worse short-term outcomes in kidney transplantation.[24] Increased Keratin 76 expression in fetal cardiomyocytes may be induced by endothelin-1 during hypoxia-induced remodeling.[25]

In 1-year survival analysis, D-dopachrome decarboxylase, leucine-rich alpha-2-glycoprotein 1, and keratin 79 were identified as statistically significant proteins. D-dopachrome decarboxylase, also known as macrophage inhibitory factor-2 (MIF-2), is involved in the modulation of immune response and has been recently introduced as a novel inflammatory mediator in CNS pathophysiology.[26] In experimental studies, DDT in cardiomyocytes mediates anti-fibrotic and anti-angiogenic effects and protects against heart failure. Patients with heart failure undergoing heart transplantation showed decreased DDT expression levels in cardiomyocytes.[27] Furthermore, DDT has been shown to protect the heart against ischemia-reperfusion injury-induced injury and contractile dysfunction.[28] Leucine-rich alpha-2-glycoprotein 1 is secreted also by activated neutrophils and promotes angiogenesis by modulating

endothelial TGFβ1 signaling and attenuates adverse cardiac remodeling.[29, 30, 31] Keratin 79 is a filament protein in endothelial cells.[32] Despite its statistical significance, the biological association between Keratin 79 and pathophysiology in heart transplant recipients remains unclear at this point.

---

[1] Saraswat M, Joenväärä S, Seppänen H, Mustonen H, Haglund C, Renkonen R. Comparative proteomic profiling of the serum differentiates pancreatic cancer from chronic pancreatitis. *Cancer Med* 2017; **6**(7):1738-1751. doi:10.1002/cam4.1107

[2] Holm M, Joenväärä S, Saraswat M, et al. Plasma protein expression differs between colorectal cancer patients depending on primary tumor location. *Cancer Med* 2020; **9**(14):5221-5234. doi:10.1002/cam4.3178

[3] Kobashigawa J, Zuckermann A, Macdonald P, et al. Report from a consensus conference on primary graft dysfunction after cardiac transplantation. *J Heart Lung Transplant* 2014; **33**(4):327-340. doi:10.1016/j.healun.2014.02.027

[4] Billingham M, Kobashigawa JA. The revised ISHLT heart biopsy grading scale. *J Heart Lung Transplant* 2005; **24**(11):1709. doi:10.1016/j.healun.2005.03.018

[5] Van Kuilenburg AB, Dobritzsch D, Meijer J, et al. ß-ureidopropionase deficiency: phenotype, genotype and protein structural consequences in 16 patients. *Biochim Biophys Acta* 2012; **1822**(7):1096-1108. doi:10.1016/j.bbadis.2012.04.001

[6] Connolly GP, Simmonds HA, Duley JA. Pyrimidines and CNS regulation. *Trends Pharmacol Sci* 1996; **17**(3):106-107. doi:10.1016/0165-6147(96)20001-x

[7] Backofen B, Jacob R, Serth K, Gossler A, Naim HY, Leeb T. Cloning and characterization of the mammalian-specific nicolin 1 gene (NICN1) encoding a nuclear 24 kDa protein. *Eur J Biochem* 2002; **269**(21):5240-5245. doi:10.1046/j.1432-1033.2002.03232.x

[8] Barutaut M, Fournier P, Peacock WF, et al. Insulin-like Growth Factor Binding Protein 2 predicts mortality risk in heart failure. *Int J Cardiol* 2020; **300**:245-251. doi:10.1016/j.ijcard.2019.09.032

[9] Azar WJ, Azar SH, Higgins S, et al. IGFBP-2 enhances VEGF gene promoter activity and consequent promotion of angiogenesis by neuroblastoma cells. *Endocrinology* 2011; **152**(9):3332-3342. doi:10.1210/en.2011-1121

[10] Gupta K, Kshirsagar S, Li W, et al. VEGF prevents apoptosis of human microvascular endothelial cells via opposing effects on MAPK/ERK and SAPK/JNK signaling. *Exp Cell Res* 1999; **247**(2):495-504. doi:10.1006/excr.1998.4359

[11] Krenn K, Klepetko W, Taghavi S, Lang G, Schneider B, Aharinejad S. Recipient vascular endothelial growth factor serum levels predict primary lung graft dysfunction. *Am J Transplant* 2007; **7**(3):700-706. doi:10.1111/j.1600-6143.2006.01673.x

[12] Li XZ, Zhang KZ, Yan JJ, et al. Serum retinol-binding protein 4 as a predictor of cardiovascular events in elderly patients with chronic heart failure. *ESC Heart Fail* 2020; **7**(2):542-550. doi:10.1002/ehf2.12591

[13] Gao W, Wang H, Zhang L, et al. Retinol-Binding Protein 4 Induces Cardiomyocyte Hypertrophy by Activating TLR4/MyD88 Pathway. *Endocrinology* 2016; **157**(6):2282-2293. doi:10.1210/en.2015-2022

[14] Khalil A, Poelvoorde P, Fayyad-Kazan M, et al. Apoliporotein L3 interferes with endothelial tube formation via regulation of ERK1/2, FAK and Akt signaling pathway. *Atherosclerosis* 2018; **279**:73-87. doi:10.1016/j.atherosclerosis.2018.10.023

[15] Gruarin P, Maglie S, De Simone M, et al. Eomesodermin controls a unique differentiation program in human IL-10 and IFN-γ coproducing regulatory T cells. *Eur J Immunol* 2019; **49**(1):96-111. doi:10.1002/eji.201847722

[16] Raveney BJ, Oki S, Hohjoh H, et al. Eomesodermin-expressing T-helper cells are essential for chronic neuroinflammation. *Nat Commun* 2015; **6**:8437. Published 2015 Oct 5. doi:10.1038/ncomms9437

[17] Chemin K, Ramsköld D, Diaz-Gallo LM, et al. EOMES-positive CD4+ T cells are increased in PTPN22 (1858T) risk allele carriers. *Eur J Immunol* 2018; **48**(4):655-669. doi:10.1002/eji.201747296

[18] Yang Z, Sharma AK, Linden J, Kron IL, Laubach VE. CD4+ T lymphocytes mediate acute pulmonary ischemia-reperfusion injury. *J Thorac Cardiovasc Surg* 2009; **137**(3):695-702. doi:10.1016/j.jtcvs.2008.10.044

[19] Peiró C, Romacho T, Azcutia V, et al. Inflammation, glucose, and vascular cell damage: the role of the pentose phosphate pathway [published correction appears in Cardiovasc Diabetol. 2017 Feb 16;16(1):25]. *Cardiovasc Diabetol* 2016; **15**:82. Published 2016 Jun 1. doi:10.1186/s12933-016-0397-2

[20] Vimercati C, Qanud K, Mitacchione G, et al. Beneficial effects of acute inhibition of the oxidative pentose phosphate pathway in the failing heart. *Am J Physiol Heart Circ Physiol* 2014; **306**(5):H709-H717. doi:10.1152/ajpheart.00783.2013

[21] Buechler C, Ritter M, Orsó E, Langmann T, Klucken J, Schmitz G. Regulation of scavenger receptor CD163 expression in human monocytes and macrophages by pro- and antiinflammatory stimuli. *J Leukoc Biol* 2000; **67**(1):97-103.

[22] Klimczak-Tomaniak D, Bouwens E, Schuurman AS, et al. Temporal patterns of macrophage- and neutrophil-related markers are associated with clinical outcome in heart failure patients. *ESC Heart Fail* 2020; **7**(3):1190-1200. doi:10.1002/ehf2.12678

[23] Clapp BR, Hirschfield GM, Storry C, et al. Inflammation and endothelial function: direct vascular effects of human C-reactive protein on nitric oxide bioavailability. *Circulation* 2005; **111**(12):1530-1536. doi:10.1161/01.CIR.0000159336.31613.31

[24] Cucchiari D, Rovira J, Paredes D, et al. Association of Brain-Dead Donors' Terminal Inflammation With Delayed Graft Function in Kidney Transplant Recipients. *Transplant Proc* 2017; **49**(10):2260-2264. doi:10.1016/j.transproceed.2017.10.003

[25] Shin AN, Dasgupta C, Zhang G, Seal K, Zhang L. Proteomic Analysis of Endothelin-1 Targets in the Regulation of Cardiomyocyte Proliferation. *Curr Top Med Chem* 2017; **17**(15):1788-1802. doi:10.2174/1568026617666161116142417

[26] Ji H, Zhang Y, Chen C, et al. D-dopachrome tautomerase activates COX2/PGE2 pathway of astrocytes to mediate inflammation following spinal cord injury. *J Neuroinflammation* 2021; **18**(1):130. Published 2021 Jun 11. doi:10.1186/s12974-021-02186-z

[27] Ma Y, Su KN, Pfau D, et al. Cardiomyocyte d-dopachrome tautomerase protects against heart failure. *JCI Insight* 2019; **4**(17):e128900. Published 2019 Sep 5. doi:10.1172/jci.insight.128900

[28] Qi D, Atsina K, Qu L, et al. The vestigial enzyme D-dopachrome tautomerase protects the heart against ischemic injury. *J Clin Invest* 2014; **124**(8):3540-3550. doi:10.1172/JCI73061

[29] Wang X, Abraham S, McKenzie JAG, et al. LRG1 promotes angiogenesis by modulating endothelial TGF-β signalling. *Nature* 2013; **499**(7458):306-311. doi:10.1038/nature12345

[30] Liu C, Lim ST, Teo MHY, et al. Collaborative Regulation of LRG1 by TGF-β1 and PPAR-β/δ Modulates Chronic Pressure Overload-Induced Cardiac Fibrosis. *Circ Heart Fail* 2019; **12**(12):e005962. doi:10.1161/CIRCHEARTFAILURE.119.005962

[31] Kumagai S, Nakayama H, Fujimoto M, et al. Myeloid cell-derived LRG attenuates adverse cardiac remodelling after myocardial infarction. *Cardiovasc Res* 2016; **109**(2):272-282. doi:10.1093/cvr/cvv273

[32] Rogers MA, Edler L, Winter H, Langbein L, Beckmann I, Schweizer J. Characterization of new members of the human type II keratin gene family and a general evaluation of the keratin gene domain on chromosome 12q13.13. *J Invest Dermatol* 2005; **124**(3):536-544. doi:10.1111/j.0022-202X.2004.23530.x